

Alma Mater Studiorum  
University of Bologna

---

FACULTY OF ENGINEERING

*DICAM*

*Department of Civil, Chemical, Environmental and Material Engineering*

Civil Engineering  
Roads, Railroads and Airports Constructions LM

*Flexible pavement design using  
Mechanistic-Empirical methods:  
the Californian approach*

*Master of Science  
thesis of:*  
Alessio Montuschi

*Supervisor:*  
Professor Giulio Dondi

*Advisors:*  
Assistant Researcher Matteo Pettinari

---

Session III

Academic year 2011/2012



Alma Mater Studiorum  
Università degli Studi di Bologna

---

FACOLTÀ DI INGEGNERIA

*DICAM*

*Dipartimento di Ingegneria Civile, Chimica, Ambientale e dei Materiali*

Ingegneria Civile  
Costruzione di Strade Ferrovie ed Aeroporti LM

*Flexible pavement design using  
Mechanistic-Empirical methods:  
the Californian approach*

***Tesi di laurea di:***  
Alessio Montuschi

***Relatore:***  
Chiar.mo Prof. Ing. Giulio Dondi

***Correlatore:***  
Dott. Ing. Matteo Pettinari

---

Sessione III

Anno Accademico 2011/2012



*To Emma and Nicole*



# *Key Words*

*Maintenance*

*Mechanistic-Empirical design*

*CalME*

*pavement performance*

*overlay*



# *Abstract*

*(English version)*

Pavement structural design is a complex task. Although the basic geometry of a road system is quite simple, everything else is not. Traffic loading is a heterogeneous mix of vehicles, axle types, and axle loads with distributions that vary with time through the day, from season to season, and over pavement design life. Since the beginning of 1900 empirical methods for design have been used, as in most of those of the American Association of State Highway and Transportation Officials (AASHTO) guides, but several developments in recent decades have offered the opportunity for more rational and rigorous pavement design procedures. A better characterization of materials and the development of constitutive models now allow a greater ability to predict the pavement response to load and climate effects, and the possibility of using dedicated softwares that use fatigue laws relating to the current materials behavior. Volumetric (Mix Design) and mechanical (Permanent deformation and Fatigue performance) characterization properties are fundamental and necessary for a realistic estimate of pavement performance.

To date, the pavement design is still based on empirical methodologies and specifications in which, starting from selected input data, the final results and the thickness layers are directly established without considering the numerous variables involved during the service life of the pavement structure. For this reason new and more realistic mechanistic methods are increasingly adopted and analyzed. The main objective of this thesis is precisely to evaluate the potential application and validation of a mechanistic-empirical approach, analyzing the outcomes of pavement simulations in which several maintenance interventions are applied. The Empirical-Mechanistic method consists of a structural model able to predict the stress and strain states within the pavement structure under the different traffic and environmental conditions, and of empirical models, that calibrated with the behavior of the materials, connect the structural response to the pavement performances.

The year 1996 marks the beginning of an extensive research project for the California aimed at the development of Empirical-Mechanistic methods for pavement design. Thanks to advances in the pavement field it has reached the first version of the software CalME, which was used for the development of this dissertation. Of the three approaches, of which the is composed (Empirical, Empirical-Mechanistic classic and Empirical-Mechanistic Incremental-Recursive), the procedure Incremental-Recursive was the application of choice. It is based on several models, which

attempt to represent the numerous variables that affect the behavior of a pavement structure. Among them, this paper is focused on fatigue damage models and accumulation of permanent deformation models achieved through a careful material characterization in the laboratory.

One of the innovations introduced by CalME with this approach is the ability to evaluate the interaction between the various layers in order to identify the ideal thicknesses in both the design and maintenance interventions.

In Chapter 1 the importance of maintenance in pavement and road fields is analyzed. The different types of pavements with relating distresses are described and the main maintenance operations are proposed. A short historical excursus on the pavement design evolution from the early empirical methods to the more complex mechanistic methods is shown, through the useful mechanistic-empirical methods, in Chapter 2. The CalME (Mechanistic Empirical Design Software) is introduced in Chapter 3. In particular, the Incremental-Recursive procedure is analyzed and the models on which it is based. The experimental research starts in Chapter 4, in which an empirical method is utilized for the design of two pavements, using the Caltrans Highway Design Manual. Finally in Chapter 5 the results of the asphalt structures simulations are shown. Consequently the results of other structure simulations subject to several maintenance interventions are presented. For each situation considered the total surface cracking, the total rutting and fatigue damage and rut depth on each layer were analyzed

The research was carried out in particular to the Pavement Research Center at the University of California, Berkeley (UCPRC), with the support of the DICAM from the University of Bologna.

# *Abstract*

*(Italian version)*

La progettazione strutturale della pavimentazione stradale è un compito complesso. Sebbene la geometria di un sistema stradale presenti meno problematiche, il dimensionamento di una struttura stradale è influenzato da numerose variabili: il carico dovuto al traffico è una miscela eterogenea di veicoli, i tipi di assi e i carichi agenti su di essi hanno distribuzioni che variano nel tempo, le condizioni climatiche non sono costanti durante l'anno e nemmeno nell'arco di una giornata. Dagli inizi del '900 si è fatto ricorso a metodi empirici per la progettazione, come in gran parte quelli dell'American Association of State Highway and Transportation Officials (AASHTO), ma diversi sviluppi negli ultimi decenni hanno offerto l'occasione per più razionali e rigorose procedure di progettazione. Una migliore caratterizzazione dei materiali e lo sviluppo di modelli costitutivi permettono ora una migliore capacità di prevedere le risposte delle pavimentazioni agli effetti di carico e clima, e la possibilità di usare softwares dedicati che utilizzano leggi di fatica relative al reale comportamento dei materiali. La caratterizzazione volumetrica e meccanica di un conglomerato bituminoso è quindi fondamentale e necessaria per una realistica previsione delle performance di una pavimentazione stradale.

Ad oggi la progettazione stradale è ancora basata su metodologie empiriche e capitolati in cui, partendo da alcuni dati in input, i risultati finali e gli spessori degli strati sono dati direttamente senza tenere conto delle numerose variabili che intervengono durante la vita utile della struttura. Per questo motivo si sta cercando di spingersi verso nuove e più realistiche metodologie meccanicistiche. Obiettivo principale di questa tesi è appunto valutare le potenzialità di applicazione di un nuovo approccio Empirico-Meccanicistico nell'ambito della progettazione delle sovrastrutture stradali, analizzando i risultati derivanti da simulazioni ottenute attraverso il CalME, software in fase di sviluppo presso l'Università di Berkeley.

La progettazione Empirico-Meccanicistica consiste di un modello strutturale capace di prevedere gli stati tenso-deformativi all'interno della pavimentazione sotto l'azione del traffico e in funzione delle condizioni climatiche e di modelli empirici, calibrati sul comportamento dei materiali, che collegano la risposta strutturale alle performance della pavimentazione.

Il 1996 segna l'inizio per la California di un estensivo progetto di ricerca mirato allo sviluppo dei metodi di progetto Empirico-Meccanicistici per le pavimentazioni stradali. Grazie ai continui progressi in campo stradale si è arrivati alla prima versione del software CalME, la cui ultima versione è stata utilizzata per questo elaborato. Dei tre approcci dei quali il programma si

componi (Empirico, Empirico-Meccanicistico classico ed Empirico-Meccanicistico Incrementale-Ricorsivo) si è utilizzata la procedura Incrementale-Ricorsiva. Essa è basata su numerosi modelli che cercano di rappresentare le variabili che condizionano il comportamento di una pavimentazione stradale. Tra tutti, in questo elaborato, ci si è soffermati sui modelli di danno da fatica e sui modelli di accumulo di deformazioni permanenti conseguiti tramite un'accurata caratterizzazione dei materiali in laboratorio. Una delle innovazioni introdotte dal CalME con tale approccio è la possibilità di valutare l'interazione tra i vari strati al fine di individuare gli spessori ideali sia in fase di progettazione che in fase di manutenzione.

Nel capitolo 1 è analizzata l'importanza della manutenzione in ambito stradale. Sono descritte le diverse tipologie di pavimentazione, i relativi ammaloramenti cui sono soggette ed introdotti i principali interventi manutentivi volti al risanamento delle stesse.

Nel capitolo 2 è esposto un breve excursus storico sull'evoluzione della progettazione stradale dai primi metodi empirici fino ai più complessi metodi meccanicistici, passando per i metodi empirico-meccanicistici ed i relativi modelli di performance utilizzati.

Nel capitolo 3 è stato descritto il CalME, Mechanistic Empirical Design Software. In particolare è stata analizzata la procedura Incrementale-Ricorsiva e i modelli che ne sono alla base.

Nel capitolo 4 è stato introdotto il programma sperimentale attraverso la definizione di due sovrastrutture stradali e dei materiali costituenti. Il dimensionamento delle stesse è stato ottimizzato secondo il manuale di progettazione attualmente in uso presso l'ente gestore delle infrastrutture stradali dello stato della California.

Infine nel capitolo 5 sono riportati i risultati delle simulazioni effettuate con le pavimentazioni in esame. Sono stati analizzate la superficie totale fessurata, l'ormaiamento totale e il danno a fatica e ormaiamento relativo a ogni strato.

La ricerca è stata eseguita presso il Pavement Research Center dell'Università di Berkeley sotto la supervisione del Prof. Carl L. Monismith, con il supporto del DICAM dell'Università di Bologna.

# Contents

<b>Key Words</b> .....	<b>vii</b>
<b>Abstract (English version)</b> .....	<b>ix</b>
<b>Abstract (Italian version)</b> .....	<b>xi</b>
<b>Contents</b> .....	<b>xiii</b>
<b>Chapter 1: Pavement Preservation</b> .....	<b>1</b>
1.1 Introduction.....	3
1.2 Pavement Preservation.....	3
1.2.1 Routine maintenance.....	4
1.2.2 Periodic maintenance.....	4
1.2.3 Urgent maintenance.....	4
1.3 Pavement Types.....	5
1.3.1 Introduction.....	5
1.3.2 Flexible Pavement.....	6
1.3.2.1 Basic Structural Elements.....	7
1.3.2.1.1 Surface Course.....	7
1.3.2.1.2 Base Course.....	8
1.3.2.1.2 Subbase Course .....	8
1.3.2.2 Flexible pavement types.....	9
1.3.3 Rigid Pavement.....	10
1.3.3.1 Basic Structural Elements.....	10
1.3.3.1.1 Surface Course.....	11
1.3.3.1.2 Base Course.....	11
1.3.3.1.2 Subbase Course .....	12
1.3.3.2 Joints.....	13

1.3.3.2.1	Contraction Joints.....	13
1.3.3.2.2	Expansion Joints.....	14
1.3.3.2.3	Isolation Joints.....	15
1.3.3.2.4	Construction Joints.....	15
1.3.3.3	Rigid pavement types.....	16
1.4	Pavement distresses.....	17
1.4.1	Introduction.....	17
1.4.2	Flexible Pavement Distresses.....	17
1.4.2.1	Fatigue (Alligator) Cracking.....	17
1.4.2.2	Block Cracking and Transverse (Thermal).....	18
1.4.2.3	Potholes.....	19
1.4.2.4	Bleeding.....	20
1.4.2.5	Rutting.....	21
1.4.2.6	Corrugation and Shoving.....	22
1.4.2.7	Ravelling and Weathering.....	22
1.4.2.8	Pumping.....	23
1.4.2.9	Longitudinal Cracking.....	23
1.4.2.10	Surface Deterioration.....	24
1.5	Maintenance and Rehabilitation.....	24
1.5.1	Introduction.....	24
1.5.2	Maintenance for flexible pavement.....	25
1.5.2.1	Crack seals.....	25
1.5.2.2	Fog seals.....	25
1.5.2.3	Slurry seals.....	26
1.5.2.4	Bituminous Surface Treatments (BST).....	26
1.5.2.5	Patches.....	27
1.5.2.6	Thin Maintenance Overlays.....	27
1.5.2.6.1	Dense Graded Thin Overlays.....	28
1.5.2.6.2	Open Graded Mixes.....	28
1.5.2.6.3	Gap Graded Mixtures.....	29
1.5.3	Rehabilitation for flexible pavement.....	29

1.5.3.1 Structural HMA Overlays.....	29
1.5.3.1.1 Engineering Judgement.....	30
1.5.3.1.2 Component Analysis.....	30
1.5.3.1.3 Non Destructive Testing with Limiting Deflection Criteria.....	30
1.5.3.1.4 Mechanistic-Empirical Analysis.....	30
1.5.3.2 Structural PCC Overlays.....	31
1.5.3.2.1 Unbounded-Classical Whitetopping.....	31
1.5.3.2.2 Bpunded-Thin composite Whitetopping.....	32
<b>Chapter 2: Evolution of Pavement Design Procedure.....</b>	<b>33</b>
2.1 Introduction .....	35
2.2 Review of Flexible Pavement Design Principles.....	35
2.2.1 Empirical Methods.....	36
2.2.2 Mechanistic-Empirical Methods.....	37
2.2.2.1 Basic Inputs and Outcomes.....	38
2.3 Pavement Design Procedure.....	42
2.3.1 The 1993 AASHTO Guide.....	43
2.3.1.1 AASHTO Road Test and Early Versions of the Guide.....	43
2.3.1.2 Current Design Equation.....	47
2.3.1.3 Input Variables.....	49
2.3.1.4 Reliability.....	53
2.3.1.5 Addition Considerations.....	54
2.3.2 M-E PDG.....	56
2.3.2.1 Design Process.....	57
2.3.2.2 Design Input.....	59
2.3.2.3 Pavement Response Models.....	65
2.3.2.4 Empirical Performance Models.....	69
2.3.2.5 Reliability.....	77

<b>Chapter 3: CalME: California Mechanistic – Empirical design software.....</b>	<b>79</b>
3.1 Introduction to CalME and CalBack.....	81
3.1.1 Overview.....	81
3.1.2 CalME.....	81
3.1.3 CalBack.....	83
3.2 CalME Design Methods: The “ <i>Caltrans</i> ” Empirical Design Methods.....	86
3.2.1 R-Value Method for New Pavements .....	86
3.2.2 Deflection Reduction Method for Rehabilitation.....	86
3.3 CalME Design Methods: The “ <i>Classical</i> ” Mechanistic-Empirical Design Method.....	89
3.3.1 Introduction.....	89
3.3.2 Pavement Response.....	90
3.3.2.1 Introduction.....	90
3.3.2.2 Boussinesque’s equations.....	92
3.3.2.3 Burmister’s Elastic Models.....	94
3.3.2.4 Odemark’s Method of the Equivalent Thickness.....	95
3.3.3 Pavement Performance.....	97
3.3.3.1 Design Criteria.....	97
3.3.3.2 Default Design Criteria in CalME.....	100
3.4 CalME Design Methods: The “ <i>Incremental-Recursive</i> ” procedure.....	102
3.4.1 Introduction.....	102
3.4.2 CalME Models used in the I-R procedure.....	104
3.4.2.1 Asphalt Concrete Master Curve.....	104
3.4.2.2 Aging of Asphalt Binder and Hardening of Asphalt Mixes.....	110
3.4.2.3 Effect of seasonal variations on unbound materials.....	111
3.4.2.4 Effect of confinement and load level variations on unbound materials...	112
3.4.2.5 Damage functions and the Time-Hardening procedure.....	113
3.4.2.6 AC Fatigue Damage model .....	116
3.4.2.7 AC Fatigue cracking evaluation.....	118
3.4.2.8 Reflection cracking in an overlay asphalt layer.....	119
3.4.2.9 Fatigue damage to cemented materials.....	120

3.4.2.10 AC Permanent shear strain accumulation.....	121
3.4.2.11 AC Rutting evaluation.....	122
3.4.2.12 Unbound materials Rutting evaluation.....	122
3.4.2.13Crushing damage.....	123

**Chapter 4: Experimental Program Description.....125**

4.1 Introduction.....	127
4.2 Pavement Structure Layers.....	127
4.3 Traffic Consideration.....	129
4.3.1 Traffic Index Calculation.....	129
4.4 Soil Characteristics.....	131
4.4.1 California R-Value.....	131
4.5 Engineering Procedures for New Projects.....	132
4.5.1 Empirical Method.....	132
4.6 Pavement design through Caltrans Highway Design Manual.....	136

**Chapter 5: Pavement Design.....139**

5.1 Pavement structure definition, Traffic and Climate.....	141
5.2 Performance Simulation Results.....	143
5.2.1 Central Coast conditions.....	143
5.2.2 Desert conditions.....	147
5.3 Performance Simulation Results, overlay applications.....	152
5.3.1 Central Coast conditions.....	152
5.3.1.1 Pavement structure A and TI=11.5.....	152

5.3.1.2 Pavement structure A and TI=13.....	156
5.3.1.3 Pavement structure B and TI=11.5.....	159
5.3.1.4 Pavement structure B and TI=13.....	162
5.3.2 Desert conditions.....	165
5.3.1.1 Pavement structure A and TI=11.5.....	165
5.3.1.2 Pavement structure A and TI=13.....	168
5.3.1.3 Pavement structure B and TI=11.5.....	171
5.3.1.4 Pavement structure B and TI=13.....	174
5.4 Result Analysis.....	177
<b><u>Conclusions</u></b> .....	<b>179</b>
<b><u>List of References</u></b> .....	<b>181</b>

*Pavement  
Preservation*



## **1.1 Introduction**

Roads are among the most important public assets in many countries. Developed countries require a core transportation network that carries approximately 80 percent of national traffic, including key roads in urban areas and roads providing sufficient access to rural areas. A portion of the overall transportation budget thus has to be spent on construction and the remainder on maintaining the core network. Many countries have tended to favor new construction, rehabilitation, or reconstruction of roads over maintenance. This has led to a steady increase in the backlog of road repairs and a loss of development impact. Road improvements bring immediate and at times dramatic benefits to road users such as improved access to hospitals, schools, and markets. Smooth roads also improve comfort, speed, safety and lower vehicle operating costs. For these benefits to be sustained, road improvements must be followed by a well planned maintenance program.

Postponing road maintenance results in high direct and indirect costs. If road defects are repaired promptly, the cost is usually modest. If defects are neglected, an entire road section may fail completely, requiring full reconstruction on average at three or more times the cost of quick repairs. Delayed maintenance has indirect costs as well. Neglected roads steadily become more difficult to use, resulting in increased vehicle operating costs (more frequent repairs, more fuel use) and a reluctance by transport operators to use the roads. This imposes a heavy burden on the economy. As passenger and freight services are curtailed, there is a consequent loss of economic and social development opportunities.

## **1.2 Pavement Preservation**

The combined effects of traffic loading and environment will cause every pavement, no matter how well-designed/constructed to deteriorate over time. Maintenance and rehabilitation are the solutions to preserve the pavement from this deterioration process. Maintenance actions help slow the rate of deterioration by identifying and addressing specific pavement deficiencies that contribute to overall deterioration. Rehabilitation is the act of repairing portions of an existing pavement to reset the deterioration process. Reconstructing an entire pavement, however, is not considered rehabilitation but rather new construction because the methods used are generally those developed for new pavement construction. Although maintenance can slow the rate of pavement deterioration, it cannot stop it. Therefore eventually the effects of deterioration need to

be reversed by adding or replacing material in the existing pavement structure and this is called rehabilitation ([www.pavementinteractive.org](http://www.pavementinteractive.org)).

The goal of maintenance is to preserve the asset, and not to upgrade it. Unlike major road works maintenance must be done regularly. Pavement maintenance comprises “activities to keep pavement, shoulders, slopes, drainage facilities and all other structures and property within the road margins as near as possible to their as-constructed or renewed condition” (PIARC 1994). It includes minor repairs and improvements to eliminate the cause of defects and to avoid excessive repetition of maintenance efforts. For management and operational convenience, road maintenance is categorized as routine, periodic, and urgent.

### **1.2.1 Routine maintenance**

Routine maintenance, which comprises small-scale works conducted regularly, aims “to ensure the daily passability and safety of existing roads in the short-run and to prevent premature deterioration of the roads” (PIARC 1994). Typical activities include roadside verge clearing and grass cutting, cleaning of silted ditches and culverts, patching, and pothole repair. For gravel roads it may include regrading every six months. Activity frequency varies, and consequently requires attention once or more per week or month.

### **1.2.2 Periodic maintenance**

Periodic maintenance, which covers activities on a section of road at regular and relatively long intervals, aims “to preserve the structural integrity of the road” (WB Maintenance website). These operations tend to be in large scale, requiring specialized equipment and personnel. They cost more than routine maintenance works and require specific identification and planning for implementation and often even design. Activities can be classified as preventive, resurfacing, overlay, and pavement reconstruction. Resealing and overlay works are generally undertaken in response to measured deterioration in road conditions. For a paved road, repaving is needed usually every eight years; for a gravel road, re-graveling is needed usually every three years.

### **1.2.3 Urgent maintenance**

Urgent maintenance is undertaken for repairs that cannot be foreseen but require immediate attention, such as collapsed culverts or landslides that block a road.

Maintenance does not include rehabilitation, building shoulders, or widening roads. If the sections to be rebuilt constitute more than 25 percent of the road’s length, the work is classified as rehabilitation and not maintenance.

## 1.3 PAVEMENT TYPES

### 1.3.1 Introduction

Generally, all surfaced pavement types can be categorized into two groups, flexible and rigid. Flexible pavements are those which are surfaced with bituminous (or asphalt) materials. These can be either in the form of HMA surface courses (generally used on higher volume roads such as the Interstate highway network) or pavement surface treatments (such as a bituminous surface treatment (BST) generally found on lower volume roads). These types of pavements are called "flexible" since the total pavement structure "deflects" or "bends" due to traffic loads. A flexible pavement structure is generally composed of several layers of materials which can allow this "flexing". On the other hand, rigid pavements are composed of a PCC surface course. Such pavements are substantially "stiffer" than flexible pavements due to the high modulus of elasticity of the PCC material. Furthermore these pavements can have reinforcing steel, which is generally used to reduce or eliminate joints. Each of these pavement types distribute loads over the subgrade in a different manner. Flexible pavement uses more flexible surface course and distributes loads over a smaller area. It relies on a combination of layers for transmitting load to the subgrade (see Figure 1). Rigid pavement, because of PCC's high elastic modulus (stiffness), tends to distribute the load over a relatively wide area of subgrade (see Figure 1.1). The concrete slab itself supplies most of a rigid pavement's structural capacity.

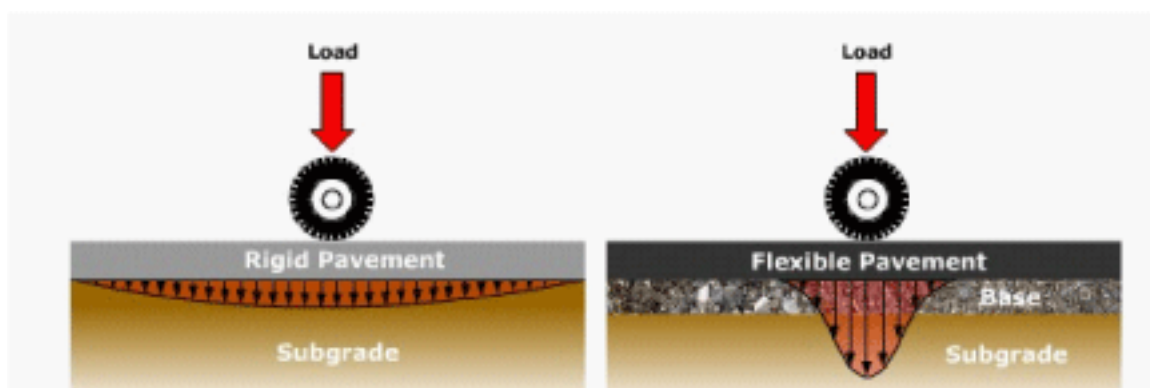


Figure 1.1. Rigid and Flexible Pavement Load Distribution.

Overall, it may be somewhat confusing as to why one pavement is used versus another. In general, state highway agencies generally select pavement type either by policy, economics, or both. Flexible pavements usually require some sort of maintenance or rehabilitation every 10 to 15 years. Rigid pavements, on the other hand, can often serve 20 to 40 years with little or no maintenance or rehabilitation. Thus, it should come as no surprise that rigid pavements are often used in urban, high traffic areas, but, naturally, there are trade-offs. For example, when a flexible pavement requires maintenance and rehabilitation, the options are generally less expensive and quicker to perform than for rigid pavements. This next subdivision to those found in Washington State Department of Transportation (WSDOT).

### **1.3.2 Flexible Pavement**

The term flexible pavement is derived by the fact that the total pavement structure deflects, or flexes, under loading. A flexible pavement structure is typically composed of several layers of material. Each layer receives the loads from the above layer, spreads this load, then passes on these loads to the next layer below. Thus, the further down in the pavement structure a particular layer is, the less load (in terms of force per area) it will carry.

In order to take maximum advantage of this property, material layers are usually arranged in order of descending load bearing capacity with the highest load bearing capacity material (and most expensive) on the top and the lowest load bearing capacity material (and least expensive) on the bottom. This section describes the typical flexible pavement structure consisting of:

- *Surface course.* This is the top layer and the layer that comes in contact with traffic. It may be composed of one or several different HMA sublayers.
- *Base course.* This is the layer directly below the HMA layer and generally consists of aggregate (either stabilized or unstabilized).
- *Subbase course.* This is the layer (or layers) under the base layer. A subbase is not always needed

### 1.3.2.1 Basic Structural Elements

A typical flexible pavement structure (see Figure 1.2) consists of the surface course underlying base and subbase courses. Each of these layers contributes to structural support and drainage. The surface course (typically an HMA layer) is the stiffest (measured by resilient modulus) and contributes the most to pavement strength. The underlying layers are less stiff but are still important to pavement strength as well as drainage and frost protection. A typical structural design results in a series of layers that gradually decrease in material quality with depth.

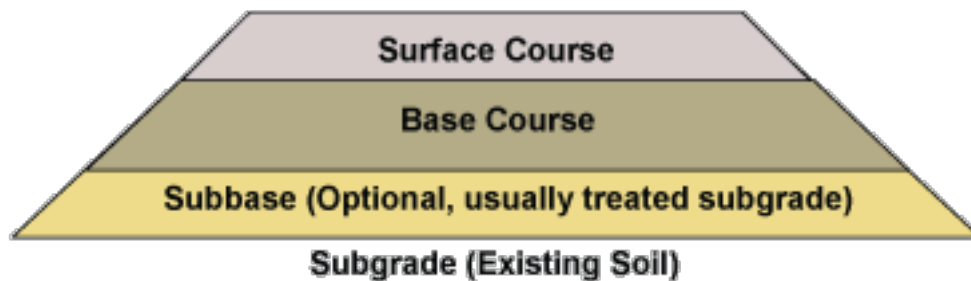


Figure 1.2. Flexible Pavement Structure.

#### 1.3.2.1.1 Surface Course

The surface course is the layer in contact with the traffic loads and normally contains the highest quality materials. It has characteristics such as friction, smoothness, noise control, rutting, shoving resistance, and drainage. In addition, it prevents excessive quantities of surface water entering into the underlying base, subbase, and subgrade. The top structural layer of material is sometimes subdivided into two layers :

1. *Wearing Course*. This is the layer in direct contact with the traffic loads. It is used to take the brunt of traffic wear and can be removed and replaced as it becomes worn. A properly designed (and funded) preservation program should be able to identify pavement surface distress while it is still confined to the wearing course. Consequently, the wearing course can be rehabilitated before distress propagates into the underlying intermediate/binder course.
2. *Intermediate/Binder Course*. This layer provides the bulk of the HMA structure. Its purpose is to distribute load.

### **1.3.2.1.2 Base Course**

The base course is immediately beneath the surface course. It provides additional load distribution and contributes to drainage and frost resistance. Base courses are usually constructed out of:

1. *Aggregate*. Base courses are most typically constructed from durable aggregates (see Figure 1.3) that will not be damaged by moisture or frost action. Aggregates can be either stabilized or unstabilized.
2. *HMA*. In certain situations where high base stiffness is desired, base courses can be constructed using a variety of HMA mixes. In relation to surface course HMA mixes, base course mixes usually contain larger maximum aggregate sizes, are more open graded and are subject to more lenient specifications.



**Figure 1.3. Limerock Base Course Undergoing Final Grading.**

### **1.3.2.1.3 Subbase Course**

The subbase course, positioned between the base course and the subgrade, functions primarily as structural support and it can also:

1. Minimize the intrusion of fines from the subgrade into the pavement structure.

2. Improve drainage.
3. Minimize frost action damage.
4. Provide a working platform for construction.

A subbase course is not always needed or used. It consists of lower quality materials than the base course but possesses higher quality material when compared to the subgrade soils. For example, a pavement constructed over a high quality, stiff subgrade may not need the additional features offered by a subbase course and can consequently be omitted from design. However, a pavement constructed over a low quality soil such as a swelling clay may require the additional load distribution characteristic that a subbase course can offer. In this scenario the subbase course may consist of high quality filler used to replace poor quality subgrade.

### **1.3.2.2 Flexible pavement types**

There are many different types of flexible pavements. Three of the more common types of HMA mix types used in the U.S.:

- *Dense-graded HMA*. Dense-graded HMA is a versatile, all-around mix making it the most common and well-understood mix type in the U.S.
- *Stone matrix asphalt (SMA)*. SMA, although relatively new in the U.S., has been used in Europe as a surface course for years to support heavy traffic loads and resist studded tire wear.
- *Open-graded HMA*. This includes both open-graded friction course (OGFC) and asphalt treated permeable materials (ATPM). Open-graded mixes are typically used as wearing courses (OGFC) or underlying drainage layers (ATPM) because of the special advantages offered by their porosity.

### 1.3.3 Rigid Pavement

Rigid pavements are so named because the pavement structure deflects very little under loading due to the high modulus of elasticity of their surface course. A rigid pavement structure is typically composed of a PCC surface course built on top of either (1) the subgrade or (2) an underlying base course. Because of its relative rigidity, the pavement structure distributes loads over a wide area with only one, or at most two, structural layers. This section describes the typical rigid pavement structure consisting of:

- *Surface course.* This is the top layer, which consists of the PCC slab.
- *Base course.* This is the layer directly below the PCC layer and generally consists of aggregate or stabilized subgrade.
- *Subbase course.* This is the layer (or layers) under the base layer. A subbase is not always needed and therefore may often be omitted.

#### 1.3.3.1 Basic Structural Elements

A typical rigid pavement structure (see Figure 1.4) consists of the surface course and the underlying base and subbase courses (if used).

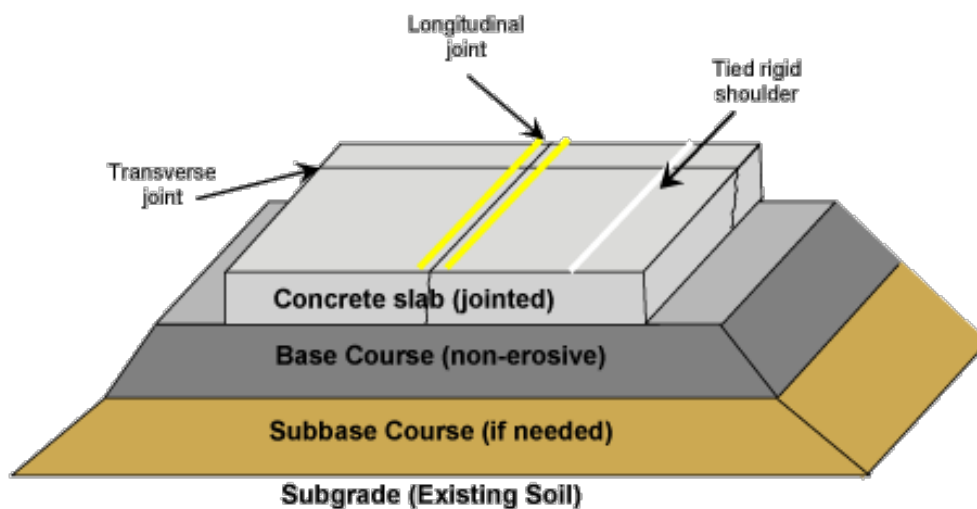


Figure 1.4. Basic Rigid Pavement Structure.

The surface course (made of PCC) is the stiffest (as measured by resilient modulus) and provides the majority of strength. The underlying layers are orders of magnitude less stiff but still make important contributions to pavement strength as well as drainage and frost protection.

### 1.3.3.1.1 Surface Course

The surface course is the layer in contact with traffic loads and is made of PCC. It provides characteristics such as friction (see Figure 1.5), smoothness, noise control and drainage. In addition, it serves as a waterproofing layer to the underlying base, subbase and subgrade. The surface course can vary in thickness but is usually between 150 mm (for light loading) and 300 mm (12 inches) (for heavy loads and high traffic). Figure 1.6 shows a 300 mm surface course (Hall, Correa, & Carpenter, 2001).



Figure 1.5. PCC Surface.



Figure 1.6. Rigid Pavement Slab (Surface Course) Thickness.

### 1.3.3.1.2 Base Course

The base course is immediately beneath the surface course. It provides (1) additional load distribution, (2) contributes to drainage and frost resistance, (3) uniform support to the pavement and (4) a stable platform for construction equipment (ACPA, 2001). Bases also help prevent subgrade soil movement due to slab pumping and are usually constructed out of:

1. *Aggregate base.* A simple base course of crushed aggregate has been a common option since the early 1900s and is still appropriate in many situations today.
2. *Stabilized aggregate or soil* (see Figure 1.7). Stabilizing agents are used to bind otherwise loose particles to one another, providing strength and cohesion. Cement

treated bases (CTBs) can be built to as much as 20 - 25 percent of the surface course strength (FHWA, 1999). However, cement treated bases (CTBs) used in the 1950s and early 1960s had a tendency to lose excessive amounts of material leading to panel cracking and settling.

3. *Dense-graded HMA*. In situations where high base stiffness is desired base courses can be constructed using a dense-graded HMA layer.
4. *Permeable HMA*. In certain situations where high base stiffness and excellent drainage is desired, base courses can be constructed using an open graded HMA. Recent research may indicate some significant problems with ATPB use.
5. *Lean concrete*. Contains less portland cement paste than a typical PCC and is stronger than a stabilized aggregate. Lean concrete bases (LCBs) can be built to as much as 25 - 50 percent of the surface course strength (FHWA, 1999). A lean concrete base functions much like a regular PCC surface course and therefore, it requires construction joints and will crack over time. These joints and cracks can potentially cause reflection cracking in the surface course if they are not carefully matched.



**Figura 1.7. Completed CTB with Curing Seal.**

### ***1.3.3.1.3 Subbase Course***

The subbase course is the portion of the pavement structure between the base course and the subgrade. It functions primarily as structural support but it can also:

1. Minimize the intrusion of fines from the subgrade into the pavement structure.
2. Improve drainage.
3. Minimize frost action damage.
4. Provide a working platform for construction.

The subbase generally consists of lower quality materials than the base course but possesses a higher quality than the subgrade soils. Appropriate materials are aggregate and high quality structural filler. A subbase course is not always needed or used.

### **1.3.3.2 Joints**

Joints are placed discontinuously in a rigid pavement surface course. The most common types of pavement joints, defined by their function, are (AASHTO, 1993): contraction, expansion, isolation and construction.

#### ***1.3.3.2.1 Contraction Joints***

A contraction joint is a sawed, formed, or tooled groove in a concrete slab that creates a weakened vertical plane. It regulates the location of the cracking caused by dimensional changes in the slab. Unregulated cracks can grow and result in an unacceptably rough surface as well as water infiltration into the base, subbase and subgrade, which can enable other types of pavement distress. Contraction joints are the most common type of joint in concrete pavements, thus the generic term "joint" generally refers to a contraction joint. Contraction joints are chiefly defined by their spacing and their method of load transfer. They are generally between 1/4 - 1/3 the depth of the slab and typically spaced every 3.5-15 m with thinner slabs having shorter spacing (see figure 1.8). Some states use a semi-random joint spacing pattern to minimize their resonant effect on vehicles. These patterns typically use a repeating sequence of joint spacing (for example: 2.7 m followed by 3.0 m followed by 4.3 m followed by 4.0 m). Transverse contraction joints can be cut at right angles to the direction of traffic flow or at an angle (called a "skewed joint").



**Figure 1.8. Rigid pavement showing contraction joint.**

### ***1.3.3.2 Expansion Joints***

An expansion joint (see figure 1.9) is placed at a specific location to allow the pavement to expand without damaging adjacent structures or the pavement itself. Up until the 1950s, it was common practice in the U.S. to use plain, jointed slabs with both contraction and expansion joints (Sutherland, 1956). However, expansion joints are not typically used today because their progressive closure tends to cause contraction joints to progressively open (Sutherland, 1956). Progressive or even large seasonal contraction joint openings cause a loss of load transfer—particularly so for joints without dowel bars.



**Figure 1.9. Joint Expansion.**

### **1.3.3.2.3 Isolation Joints**

An isolation joint (see figure 1.10) is used to lessen compressive stresses that develop at T- and unsymmetrical intersections, ramps, bridges, building foundations, drainage inlets, manholes, and anywhere differential movement between the pavement and a structure (or another existing pavement) may take place (ACPA, 2001). They are typically filled with a joint filler material to prevent water and dirt infiltration.



**Figure 1.10. Roofing paper used for an isolation joint.**

### **1.3.3.2.4 Construction Joints**

A construction joint (see figure 1.11) is a joint between slabs that results when concrete is placed at different times. This type of joint can be further broken down into transverse and longitudinal construction joints. Longitudinal construction joints also allow slab warping without appreciable separation or cracking of the slabs.



Figure 1.11. Construction joint.

### **1.3.3.3 Rigid pavement types**

Rigid pavements are differentiated into three major categories by their means of crack control:

- *Jointed plain concrete pavement (JPCP)*. This is the most common type of rigid pavement. JPCP controls cracks by dividing the pavement up into individual slabs separated by contraction joints. Slabs are typically one lane wide and between 3.7 m and 6.1 m long. JPCP does not use any reinforcing steel but does use dowel bars and tie bars.
- *Jointed reinforced concrete pavement (JRCP)*. As with JPCP, JRCP controls cracks by dividing the pavement up into individual slabs separated by contraction joints. However, these slabs are much longer than JPCP slabs, so JRCP uses reinforcing steel within each slab to control within-slab cracking. This pavement type is no longer constructed in the U.S. due to long-term performance problems.
- *Continuously reinforced concrete pavement (CRCP)*. This type of rigid pavement uses reinforcing steel rather than contraction joints for crack control. Cracks typically appear every 1.1-2.4 m and are held tightly together by the underlying reinforcing steel.

## **1.4 PAVEMENT DISTRESSES**

### **1.4.1 Introduction**

In this section, various types of asphalt pavement distress classes are briefly discussed and a subset of interest is defined. These definitions conform to those found in US department of transportation distress identification manual (Federal Highway Administration, 2003) and many of the images utilized are from the LTPP Distress Identification Manual.

### **1.4.2 Flexible Pavement Distress**

The most commonly seen distresses on flexible pavement surfaces include cracking, rutting, pothole, pumping, bleeding and surface deterioration.

#### **1.4.2.1 Fatigue (Alligator) Cracking**

Fatigue (also called alligator) cracking, which is caused by fatigue damage, is the principal structural distress which occurs in asphalt pavements with granular and weakly stabilized bases. Alligator cracking first appears as parallel longitudinal cracks in the wheelpaths, and progresses into a network of interconnecting cracks resembling chickenwire or the skin of an alligator. Alligator cracking may progress further, particularly in areas where the support is weakest, to localized failures and potholes.

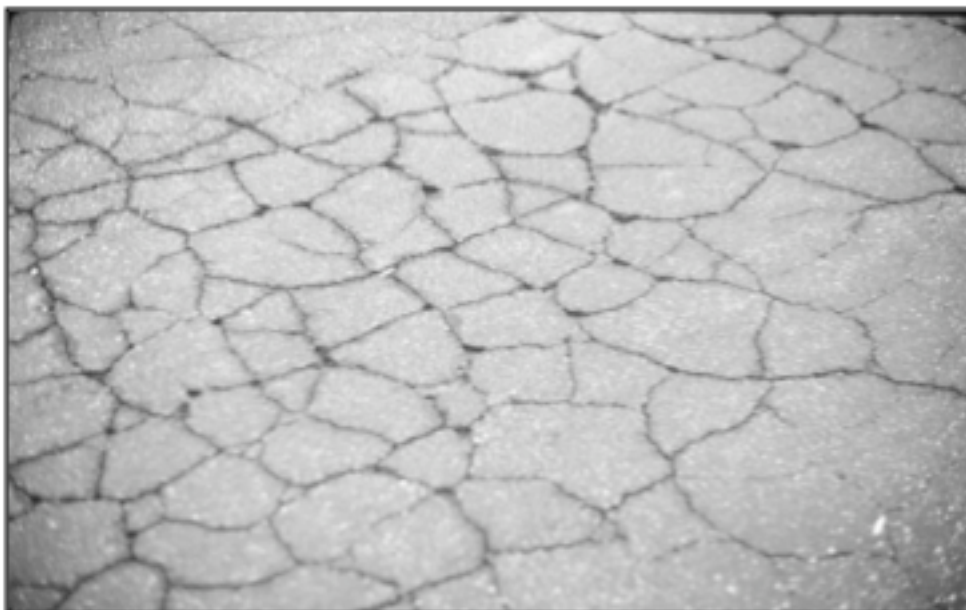


**Figura 1.14. Fatigue (alligator) cracking in flexible pavement.**

Factors which influence the development of alligator cracking are:

- the number and magnitude of applied loads;
- the structural design of the pavement (layer materials and thicknesses);
- the quality and uniformity of foundation support;
- the consistency of the asphalt cement;
- the asphalt content;
- the air voids and aggregate characteristics of the asphalt concrete mix;
- the climate of the site (i.e., the seasonal range and distribution of temperatures).

Considerable laboratory research into the fatigue life of asphalt concrete mixes has been conducted. However, attempting to infer from such laboratory tests how asphalt concrete mix properties influence asphalt pavement fatigue life requires consideration of the mode of laboratory testing (constant stress or constant strain) and the failure criterion used. Constant-stress testing suggests that any asphalt cement property (e.g., lower penetration, higher viscosity) or mix property which increases mix stiffness will increase fatigue life. Constant-strain testing suggests the opposite: that less brittle mixes (e.g., higher penetrations, lower viscosities) exhibit longer fatigue lives. The prevailing recommendations are that low-stiffness (low viscosity) asphalt cements should be used for thin asphalt concrete layers (i.e., less than 15 cm), and that the fatigue life of such mixes should be evaluated using constant-strain testing, while high-stiffness (high viscosity) asphalt cements should be used for asphalt concrete layers 15 cm and thicker, and the fatigue life of such mixes should be evaluated using constant-stress testing. In practice, however, it is not common to modify the mixture stiffness for different asphalt concrete layer thicknesses (FHWA, 2003).

#### **1.4.2.2 Block Cracking and Transverse (Thermal)**

Block cracking is the cracking of an asphalt pavement into rectangular pieces ranging from approximately 30 cm to 300 cm on a side. Block cracking occurs over large paved areas such as parking lots, as well as roadways, primarily in areas not subjected to traffic loads, but sometimes also in loaded areas. Thermal cracks typically develop transversely across the traffic lanes of a roadway, sometimes at such regularly spaced intervals that they may be mistaken for reflection cracks from an underlying concrete pavement or stabilized base.



**Figura 1.15. Medium severity longitudinal cracking.**

Block cracking and thermal cracking are both related to the use of an asphalt cement which is or has become too stiff for the climate. Both types of cracking are caused by shrinkage of the asphalt concrete in response to low temperatures, and progress from the surface of the pavement downward. The key to minimizing block and thermal cracking is using an asphalt cement of sufficiently low stiffness (high penetration), which is nonetheless not overly temperature-susceptible (i.e., likely to become extremely stiff at low temperatures regardless of its penetration index at higher temperatures).

### **1.4.2.3 Potholes**

A pothole is a bowl-shaped hole through one or more layers of the asphalt pavement structure, between about 15 and 90 centimeters in diameter. Potholes begin to form when fragments of asphalt concrete are displaced by traffic wheels, e.g., in alligator-cracked areas. Potholes grow in size and depth as water accumulates in the hole and penetrates into the base and subgrade, weakening support in the vicinity of the pothole.



**Figura 1.16. High severity pothole.**

#### **1.4.2.4 Bleeding**

Bleeding is the accumulation of asphalt cement material at the pavement surface, beginning as individual drops which eventually coalesce into a shiny, sticky film. Bleeding is the consequence of a mix deficiency: an asphalt cement content in excess of that which the air voids in the mix can accommodate at higher temperatures (when the asphalt cement expands). Bleeding occurs in hot weather but is not reversed in cold weather, so it results in an accumulation of excess asphalt cement on the pavement surface. Bleeding reduces surface friction and is therefore a potential safety hazard.

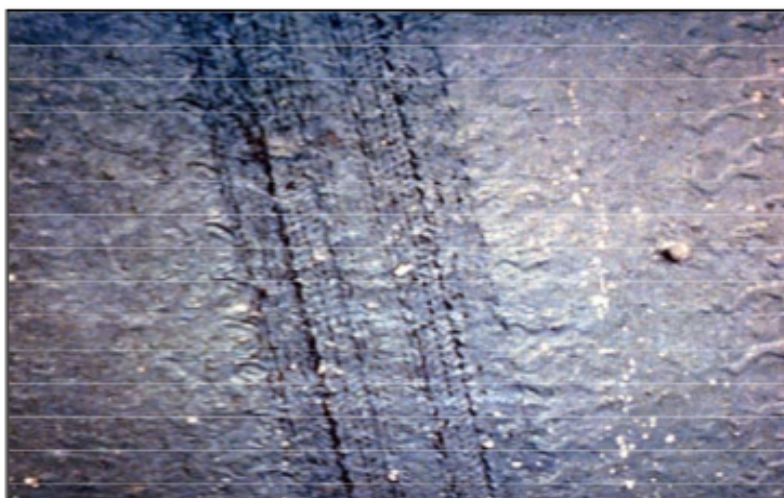


**Figura 1.17. Tire marks evident in high-severity bleeding.**

### **1.4.2.5 Rutting**

Rutting is the formation of longitudinal depression of the wheelpaths, most often due to consolidation or movement of material in either the base and subgrade or in the asphalt concrete layer. Another, unrelated, cause of rutting is abrasion due to studded tires and tire chains. Deformation which occurs in the base and underlying layers is related to the thickness of the asphalt concrete surface, the thickness and stability of the base and subbase layers, and the quality and uniformity of subgrade support, as well as the number and magnitude of applied loads.



**Figura 1.18. Rutting**

Deformation which occurs only in the asphalt concrete layer may be the result of either consolidation or plastic flow. Consolidation is the continued compaction of asphalt concrete by traffic loads applied after construction. Consolidation may produce significant rutting in asphalt layers which are very thick and which are compacted during construction to initial air void contents considerably higher than the long-term air void contents for which the mixes were designed. Plastic flow is the lateral movement of the mix away from the wheelpaths, most often as a result of excessive asphalt content, exacerbated by the use of small, rounded aggregates and/or inadequate compaction during construction. Asphalt cement stiffness is believed to play a relatively minor role in rutting resistance of asphalt mixes which contain well-graded, angular, rough-textured aggregates. Stiffer asphalt cements can increase rutting resistance to an extent, but the tradeoff is that mixes containing stiffer cements are more prone to cracking in cold weather. Wheelpath ruts greater than a third to a half an inch in depth are considered by many highway agencies to pose a safety hazard, due to the potential for hydroplaning, wheel spray, and

vehicle handling difficulties.

#### **1.4.2.6 Corrugation and Shoving**

Corrugations are deviations of the pavement surface from its original cross section and are generally caused by excessive bitumen, improper aggregate gradation in the pavement, insufficient compaction of the mix or low interparticle friction to a degree that causes an unstable pavement with low resistance to traffic loads. Grooving, rutting, and shoving will also occur where the pavement is unstable. These distresses cause considerable annoyance to motorists. Repairs will normally involve removing the corrugated material and replacing it with new asphalt concrete.

#### **1.4.2.7 Ravelling and weathering**

Ravelling and weathering are progressive deterioration of an asphalt concrete surface as a result of loss of aggregate particles (ravelling) and asphalt binder (weathering) from the surface downward. Ravelling and weathering occur as a result of loss of bonding between aggregates and the asphalt binder. This may occur due to hardening of the asphalt cement, dust on the aggregate which interferes with asphalt adhesion, localized areas of segregation in the asphalt concrete mix where fine aggregate particles are lacking, or low in-place density of the mix due to inadequate compaction. High air void contents are associated with more rapid aging and increased likelihood of ravelling. Increased asphalt film thickness can significantly reduce the rate of aging and offset the effects of high air voids. Surface softening and aggregate dislodging due to oil spillage are also classified as ravelling.

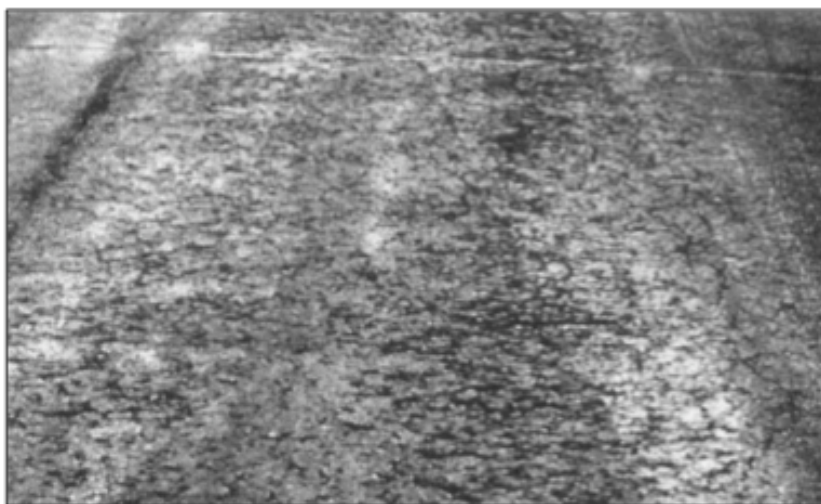


**Figura 1.19. High severity ravelling**

Ravelling and weathering may pose a safety hazard if deteriorated areas of the surface collect enough water to cause hydroplaning or wheel spray. Loose debris on the pavement surface which

may also be picked up by vehicle tires is also a potential safety hazard.

#### **1.4.2.8 Pumping**

Pumping is the ejection of water and erodible fines from under a pavement under heavywheel loads. On asphalt pavements, pumping is typically evidenced by light-colored stains on the pavement shoulder near joints and cracks.



**Figura 1.20. Water bleeding and pumping**

The major factors which contribute to pumping are the presence of excess water in the pavement structure, erodible base or subgrade materials, and high volumes of high-speed, heavy wheel loads.

#### **1.4.2.9 Longitudinal Cracking**

Non-wheelpath longitudinal cracking in an asphalt pavement may reflect up from the edges of an underlying old pavement or from edges and cracks in a stabilized base, or may be due to poor compaction at the edges of longitudinal paving lanes. Longitudinal cracking may also be produced in the wheelpaths by the application of heavy loads or high tire pressures. It is important to distinguish between non-wheelpath and wheelpath longitudinal cracking when conducting condition surveys; only wheelpath longitudinal cracking should be considered along with alligator cracking in assessing the extent of load-related damage which has been done to the pavement.



**Figura 1.21. Medium severity longitudinal cracking.**

### **3.2.10 Surface deterioration**

Surface deterioration such as raveling, popouts, joint spalling and other surface type deterioration allows moisture to penetrate to steel reinforcing, causing further distress. Ride quality also becomes uncomfortable. Repairs are to be made as soon as possible when a section of a roadway is considered to have a severe condition of this type.

## **1.5 Maintenance and Rehabilitation**

### **1.5.1 Introduction**

Asphalt pavement is both durable and resilient, as it must be. Asphalt pavement takes a beating on a daily basis. Between regular traffic and environmental conditions pavement must be resilient. However, over time, even the toughest asphalt will start to deteriorate. Maintenance and rehabilitation are the solutions to slow down and may reset this deterioration process. Maintenance actions, such as crack sealing, joint sealing, fog seals and patching are typically applied to pavements in good condition having significant remaining service life. Rehabilitation involves structural enhancements that extend the service life of an existing pavement and/or improve its load carrying capacity. For instance, removing and replacing the wearing course in a pavement provides new wearing course material on which the deterioration process begins anew. Reconstructing an entire pavement, however, is not

considered rehabilitation but rather new construction because the methods used are generally those developed for new pavement construction. These definitions conform to those found in Washington State Department of Transportation (WSDOT).

## **1.5.2 Maintenance for flexible pavement**

Pavement maintenance describes all the methods and techniques used to preserve pavement condition, safety, and ride quality, and therefore aid a pavement in achieving its design life. The performance of a pavement is directly tied to the timing, type and quality of the maintenance it receives. This section, taken largely from Roberts et al. (Roberts, 1986), describes the more common U.S. preventative and corrective maintenance options for HMA pavement.

### **1.5.2.1 Crack Seals**

Crack seal products are used to fill individual pavement cracks to prevent entry of water or other non-compressible substances such as sand, dirt, rocks or weeds. Crack sealant is typically used on early stage longitudinal cracks, transverse cracks, reflection cracks and block cracks. Alligator cracks are most often too extensive to justify filling with crack sealer; they usually require an area treatment such as a patch or reconstruction. Crack filler material is typically some form of rubberized asphalt or sand slurry. Before applying crack sealant, cracks need to be routed out and cleaned. Reported average performance life ranges from about 3 - 8 years.

### **1.5.2.2 Fog Seals**

A fog seal is a light application of a diluted slow-setting asphalt emulsion to the surface of an aged (oxidized) pavement surface. Fog seals are low-cost and are used to restore flexibility to an existing HMA pavement surface. They may be able to temporarily postpone the need for a surface treatment or non-structural overlay. An excessive application rate may result in a thin asphalt layer on top of the original HMA pavement. This layer can be very smooth and cause a loss of skid resistance. Sand should be kept in reserve to blot up areas of excess application.

### **1.5.2.3 Slurry Seals**

A slurry seal is a homogenous mixture of emulsified asphalt, water, well-graded fine aggregate and mineral filler that has a creamy fluid-like appearance when applied. Slurry seals are used to fill existing pavement surface defects as either a preparatory treatment for other maintenance treatments or as a wearing course. There are three basic aggregate gradations used in slurry seals:

1. *Type I (fine)*. This type has the finest aggregate gradation (most are smaller than the 2.36 mm (No. 8) sieve) and is used to fill small surface cracks and provide a thin covering on the existing pavement. Type I aggregate slurries are sometimes used as a preparatory treatment for HMA overlays or surface treatments. Type I aggregate slurries are generally limited to low traffic areas.
2. *Type II (general)*. This type is coarser than a Type I aggregate slurry (it has a maximum aggregate size of 6.4 mm) and is used to (1) treat existing pavement that exhibits moderate to severe raveling due to aging or (2) to improve skid resistance. Type II aggregate slurry is the most common type.
3. *Type III (coarse)*. This type has the most coarse gradation and is used to treat severe surface defects. Because of its aggregate size, it can be used to fill slight depressions to prevent water ponding and reduce the probability of vehicle hydroplaning.

### **1.5.2.4 Bituminous Surface Treatments (BST)**

A bituminous surface treatment, also known as a seal coat or chip seal, is a thin protective wearing surface that is applied to a pavement or base course. BSTs can provide: a waterproof layer to protect the underlying pavement, increased skid resistance, a fill for existing cracks or raveled surfaces, an anti-glare surface during wet weather and an increased reflective surface for night driving.

A single layer BST is constructed in the following steps:

1. *Surface preparation*. Surface defects, such as potholes, are repaired and the existing surface is cleaned.
2. *Asphalt material application*. Typically, an asphalt emulsion is applied from a spray truck to the surface of the existing pavement.

3. *Aggregate application.* A thin aggregate cover (only one stone thick) is spread over the asphalt material before it has set. The aggregate usually has a uniform gradation.
4. *Aggregate embedding.* A roller (usually a pneumatic tire roller) is used to push the aggregate into the asphalt material and seat it firmly against the underlying pavement. It is common to place an aggregate "chokestone" on top of the uniformly graded larger aggregates after embedment. Chokestone is essentially a finer aggregate gradation used to make a more dense aggregate matrix at the level of embedment. This more dense matrix helps prevent excessive aggregate loss due to traffic.

### **1.5.2.5 Patches**

Patches are a common method of treating an area of localized distress. Patches can be either full-depth where they extend from the pavement surface to the subgrade or partial where they do not extend through the full depth of existing pavement. Full-depth patches are necessary where the entire depth of pavement is distressed. Often times, the underlying base, subbase or subgrade material is the root cause of the distress and will also need repair. Partial depth patches are used for pavement distresses like raveling, rutting, delamination and cracking where the depth of crack does not extend through the entire pavement depth. Patching material can be just about any HMA or cold mix asphalt material as well as certain types of slurries. Typically some form of HMA is used for permanent patches, while cold mix is often used for temporary emergency repairs.

### **1.5.2.6 Thin Maintenance Overlays**

Maintenance overlays are defined as thin treatments using a hot mix system. A thin treatment is a non-structural layer and is applied as a maintenance treatment, either corrective or preventive. In the U.S, thin treatments are less than 37.5 mm in thickness. In Caltrans, thin blankets are 30 mm thick. Historically, three maintenance overlay types have been used extensively by Caltrans, either alone or in combination with other treatments.

They include:

- Dense Graded Thin Blankets (Type A and B)
- Open Graded (Conventional Type O and Type O-High Binder)
- Gap Graded Mixes (Type G)

The different mixes are defined based on their aggregate grading, binder content, and voids content. Figure 1.22 illustrates, in general, the differences in aggregate structure for these mix types.

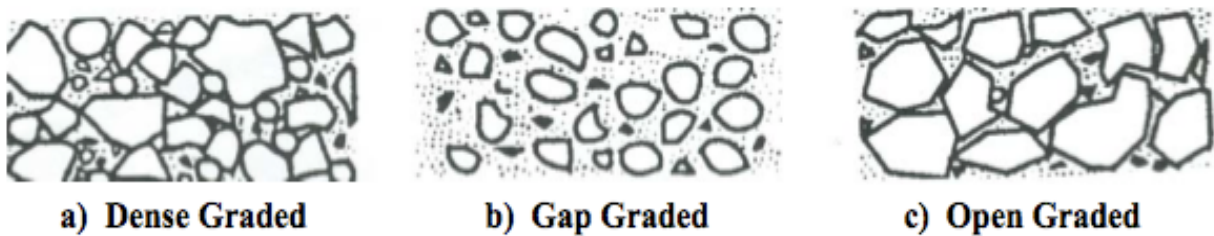


Figure 1.22. Stone matrices created by different gradings

#### ***1.5.2.6.1 Dense Graded Thin Overlays***

Dense graded mixtures have an aggregate structure that is continuously graded (sized) from the largest to the smallest aggregate in the system. Dense graded mixtures have relatively low air void contents and are designed as an abrasion resistant and functionally impermeable wearing course. Historically, dense graded mixtures have been the most commonly used mix type for overlaying asphalt or portland cement concrete pavements. Conventional dense graded thin overlays should only be placed on structurally sound pavements due to the fact that they offer little structural improvement, but can renew the surface in terms of functional performance (i.e., ride quality). They can be used to mitigate raveling, minor cracking, minor surface irregularities, skid problems, and pavement water proofing.

#### ***1.5.2.6.2 Open Graded Mixes***

Open Graded Asphalt Concrete (OGAC), also referred to as Open Graded Friction Course (OGFC), is a surface course with an aggregate gradation that provides an open void structure as compared with conventional dense graded asphalt concrete. Air void content typically ranges between 15 to 25% in OGAC resulting in a highly permeable mixture relative to DGAC (which normally is relatively impermeable). The principal benefit derived from OGAC mixtures is a significant reduction in splash and spray relative to DGAC mixtures and PCC pavements. Other benefits include a reduction in tire noise and an increase in the frictional characteristics relative to DGAC mixtures.

### **1.5.2.6.3 Gap Graded Mixtures**

Gap graded mixtures are, in general, solely Rubberized Asphalt Concrete (RAC) Type G which uses asphalt rubber binders. A gap graded mixture consists of an aggregate grading that has a missing fraction. The gap (missing fraction) is used to accommodate the asphalt rubber binder. This is intended to allow for stone on stone contact for deformation resistance and the extra binder has been found to aid in fatigue and reflection cracking resistance. The increase in voids allows the mix to accommodate the larger particulate rubber present in asphalt rubber binders and may be 7 to 9 % by weight with asphalt rubber binders. The purpose of gap grading is to provide improved stone-to-stone contact by reducing the fine aggregate content so as to provide a strong aggregate skeleton that creates space for more engineered binder than a dense graded mix can hold. Gap graded thin overlays should only be placed on structurally sound pavements because they offer no structural improvement, but they can renew the surface in terms of functional performance (e.g., ride quality).

## **1.5.3 Rehabilitation for flexible pavement**

The combined effects of traffic loading and the environment will cause pavements to deteriorate over time. Although maintenance can slow the rate of deterioration, it cannot stop it. Therefore, eventually the effects of deterioration need to be reversed by adding or replacing material in the existing pavement structure. This is called rehabilitation. Formally, rehabilitation can be defined as (Hall, Correa, & Carpenter, 2001)"...a structural or functional enhancement of a pavement which produces a substantial extension in service life, by substantially improving pavement condition and ride quality."

### **1.5.3.1 Structural HMA Overlays**

Structural overlays are used to increase pavement structural capacity. Therefore, they are considered rehabilitation, although they typically have some maintenance-type benefits as well. Asphalt concrete structural overlay design can be broadly categorized into the following:

- Engineering judgment
- Component analysis
- Non-destructive testing with limiting deflection criteria

- Mechanistic-empirical analysis

#### **1.5.3.1.1 Engineering Judgment**

This classification of overlay design is the most subjective of the four listed and can be heavily influenced by political and budgetary constraints. Selection of overlay thickness and the associated materials is often based on local knowledge of existing conditions, which can result in cost effective solutions; however, local expertise is fragile and subject to retirements, agency reorganizations, etc. Currently, more agencies appear to be relying on quantifiable overlay design approaches but tempered with local expertise.

#### **1.5.3.1.2 Component Analysis**

This approach to overlay design essentially requires that the total pavement structure be developed as a new design for the specified service conditions and then compared to the existing pavement structure (taking into account pavement condition, type, and thickness of the pavement layers). Current component design procedures require substantial judgment to effectively use them. This judgment is mainly associated with selection of "weighting factors" to use in evaluating the structural adequacy of the existing pavement layers (i.e., each layer of the pavement structure is assigned a layer coefficient often on the basis of experience).

#### **1.5.3.1.3 Non-destructive Testing with Limiting Deflection Criteria**

Pavement surface deflection measurements can be used to determine pavement structural properties, which can then be used to determine the required amount of additional pavement structure. Essentially, a pavement's surface deflection in response to a known loading is used as a measure of effective strength. This "effective strength" is influenced by a variety of factors including material properties (including subgrade), thickness of pavement layers, and environmental effects. Most currently used deflection based overlay design procedures do not attempt to isolate material properties of individual pavement layers.

#### **1.5.3.1.4 Mechanistic-Empirical Analysis**

Mechanistic-empirical based design methods are useful in overlay design as well as new pavement design. Their greatest advantage is the versatility provided in evaluating different materials under various environments and pavement conditions. Mechanistic-empirical procedures provide a basis for rationally modeling pavement systems. As these models improve, better correlations can be expected between design and performance parameters. In many places these procedures have replaced limiting deflection overlay methods, since the latter do not

account for subsurface material properties. Mechanistic-empirical overlay design is essentially the same as mechanistic-empirical structural design for new pavements but with the addition of more evaluation locations.

### **1.5.3.2 Structural PCC Overlays**

A PCC overlay of an existing flexible pavement, called "whitetopping", is a newer, viable rehabilitation alternative for flexible pavements. The overlaid rigid layer offers a reasonably thin, highly durable wearing course with a significant structural capacity. Although there are risks, whitetopping can be effective for almost all applications. They have been successfully used on interstate highways, state primary and secondary roads, intersections, etc. as well as major airport and general aviation runways, taxiways, and aprons. This subsection covers:

- Unbonded PCC overlays, often called "classical whitetopping"
- Bonded PCC overlays, often called "thin composite whitetopping"

#### ***1.5.3.2.1 Unbonded - Classical Whitetopping***

Classical whitetopping is an unbonded PCC overlay of an existing flexible pavement. Because there is no bond, the existing flexible pavement is assumed to function only as a base for the new PCC overlay. Most often, the PCC overlay is placed directly on the flexible pavement surface after sweeping to remove loose debris. Generally, classical whitetopping works well as long as rut and pothole depths in the existing flexible pavement are less than 50 mm. If rut or pothole depths are deeper, the potholes are filled or the surface is milled. All three types of rigid pavement (JPCP, JRCP and CRCP) have been successfully used as classical whitetopping. The chief advantage of classical whitetopping is that it requires minimal surface preparation. However, minimum overlay thicknesses tend to be in the 125-175 mm range, which is quite thick and possibly unsuitable in situations where a specific elevation must be maintained such as in curbed areas or under bridges. The design procedure contained in the 1993 AASHTO *Guide* is virtually identical to the AASHTO empirical design for new rigid pavements with one exception: the effective modulus of subgrade reaction ( $k$ ) is determined based on the existing flexible pavement resilient modulus. Although perfectly acceptable, this method gives little credit to the existing pavement's remaining strength.

#### **1.5.3.2.2 Bonded - Thin Composite Whitetopping**

Thin composite whitetopping is a PCC overlay intentionally bonded to an existing flexible pavement with a PCC slurry or grout in order to create a composite pavement section. This composite section, acting as a single layer, is thicker than just the PCC overlay and thus, results in substantially reduced maximum slab tensile stresses (on the order of 1/2 for edge stresses and 1/4 for corner stresses). Overlay thicknesses tend to be 50 - 175 mm thick but can be thicker for high volume roads; overlays in the 50 - 100 mm range are often referred to as "ultra-thin whitetopping" (UTW). Thin white topping (i.e., bonded PCC overlay greater than 100 mm thick) is considered appropriate for all situations and traffic levels. UTW as conceived and developed in the early 1990's is intended more for lower-volume roads, vehicular parking areas and light duty. The chief advantage of thin composite whitetopping is that it can be made thinner than classical whitetopping because of the composite layer action. However, issues with slab size, joint location and bonding effectiveness can complicate its use.

*Evolution of Pavement  
Design Procedure*



## 2.1 Introduction

Pavement structural design is a complex task. Although the basic geometry of a pavement system is quite simple, everything else is not. Traffic loading is a heterogeneous mix of vehicles, axle types, and axle loads with distributions that vary with time throughout the day, from season to season, and over the pavement design life. Pavement materials respond to these loads in complex ways influenced by stress state and magnitude, temperature, moisture, time, loading rate, and other factors. Exposure to severe environmental conditions ranging from subzero cold to burning heat and from dried to saturated moisture states adds further complications. It should be no wonder, then, that the profession has resorted to largely empirical methods like the American Association of State Highway and Transportation Officials (AASHTO) guides for pavement design (AASHTO, 1993).

Several developments over recent decades have offered an opportunity for more rational and rigorous pavement design procedures. Advances in computational mechanics and in the computers available for performing the calculations have greatly improved our ability to predict pavement response to load and climate effects. Improved material characterization and constitutive models make it possible to incorporate nonlinearities, rate effects, and other realistic features of material behavior. Large databases now exist for traffic characteristics, site climate conditions, pavement material properties, and historical performance of in-service pavement sections.

## 2.2 Review of Flexible Pavement Design Principles

Before the 1920s, pavement design consisted basically of defining thicknesses of materials that would provide strength and protection to a soft, weak subgrade. Pavements were designed against subgrade shear failure. Engineers used their experience based on successes and failures of previous projects. Since then, traffic volume has increased and the design criteria have changed. As important as providing subgrade support, it was equally important to evaluate pavement performance through ride quality and other surface distresses that increase the rate of deterioration of pavement structures. Performance became the focus point of pavement designs and methods based on laboratory test data or test track experiments were developed (empirical methods). Meanwhile, new materials started to be used in pavement structures that provided better subgrade protection, but with their own failure modes. New design criteria were required

to incorporate such failure mechanisms (e.g., fatigue cracking and permanent deformation in the case of asphalt concrete). The Asphalt Institute method (Asphalt Institute, 1982, 1991) and the Shell method (Claussen, 1977; Shook, 1982) are examples of procedures based on asphalt concrete's fatigue cracking and permanent deformation failure modes. These were the first to use linear-elastic theory of mechanics to compute structural responses (in this case strains) in combination with empirical models to predict number of loads to failure for flexible pavements. The dilemma is that pavement materials do not exhibit the simple behavior assumed in isotropic linear-elastic theory. Nonlinearities, time and temperature dependency, and anisotropy are some examples of complicated features often observed in pavement materials. In this case, advanced modeling is required to predict performance mechanistically. The mechanistic design approach is based on the theories of mechanics and relates pavement structural behavior and performance to traffic loading and environmental influences. Progress has been made in recent years on isolated pieces of the mechanistic performance prediction problem, but the reality is that mechanistic methods are not yet available for practical pavement design. The mechanistic-empirical approach is a hybrid approach. Empirical models are used to fill in the gaps that exist between the theory of mechanics and the performance of pavement structures. Simple mechanistic responses are easy to compute with assumptions and simplifications (i.e., homogeneous material, small strain analysis, static loading as typically assumed in linear elastic theory), but they by themselves cannot be used to predict performance directly; some type of empirical model is required to make the appropriate correlation. Mechanistic-empirical methods are considered an intermediate step between empirical and fully mechanistic methods (NCHRP 1-37A, 2004).

### **2.2.1 Empirical Methods**

An empirical design approach is one that is based solely on the results of experiments or experience. Observations are used to establish correlations between the inputs and the outcomes of a process. Empirical approaches are often used as an expedient when it is too difficult to define theoretically the precise cause and effect relationships of a phenomenon. The first empirical methods for flexible pavement design date around 1920s when the first soil classifications were developed with the Public Roads (PR) soil classification system (Hogentogler & Terzaghi, 1929). In 1929, the California Highway Department developed a method using the California Bearing Ratio (CBR) strength test (Huang, 2004). The CBR method related the material's CBR value to the required thickness to provide protection against subgrade shear failure. The thickness computed was defined for the standard crushed stone used in the definition of the CBR test. Several methods based on subgrade shear failure criteria were developed after the CBR

method. Barber (1946) used Terzaghi's bearing capacity formula to compute pavement thickness, while McLeod (1953) applied logarithmic spirals to determine bearing capacity of pavements. However, with increasing traffic volume and vehicle speed, new materials were introduced in the pavement structure to improve performance and smoothness. Consequently the shear failure was no longer the main design criterion. The first attempt to consider a structural response as a quantitative measure of pavement structural capacity was measuring surface vertical deflection. A few methods were developed based on the theory of elasticity for soil mass. These methods estimated layer thickness based on a limit surface vertical deflection. The first one published was developed by the Kansas State Highway Commission, in 1947, in which Boussinesq's equation was used and the deflection of subgrade was limited to 2.54 mm. Later in 1953, the U.S Navy applied Burmister's two-layer elastic theory and limited the surface deflection to 6.35 mm. The deflection methods were most appealing to practitioners because deflection is easy to measure in the field. However, failures in pavements are caused by excessive stress and strain rather than deflection. After 1950, experimental tracks started to be used for gathering pavement performance data. Regression models were developed linking the performance data to design inputs. The empirical AASHTO method (AASHTO, 1993), based on the AASHTO Road Test from the late 1950s, is the most widely used pavement design method today. The AASHTO design equation is a regression relationship between the number of load cycles, pavement structural capacity, and performance, measured in terms of serviceability. The concept of serviceability was introduced in the AASHTO method as an indirect measure of the pavement's ride quality. The serviceability index is based on surface distresses commonly found in pavements. The biggest disadvantage of regression methods is the limitation on their application. As is the case for any empirical method, regression methods can be applied only to the conditions similar to those for which they were developed.

### **2.2.2 Mechanistic-Empirical Methods**

Mechanistic-empirical (M-E) methods represent one step forward from empirical methods. The induced state of stress and strain in a pavement structure due to traffic loading and environmental conditions is predicted using theory of mechanism. Empirical models link these structural responses to distress predictions. Kerkhoven & Dormon (1953) first suggested the use of vertical compressive strain on the top of subgrade as a failure criterion to reduce permanent deformation. Saal & Pell (1960) published the use of horizontal tensile strain at the bottom of asphalt layer to minimize fatigue cracking. Dormon & Metcalf (1965) first used these concepts for pavement design. The Shell method (Claussen, 1977) and the Asphalt Institute method (Shook, 1982; AI,

1992) incorporated strain-based criteria in their mechanistic-empirical procedures. Several studies over the past fifteen years have advanced mechanistic-empirical techniques. Most of work, however, was based on variants of the same two strain-based criteria developed by Shell and the Asphalt Institute such as the M-E procedures of WSDOT and NCDOT. The National Cooperative Highway Research Program (NCHRP) 1-26 project report, Calibrated Mechanistic Structural Analysis Procedures for Pavements (1990), provided the basic framework for most of the efforts attempted by state DOTs. WSDOT and NCDOT developed similar M-E frameworks incorporating environmental variables (e.g., asphalt concrete temperature to determine stiffness) and cumulative damage model using Miner’s Law with the fatigue cracking criterion. MNDOT adopted a variant of the Shell’s fatigue cracking model developed in Illinois (Thompson, 1985) and the Asphalt Institute’s rutting model.

The availability of computer based packages for mechanistic analysis provided a powerful tool for pavement engineers. A summary listing of some of the more well known programs is shown in Table 2.1. It can be seen that multi-layer elastic (MLE) is the most widely adopted theoretical basis. Because of the assumptions involved, including homogeneous isotropic and linear elastic material properties, no shear stresses at the surface and uniformly distributed load, strictly speaking, elastic layer theory is not a good model of a pavement structure yet the basic conclusion is that elastic layer theory is a useful model for the analysis of pavements provided the input data is properly formatted and the output is properly interpreted. Finite element and viscoelastic layer theory have seen more limited use, possibly because of the difficulty in obtaining the required materials input and the complexity involved.

**Table 2.1. Summary of Some Computer-Based Analytical Solutions for Asphalt Concrete Pavements**

Program	Theoretical Basis	No. Layers (max)	No. of Loads (max)	Program Source
CHEV5L	MLE	5	1	Chevron Research
BISAR	MLE	5	10	Shell International
ELSYM MLE	MLE	5	10	FHWA
PDMAP (PSAD)	MLE	5	2	NCHRP Project 1-10
JULEA	MLE	5	4+	USACE WES
CIRCLY	MLE	5+	100	MINCAD, Australia
VESYS	MLE o MLVE	5	2	FHWA
VEROAD	MLVE	15 (resulting in half space)		Delf Technical University
ILLIPAVE	FE		1	University of Illinois
FENLAB	FE		1	University of Nottingham
SAPSI-M	Layered, damped elastic medium	N layers resting on elastic half-space or rigid base	Multiple	Michigan State University/UNiversity of California Berkeley

MLE – multilayer elastic

MLVE – multilayer viscoelastic

FE – finite element

### **2.2.2.1 Basic Inputs and Outcomes of a M-E Design Analysis**

Any pavement design procedure should incorporate a range of relevant factors or variables as inputs, and be able to predict outcomes in terms of serviceability- age history (e.g. International Roughness Index vs. age and/or accumulated traffic loads) as a minimum. In addition, it is desirable to have the capability of predicting the following measures of deterioration or damage, also as a function of age and/or accumulated traffic loads:

- Fatigue cracking
- Permanent deformation or rutting
- Thermally associated cracking

Basic inputs can be divided in: environment, structure, construction, traffic and maintenance.

Concerning environment factors is necessary to consider moisture, radiation, temperature (min., max., days, etc.), freeze-thaw cycles. For structure factors, layer thicknesses, layer types and properties, subgrade type and properties and possible variations in thickness and properties should be analyzed. For maintenance factors instead treatments type, timing, quality and methods should be considered. Furthermore construction factors are timing, methods, variance and as-built quality. Finally, for the traffic factors it is necessary to consider axle group, loads, tyre types and pressure, axle spacing, speed and repetitions.

The mechanistic part of the analysis of course only calculates a primary response(s), such as stress, strain and deformation at critical points in the pavement structure. Thus, a complete design analysis must relate primary response(s) to performance (e.g. IRI vs. age) and accumulated deterioration. In turn, this means an M-E design analysis must be calibrated to observed or measured field performance and this represents a major challenge.

There are many mechanistic-empirical (analytically-based) design procedures which have been developed. Some, while not used, have served as the basis for other procedures. Several such procedures are briefly summarized in Table 2.2. Figure 2.1 illustrates a simplified framework which the procedures generally follow. All the procedures idealize the pavement structure as a multilayer elastic or viscoelastic system using programs like those described in Table 2.2. While the procedures listed in Table 2.2 all received impetus from the 1962 Conference, the U.S. Navy was using a pavement design procedure in the 1950's for airfield pavements which incorporated results of Burmister's solution for a two-layer elastic solid. A plate bearing test was used to measure the subgrade modulus and the thickness required was based on the requirement that the

computed surface deflection not exceed 5 mm for the specific aircraft. The procedures listed in Table 2.2 all consider the fatigue and rutting modes of distress in establishing pavement structures.

The linear sum of cycle ratios cumulative damage hypothesis is used in the majority of the methods to assess the effects of mixed traffic and environmental influences on fatigue cracking. Those procedures using a subgrade strain procedure incorporate a form of the linear sum of cycle ratios (based on compressive strain) for the same purpose. A few of the methods make use of the time-hardening procedure to estimate the cumulative effects of traffic and environment on rutting in the asphalt concrete (e.g., the Shell International and the proposed AASHTO Guide methods).

Table 2.2 Examples of Analytically Based Design Procedures

Organization	Pavement Representation	Distress Modes	Environmental Effects	Pavement Materials	Design Format
Shell International Petroleum Co., Ltd., London, England (36, 90, 92, 93)	Multilayer elastic solid	fatigue in treated layers; rutting: · subgrade strain · estimate in asphalt bound layer	temperature	asphalt concrete, untreated aggregate, cement stabilized aggregate	design charts; the computer program BISAR is used for analysis
National Cooperative Highway Research Program (NCHRP) Project 1-10B Procedure (AASHTO) (20)	Multilayer elastic solid	fatigue in treated layers; rutting	temperature	Asphalt concrete, asphalt stabilized bases, untreated aggregates	Design charts; computer program (MTC093)
The Asphalt Institute, Lexington, KY (MS-1, MS-11, MS-23) (39, 94, 95)	Multilayer elastic solid	Fatigue in asphalt treated layers; Rutting: · subgrade strain	Temperature, freezing and thawing	Asphalt concrete, asphalt emulsion, treated bases, untreated aggregate	Design charts; computer program DAMA
Laboratoire Central de Ponts et Chaussées (LCPC) (96, 97)	Multilayer elastic solid	Fatigue in treated layers; rutting	Temperature	Asphalt concrete, asphalt-treated bases, cement stabilized aggregates, untreated aggregates	Catalogue of designs; computer program (ELIZE) for analysis
Centre de Recherches Routières, Belgium (98)	Multilayer elastic solid	Fatigue in treated layers; rutting	Temperature	Asphalt concrete, asphalt-stabilized bases, untreated aggregates	Design charts; computer program (MTC093)
National Institute for Transportation and Road Research (NITRR) South Africa (99, 100, 101)	Multilayer elastic solid	Fatigue in treated layers; rutting: · subgrade strain · shear in granular layers	Temperature	Gap-graded asphalt mix, asphalt concrete, cement-stabilized aggregate, untreated aggregate	Catalogue of designs; computer program
National Cooperative Highway Research Program (NCHRP) Project 1-26 Procedure (AASHTO) (102)	Finite element idealization; multilayer elastic solid	Fatigue in treated layers; rutting: · subgrade strain	Temperature	Asphalt concrete, untreated aggregates	ILLI-PAVE; elastic layer programs (e.g., ELSYM)
Federal Highway Administration U.S. DOT, Washington, D.C. (103)	Multilayer elastic or viscoelastic solid	Fatigue in treated layers; Rutting: · estimate at surface Serviceability (as measured by PSI)	Temperature	Asphalt concrete, cement stabilized aggregate, untreated aggregate, sulphur-treated materials	Computer program: VESYS
University of Nottingham, Great Britain (104, 105)	Multilayer elastic solid	Fatigue in treated layers; rutting: · subgrade strain	Temperature	Continuous or gap-graded asphalt mixes of known volumetrics on standard UK materials	Design charts; computer program (ANPAD) for analysis and design
Austrroads (106)	Multilayer elastic solid	Fatigue in treated layers; rutting: · subgrade strain	Temperature, moisture	Asphalt concrete, untreated aggregates, cement stabilized aggregates	Design charts, computer program CIRCLY
National Cooperative Highway Research Program (NCHRP) Project 1-37A (Proposed AASHTO Guide) (30)	Multilayer elastic	Fatigue in treated layers; rutting: · subgrade strain · asphalt concrete, time hardening Low temperature cracking	Temperature, Moisture	Asphalt concrete, untreated aggregates, chemical stabilized materials	Computer program JULEA

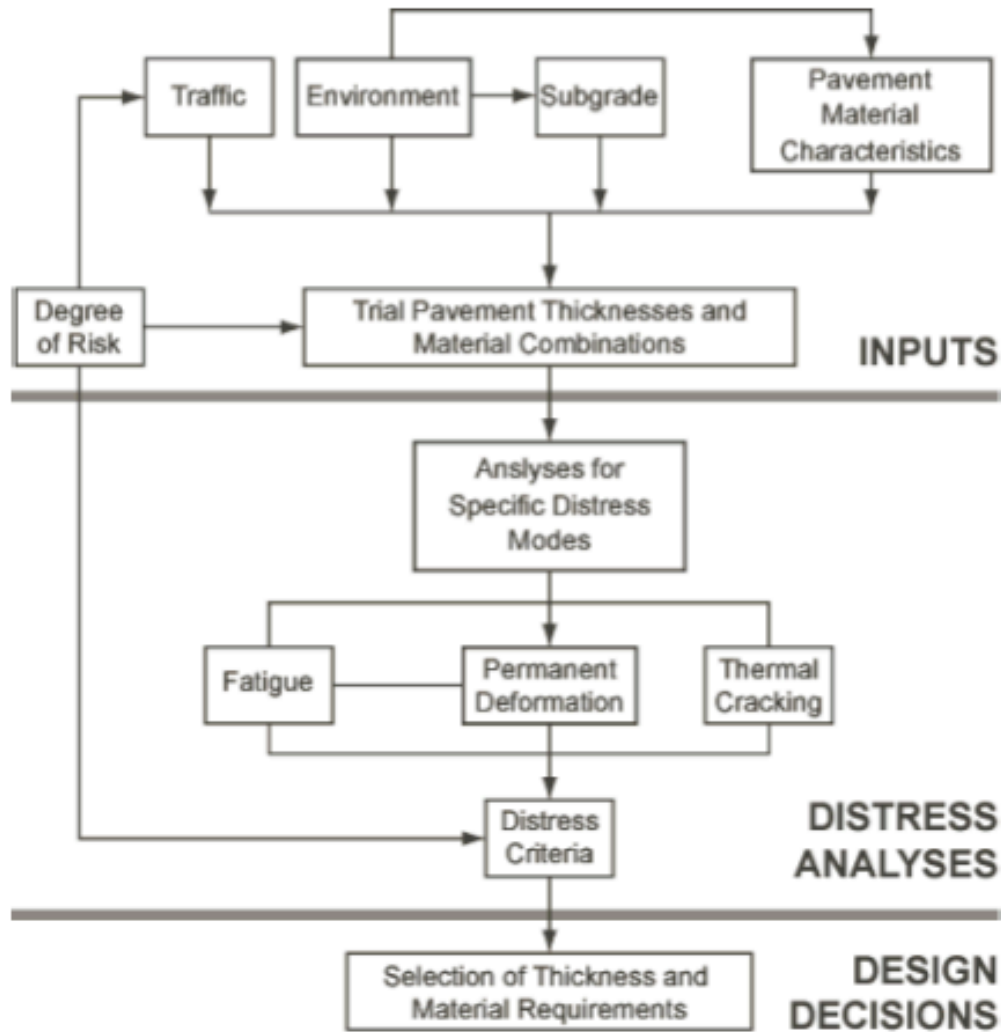


Figure 2.1. Simplified design/analysis framework

## 2.3 Pavement Design Procedure

The current 1993 AASHTO Guide and the new M-EPDG for flexible pavements are described in this chapter. The 1993 AASHTO is the latest version of AASHTO Guide for pavement design and analysis and is a largely empirical method based primarily on the AASHO Road Test conducted in the late 1950s. Over the years adjustments and modifications have been made in an effort to upgrade and expand the limits over which the AASHTO guide is valid (HRB, 1962; AASHTO, 1972, 1986, 1993).

A 1996 workshop meant to develop a framework for improving the 1993 Guide recommended instead the development of a new guide based as much as possible on mechanistic principles. The M-E PDG developed in NHCRP 1-37A is the result of this effort. Following independent reviews and validations that have been ongoing since its initial release in April, 2004, the M-E PDG is expected to be adopted by AASHTO as the new national pavement design guide. This

chapter is divided in two sections. The first describes the AASHTO Guide and its revisions since its first edition dated 1961, with the original empirical equations derived from the AASHO Road Test, to its latest dated 19931 (HRB, 1961, 1962; AASHTO, 1972, 1986, 1993). second part explains in some detail the new M-E PDG procedure (NCHRP, 2004).

### **2.3.1 The 1993 AASHTO Guide**

The 1993 AASHTO Guide is the latest version of the AASHTO Interim Pavement Design Guide, originally released in 1961. The evolution of the AASHTO Guide is outlined, followed by a description of the current design equation and input variables.

#### ***2.3.1.1 AASHO Road Test and Early Versions of the Guide***

After two successful road projects, the Road Test One-MD and the WASHO Road Test (Western Association of State Highway Officials), in 1955 the Highway Research Board (HRB) approved the construction of a new test track project located in Ottawa, Illinois. The main objective of the AASHO Road Test was to determine the relation between the number of repetitions of specified axle loads (different magnitudes and arrangements) and the performance of different flexible and rigid pavement structures.

##### *The Concept of Serviceability and Structural Number*

The performance of various pavements is a function of their relative ability to serve traffic over a period of time. The concept of serviceability is supported by five fundamental assumptions: (1) highways are for the comfort of the traveling user; (2) the user's opinion as to how a highway should perform is highly subjective; (3) there are characteristics that can be measured and related to user's perception of performance; (4) performance may be expressed by the mean opinion of all users; and (5) performance is assumed to be a reflection of serviceability with increasing load applications.

Based on these assumptions the definition of present serviceability is: —The ability of a specific section of pavement to serve high speed, high volume, and mixed traffic in its existing condition. (HRB, 1962) The Present Serviceability Ratio (PSR) is the average of all users' ratings of a specific pavement section on a scale from 5 to 0 (being 5 very good and 0 very poor). The mathematical correlation of pavement distresses observed during visual surveys and profile measurements (roughness) with PSR is termed the Present Serviceability Index (PSI); PSI is the measure of performance in the AASHTO design equation. The correlation between PSI and

typical flexible pavement distresses observed during the AASHO Road Test is represented by the following equation (HRB, 1962):

$$PSI = 5.03 - 1.91 \times \log(1 + SV) - 1.38 RD^2 - 0.01 \sqrt{C + P}$$

**Equation 2.1**

in which:

SV = mean of slope variance in the wheel paths

RD = mean rut depth (inch)

C = cracking (ft<sup>2</sup>/1000 ft<sup>2</sup>)

P = patching (ft<sup>2</sup>/1000 ft<sup>2</sup>)

### *1961 Interim Guide*

The first results from data collected at the AASHO Road Test were released in the form of Highway Research Board reports (HRB, 1961, 1962). The original design equation was empirically developed for the specific subgrade type, pavement materials and environmental conditions at the location of the AASHO Road Test as follows:

$$\log(W_{18}) = 9.36 \times \log(SN + 1) - 0.20 + \frac{\log(4.2 - p_t)/(4.2 - 1.5)}{0.4 + 1094/(SN + 1)^{5.19}}$$

**Equation 2.2**

in which:

W<sub>18</sub> = accumulated 18 kip equivalent single axle load for the design period

p<sub>t</sub> = terminal serviceability at the end of design life

SN = structural number

The structural number (SN) is the parameter that represents the pavement structural strength. It is given as the sum of the product of each layer thickness by its structural layer coefficient, which is an empirical coefficient representing each layer's relative contribution to the pavement strength:

$$SN = a_1 D_1 + a_2 D_2 + a_3 D_3$$

**Equation 2.3**

in which:

a<sub>1</sub>, a<sub>2</sub>, a<sub>3</sub> = structural layer coefficients for surface, base, and subbase

D<sub>1</sub>, D<sub>2</sub>, D<sub>3</sub> = thicknesses for surface, base, and subbase

Equation 2 is solved for the structural number for a given traffic and terminal serviceability criterion. The layer thicknesses are determined from Equation 3. Note that there is not a unique solution for the layer thicknesses.

### 1972 Interim Guide

The 1972 Interim Design Guide was the first attempt to extend the empirical relationships developed at the AASHO Road Test to a broader range of materials and environmental conditions. This version also included the first step towards an overlay design procedure. Some of the added features for flexible pavement designs are described below.

An empirical soil support ( $S_i$ ) scale was developed to reflect the influence of different local subgrade soils in Equation 2. The scale ranged from 1 to 10, with 10 corresponding to crushed stone materials and 1 to highly plastic clays. The A-6 subgrade soil at the AASHO Road Test was defined as  $S_i$  value of 3. All other values were to be set by local agency experience, but there were no guidelines on how to determine these values.

There was also a new regional factor  $R$  for adjusting the structural number for local environment, estimated from serviceability loss rates in the AASHO Road Test. These values varied between 0.2 and 5.0, with an annual average of about 1.0. Table 2.3 summarizes the recommended values for  $R$ .

**Table 2.3. Recommended values for Regional Factor  $R$  (AASHTO, 1972)**

Roadbed material condition	$R$
Frozen to depth of 5'' or more (winter)	0.2 - 1.0
Dry (summer and fall)	0.3 - 1.5
Wet (spring thaw)	4.0 - 5.0

The 1972 Interim Guide also specified ranges for structural layer coefficients applicable to materials other than those used during the AASHO Road Test. The values were based on a survey of state highway agencies that were using the 1961 Interim Guide. Table 2.4 summarizes these values for different layer applications.

**Table 2.4 ranges of structural layer coefficients (AASHTO,1972).**

Coefficient	Range
a <sub>1</sub> (surface course)	0.17 – 0.45
a <sub>2</sub> (untreated base)	0.05 – 0.18
a <sub>2</sub> (subbase)	0.05 - 0.14

Equation (2.2) was modified to account for the new input terms:

$$\log(W_{18}) = 9.36 \times \log(SN + 1) - 0.20 + \frac{\log(4.2 - p_t)/(4.2 - 1.5)}{0.4 + 1094/(SN + 1)^{5.19}} + \log \frac{1}{R} + 0.372(S_i - 3)$$

**Equation 2.4**

in which:

R = regional factor

S<sub>i</sub> = soil support value

and other terms are as previously defined

### *1986 and 1993 Guides*

The 1986 revision of the 1972 Interim Guide added more features to the design procedure. The focus was on four important issues: (1) better characterization of the subgrade and unbound materials, (2) incorporation of pavement drainage, (3) better consideration of environmental effects, and (4) incorporation of reliability as a factor into the design equation.

In the 1986 version of the AASHTO Guide, the subgrade was for the first time characterized by its resilient modulus MR, a fundamental engineering material property. The structural layer coefficients for unbound materials were also related quantitatively to resilient modulus by empirical equations.

Drainage quality was incorporated in the design process by introducing empirical drainage coefficients into the structural number equation.

$$SN = a_1 D_1 + a_2 D_2 m_2 + a_3 D_3 m_3$$

**Equation 2.5**

in which m<sub>2</sub>, m<sub>3</sub> are drainage coefficients for base and subbase and the other terms are as previously defined.

Recommended values for the drainage coefficients are defined based on the quality of drainage and period of exposure to moisture levels near saturation.

Environmental effects were also considered in two additional distinct ways: (1) separation of total serviceability losses into traffic and environmental components, and (2) estimation of an effective subgrade resilient modulus that reflects seasonal variations due primarily to moisture susceptibility. The loss in serviceability  $\Delta PSI$  was decomposed into three components:

$$\Delta PSI = \Delta PSI_{TR} + \Delta PSI_{SW} + \Delta PSI_{FH}$$

Equation 2.6

in which  $\Delta PSI_{TR}$ ,  $\Delta PSI_{SW}$ ,  $\Delta PSI_{FH}$  are the losses of PSI attributed to traffic, swelling and frost heave, respectively.

Appendix G in the 1986 AASHTO Guide describes in more detail the methods for evaluating these environmental losses, which depend on the swell/frost heave rate, probability of swell frost heave, and maximum potential serviceability loss.

Reliability was introduced into the 1986 AASHTO Guide to account for the effects of uncertainty and variability in the design inputs. Although it represents the uncertainty of all inputs, it is very simply incorporated in the design equation through factors that modify the allowable design traffic ( $W_{18}$ ).

There were few changes to the flexible pavement design procedure between the 1986 version and the current 1993 version. Most of the enhancements were geared towards rehabilitation, the of nondestructive testing for evaluation of existing pavements, and backcalculation of layer moduli for determination of the layer coefficients. The design equation did not change from the 1986 to 1993 version. The complete description of the 1993 AASHTO Guide is presented in the following subsections.

### 2.3.1.2 Current design equation

The 1993 AASHTO Guide specifies the following empirical design equation for flexible pavements:

$$\log(W_{18}) = Z_R \times S_0 + 9.36 \times \log(SN + 1) - 0.20 + \frac{\log(\Delta PSI)/(4.2 - 1.5)}{0.4 + 1094/(SN + 1)^{5.19}} + 2.32 \times \log(MR) - 8.07$$

Equation 2.7

in which:

$W_{18}$  = accumulated 18 kip equivalent single axle load for the design period

$Z_R$  = reliability factor

$S_0$  = standard deviation

SN = structural number

$\Delta$ PSI = initial PSI – terminal PSI

MR = subgrade resilient modulus (psi)

The solution of Equation 2.7 follows the same procedure described before for the previous versions of the Guide. Given all the inputs, Equation 2.7 is solved for the structural number (SN) and then the layer thicknesses can be computed. The solution is not unique and different combination of thicknesses can be found. Additional design constraints, such as costs and constructability, must also be considered to determine the optimal final design. The 1993 Guide recommends the top-to-bottom procedure in which each of the upper layers is designed to provide adequate protection to the underlying layers. Figure # illustrates the procedure for a 3-layer flexible pavement. The steps in this case are as follows:

- Calculate  $SN_1$  required to protect the base, using  $E_2$  as MR in Equation 2.7, and compute the thickness of layer 1 as:

$$D_1 \geq \frac{SN_1}{a_1}$$

- Calculate  $SN_2$  required to protect the subgrade, using Equation 2.7, now with the subgrade effective resilient modulus as MR. The thickness of the base is computed as:

$$D_2 \geq \frac{SN_2 - a_1 D_1}{a_2 m_2}$$

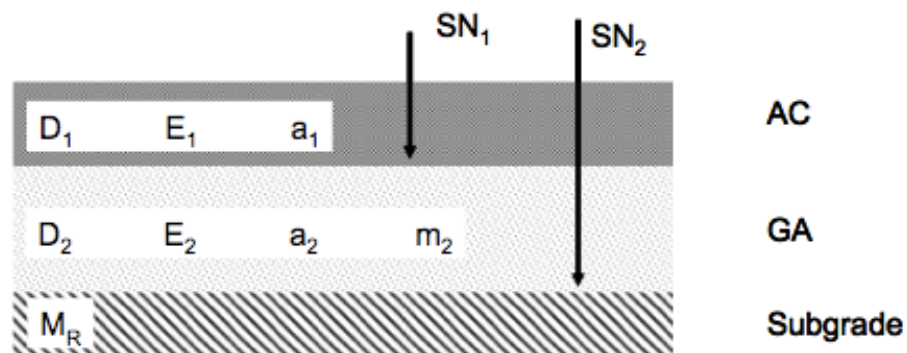


Figure 2.2. General procedure for computing thickness

### **2.3.1.3 Input variables**

The input variables required for the 1993 AASHTO guide are summarized in this section and the most important recommendations are described. Additional guidance can be found in the AASHTO Guide itself (AASHTO, 1993) and in standard textbooks (Huang, 2004).

Design period and serviceability loss are the initial inputs to be defined. Serviceability loss is defined as the difference between initial and terminal serviceability. Initial serviceability is the condition immediately after pavement construction. The conventional value is 4.2 (the average initial serviceability value at the AASHO Road Test). Terminal serviceability is the value at which the pavement is no longer capable of providing adequate service and major rehabilitation is required. Most state agencies have their own specification, although the 1993 AASHTO Guide recommends a terminal PSI of 2.5 for major highways and 2.0 for low volume roads, unless otherwise specified.

The other input variables are separated into three groups: (a) traffic, (b) material properties, and (c) environmental effects

#### *Traffic*

Vehicle and load distributions grouped by axle type are used to transform mixed traffic into a unified traffic parameter that can be used in the design equation. The mixed traffic is converted into one parameter called the Equivalent Single Axle Load (ESAL). ESALs are defined as the number of 18-kip single axles that causes the same pavement damage as caused by the actual mixed axle load and axle configuration traffic. The damage associated with the equivalent axle can be defined in numerous ways; in the 1993 AASHTO Guide it is defined in terms of serviceability. The 18-kip single axle load was chosen because it was the maximum legal load permitted in many states at the time of the AASHO Road Test (Zhang, 2000).

The first step in calculating ESALs for mixed traffic is to establish first the load equivalent factor (LEF) of every axle of the traffic distribution. In the 1993 AASHTO Guide, LEFs were developed based on empirical data obtained from the AASHO Road Test. The AASHTO LEFs consider the following variables:

- Axle load
- Axle configuration (e.g., single, tandem, etc.)
- Structural number (for flexible pavements)
- Terminal serviceability

The computation of LEFs for flexible pavements is based on the following equations (Huang, 2004):

$$LEF = \frac{W_{t18}}{W_{tx}}$$

Equation 2.8a

$$\log \frac{W_{tx}}{W_{t18}} = 4.79 \log(18 + 1) - 4.79 \log(L_x - L_2) + 4.33 \log L_2 + \frac{G_t}{\beta_{tx}} - \frac{G_t}{\beta_{18}}$$

Equation 2.8b

$$G_t = \log \left( \frac{4.2 - p_t}{4.2 - 1.5} \right)$$

Equation 2.8cc

$$\beta_x = 0.40 + \frac{0.081(L_x + L_2)^{3.23}}{(SN + 1)^{5.19} L_2^{3.23}}$$

Equation 2.8d

in which:

$W_{tx}$  = number of x-axle load applications applied over the design period

$W_{t18}$  = number of equivalent 18-kip (80 kN) single axle loads over the design period

$L_x$  = load on one single axle, or a set of tandem or tridem, in kip

$L_2$  = axle code (1 for single axle, 2 for tandem, and 3 for tridem)

SN = structural number of the designed pavement

$p_t$  = terminal serviceability

$\beta_{18} = \beta_x$  for  $L_x = 18$  kip and  $L_2 = 1$

With LEF calculated for every load group, the second step is to compute the truck factor Tf as follows:

$$T_f = \sum_i (p_i \times LEF_i) \times A$$

Equation 2.9

in which:

$p_i$  = percentage of repetitions for ith load group

$LEF_i$  = LEF for the ith load group (e.g., single-12kip, tandem-22kip, etc.)

A = average number of axles per truck

The number of ESALs is calculated as follows:

$$ESAL = AADT \times T \times T_f \times G \times D \times L \times 365 \times Y$$

Equation 2.10

in which:

AADT = annual average daily traffic

T = percentage of trucks

G = growth factor

D = trucks in design direction (%)

L = trucks in design lane (%)

Y = design period

### Material Properties

The fundamental material property in the 1993 AASHTO Guide is the resilient modulus. Since the framework was constructed based upon structural layer coefficients, empirical relationships were developed to correlate resilient modulus with structural layer coefficient. Figure 2.3 summarizes the relationship for the layer coefficient  $a_1$  for asphalt concrete.

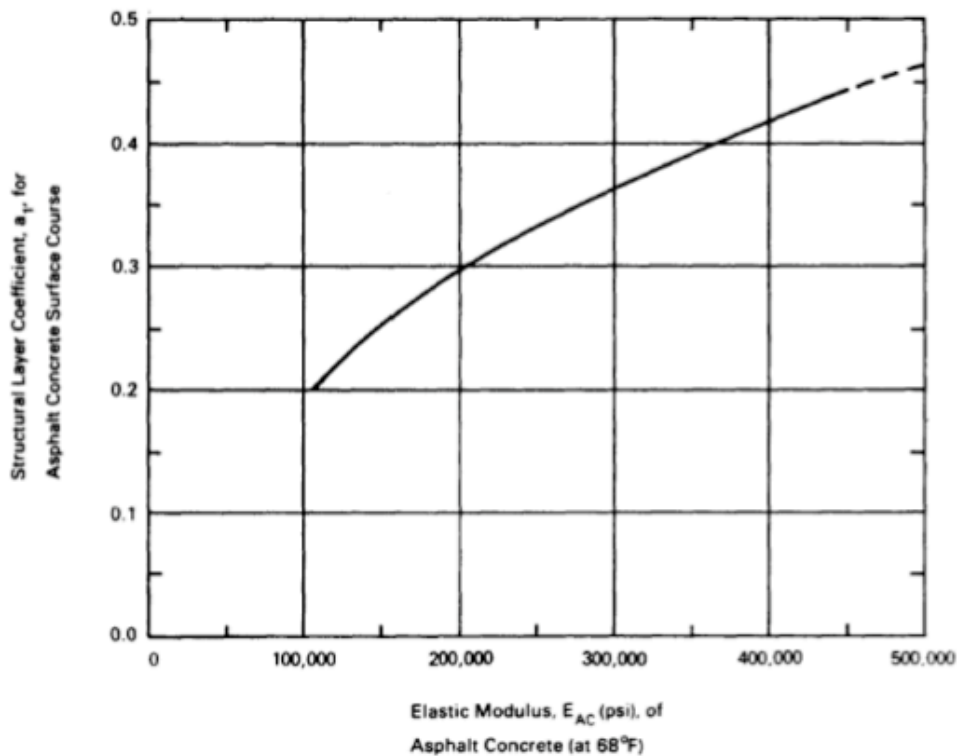


Figure 2.3. Chart for estimating layer coefficient for asphalt concrete based on elastic modulus (AASHTO, 1993)

The layer coefficient  $a_2$  for nonstabilized base materials is given by:

$$a_2 = 0.249 \log E_2 - 0.977$$

**Equation 2.11**

And the layer coefficient  $a_3$  for nonstabilized subbase materials is given by:

$$a_3 = 0.227 \log E_3 - 0.839$$

**Equation 2.12**

in which:

$E_2$  = resilient modulus of unbound base layer materials

$E_3$  = resilient modulus of unbound subbase layer materials

The layer coefficients in the AASHO Road Test were assumed equal to 0.44 for asphalt concrete, which corresponds to a  $M_R = 450,000$  psi; 0.14 for the granular base, corresponding to  $M_R = 30,000$  psi; and 0.11 for the subbase, equivalent to  $M_R = 15,000$  psi.

The subgrade is characterized solely by its resilient modulus in Equation 7. There are also several correlations between  $M_R$  and other soil properties that can be found in the literature. Most of them relate  $M_R$  to CBR or R-Value (Asphalt Institute, 1982; Huang, 1993; NCHRP, 2004).

*Environmental Effects*

Environmental effects (other than swelling and frost heave) are accounted for in two input parameters in the 1993 AASHTO Guide, the seasonally-adjusted subgrade resilient modulus and the drainage coefficient  $m_i$  applied to the structural number in Equation 2.5.

It is recommended that an effective subgrade resilient modulus be used to represent the effect of seasonal variations, especially for moisture-sensitive fine-grained soils or for locations with significant freeze-thaw cycles (AASHTO, 1993). The effective resilient modulus is the equivalent modulus that would result in the same damage to the pavement as if seasonal modulus were used.

The relative damage  $u$  is describe by the following empirical relationship:

$$u_r = 1.18 \times 10^8 M_R^{-2.32}$$

**Equation 2.13**

The average relative damage ( $u_f$ ) is computed by taking the average of  $u_r$  of all seasons. The effective subgrade resilient modulus is then given by:

$$M_R = 3015 \times u_f^{-0.431}$$

**Equation 2.14**

The drainage coefficient is related to the material's permeability and the amount of time that the material is expected to be at near saturation conditions. Table 2.5 shows recommended drainage coefficients for unbound materials. However, in practice it is difficult to assess the quality of

drainage or the percentage of time the material is exposed to near saturation conditions, and most agencies use drainage coefficient values of 1.0, relying mostly on the effective subgrade resilient modulus as the climatic-sensitive input parameter.

**Table 2.5. Recommended drainage coefficients for unbound bases and subbases in flexible pavements (Huang,1993)**

Quality of drainage		Percentage of time pavement structure exposed to moisture levels approaching saturation			
Rating	Water removed within	Less than 1%	1-5%	5-25%	Greater than 25%
Excellent	2 hours	1.40-1.35	1.35-1.30	1.30-1.20	1.20
Good	1 day	1.35-1.25	1.25-1.15	1.15-1.00	1.00
Fair	1 week	1.25-1.15	1.15-1.05	1.00-0.80	0.80
Poor	1 month	1.15-1.05	1.05-0.80	0.80-0.60	0.60
Very poor	Never drain	1.05-0.95	0.95-0.75	0.75-0.40	0.40

### 2.3.1.4 Reliability

There are many sources for uncertainties in pavement design problems – e.g., traffic prediction, material characterization and behavior modeling, environmental conditions, etc. – as well as variability during construction and maintenance. The uncertainty comes not only from data collection, but also from the lack of input parameters required to better characterize traffic, materials and environmental conditions. The reliability factor was introduced in the design equation to account for these uncertainties. Reliability is defined as the probability that the design pavement will achieve its design life with serviceability higher than or equal to the specified terminal serviceability. Although the reliability factor is applied directly to traffic in the design equation, it does not imply that traffic is the only source of uncertainty.

Table 2.6 suggests appropriate levels of reliability for various highway classes. There is some guidance on how reliability is considered. High volume and high speed highways have higher reliability factors than minor roads and local routes. The standard deviation ( $S_0$ ) and reliability factor ( $Z_R$ ) parameters in the design equation are respectively defined as the standard deviation of uncertainties and the area under a normal distribution curve for  $p < \text{reliability}$ . The parameter  $Z_R$  can be retrieved from Table 2.7 The 1993 AASHTO Guide recommends values for  $S_0$  between 0.35 and 0.45 for flexible pavements.

**Table 2.6. Suggested levels of reliability for various highway classes (AASHTO, 1993)**

Functional classification	Recommended level of reliability	
	Urban	Rural
Interstate and freeways	85-99.9	80-99.9
Principal arterials	80-99	75-95
Collectors	80-95	75-95
Locals	50-80	50-80

**Table 2.7.  $Z_R$  values for various levels of reliability (Huang, 1993)**

Reliability	$Z_R$	Reliability	$Z_R$
50	0.000	93	-1.476
60	-0.253	94	-1.555
70	-0.524	95	-1.645
75	-0.674	96	-1.751
80	-0.841	97	-1.881
85	-1.037	98	-2.054
90	-1.282	99	-2.327
91	-1.340	99.9	-3.090
92	-1.405	99.99	-3.750

### **2.3.1.5 Additional Considerations**

Several researchers have studied the AASHTO Guide in all its versions. This section summarizes the relevant findings gathered from the literature that discuss conflicting issues such as traffic, material properties, environmental conditions, and parametric sensitivity of the design equation. Serviceability cannot be directly measured in the field. A panel of users is required to provide subjective assessments of serviceability. This value is the Present Serviceability Ratio (PSR). The correlation of PSR with measured distresses is the Present Serviceability Index (PSI). PSI is the input parameter of the design equation, not the PSR, because determining PSR is very subjective, not to mention expensive and time consuming. Alternative approaches are available correlating PSI with roughness, which is a more reliable, and more easily measured parameter than the recommended distresses given in Eq. (2.1) (Al-Omari and Darter, 1994; Gulen et al., 1994).

Traffic has been a controversial parameter in the 1993 AASHTO Guide and its earlier versions. The fact that it relies on a single value to represent the overall traffic spectrum is questionable. The method used to convert the traffic spectra into ESALs by applying LEFs is questionable. The AASHTO LEFs consider serviceability as the damage equivalency between two axles. Zhang et al. (2000) have found that Eq. (2.8), used to determine LEFs, is inconsistent with capturing damage in terms of equivalent deflection, which is easier to measure and validate. However quantifying damage equivalency in terms of serviceability or even deflections is not enough to represent the complex failure modes of flexible pavements.

Several studies have been conducted to investigate effects of different load types and magnitudes on damage of pavement structures using computed mechanistic pavement responses (Sebaaly and Tabatabaee, 1992; Zaghoul and White, 1994). Hajek (1995) proposed a general axle load equivalent factor – independent from pavement-related variables and axle configurations, based only on axle load – suitable for use in pavement management systems and simple routine design projects.

Today it is widely accepted that load equivalency factors are a simple technique for incorporating mixed traffic into design equations and are well suited for pavement management systems.

However pavement design applications require more comprehensive procedures. Mechanistic-empirical design procedures take a different approach for this problem; different loads and axle geometrics are mechanistically analyzed to determine directly the most critical structural responses that are significant to performance predictions, avoiding the shortcut of load equivalency factors.

Layer coefficients have also been of interest to those developing and enhancing pavement design methods. Several studies have been conducted to find layer coefficients for local and new materials (Little, 1996; Richardson, 1996; MacGregor et al., 1999). Coree and White (1990) presented a comprehensive analysis of layer coefficients and structural number. They showed that the approach was not appropriate for design purposes. Baladi and Thomas (1994), through a mechanistic evaluation of 243 pavement sections designed with the 1986 AASHTO guide, demonstrated that the layer coefficient is not a simple function of the individual layer modulus, but a function of all layer thicknesses and properties.

There are several studies in the literature of the environmental influences in the AASHTO method. There are two main environmental factors that impact service life of flexible pavements: moisture and temperature. The effect of moisture on subgrade strength has been well documented in past years and uncountable publications about temperature effects on asphalt

concrete are available. Basma and Al-Suleiman (1991) suggested using empirical relations between moisture content and resilient modulus directly in the design Eq. (2.7). The variation of the structural number with moisture content was defined as  $\Delta SN$  and was used to adjust the calculated SN. Basma and Al-Suleiman (1991) also suggested using a nomograph containing binder and mixture properties to determine the layer coefficient for asphalt concrete layer. Noureldin et al. (1996) developed an approach for considering temperature effects in the 1993 AASHTO design equation. In their approach, the mean annual pavement temperature is used to compute temperature coefficients that modify the original asphalt concrete layer coefficient used to compute the structural number.

The 1993 AASHTO Guide and its earlier versions were developed based on results from one test site trafficked over two years with a total of slightly over one million ESALs. From this test track, which was built with the same materials varying only thicknesses, the design equation was developed. Studies have shown that despite of the adjustments made over the years to the design equation in attempts to expand its suitability to different climate regions and materials, the design of flexible pavements still lacks accuracy in performance predictions and in ability to include different materials and their complex behavior.

### **2.3.2 M-E PDG**

The M-E PDG developed in NCHRP 1-37A is a mechanistic-empirical (M-E) method for designing and evaluating pavement structures. Structural responses (stresses, strains and deflections) are mechanistically calculated based on material properties, environmental conditions, and loading characteristics. These responses are used as inputs in empirical models to compute distress performance predictions. The M-E PDG was released in draft form at the conclusion of NCHRP 1-37A in April, 2004 (NCHRP, 2004).

The M-E PDG still depends on empirical models to predict pavement performance from calculated structural responses and material properties. The accuracy of these models is a function of the quality of the input information and the calibration of empirical distress models to observed field performance. Two types of empirical models are used in the M-E PDG. One type predicts the distress directly (e.g., rutting model for flexible pavements, and faulting for rigid); the other type predicts damage which is then calibrated against measured field distress (e.g., fatigue cracking for flexible pavements, and punchout for rigid).

### **2.3.2.1 Design Process**

The M-E PDG is not as direct as the 1993 AASHTO guide, in which the structure's thicknesses are obtained directly from the design equation. Instead an iterative process is used in which predicted performance of selected pavement structure is compared against the design criteria as shown in Figure 2.5. The structure and/or material selection are adjusted until a satisfactory design is achieved. A step-by-step description is as follows:

- Definition of a trial design for specific site subgrade support, material properties, traffic loading, and environmental conditions;
- Definition of design criteria for acceptable pavement performance at the end of the design period (i.e., acceptable levels of rutting, fatigue cracking, thermal cracking, and roughness);
- Selection of reliability level for each one of the distresses considered in the design;
- Calculation of monthly traffic loading and seasonal climate conditions (temperature gradients in asphalt concrete layers, moisture content in unbound granular layers and subgrade);
- Modification of material properties in response to environmental conditions;
- Computation of structural responses (stresses, strains and deflections) for each axle type and load and for each time step throughout the design period;
- Calculation of predicted distresses (e.g., rutting, fatigue cracking) at the end of each time step throughout the design period using the calibrated empirical performance models;
- Evaluation of the predicted performance of the trial design against the specified reliability level. If the trial design does not meet the performance criteria, the design (thicknesses or material selection) must be modified and the calculations repeated until the design is acceptable.

The M-E PDG is implemented in software in which all of above steps are performed automatically, except for the pavement structure and material selection.

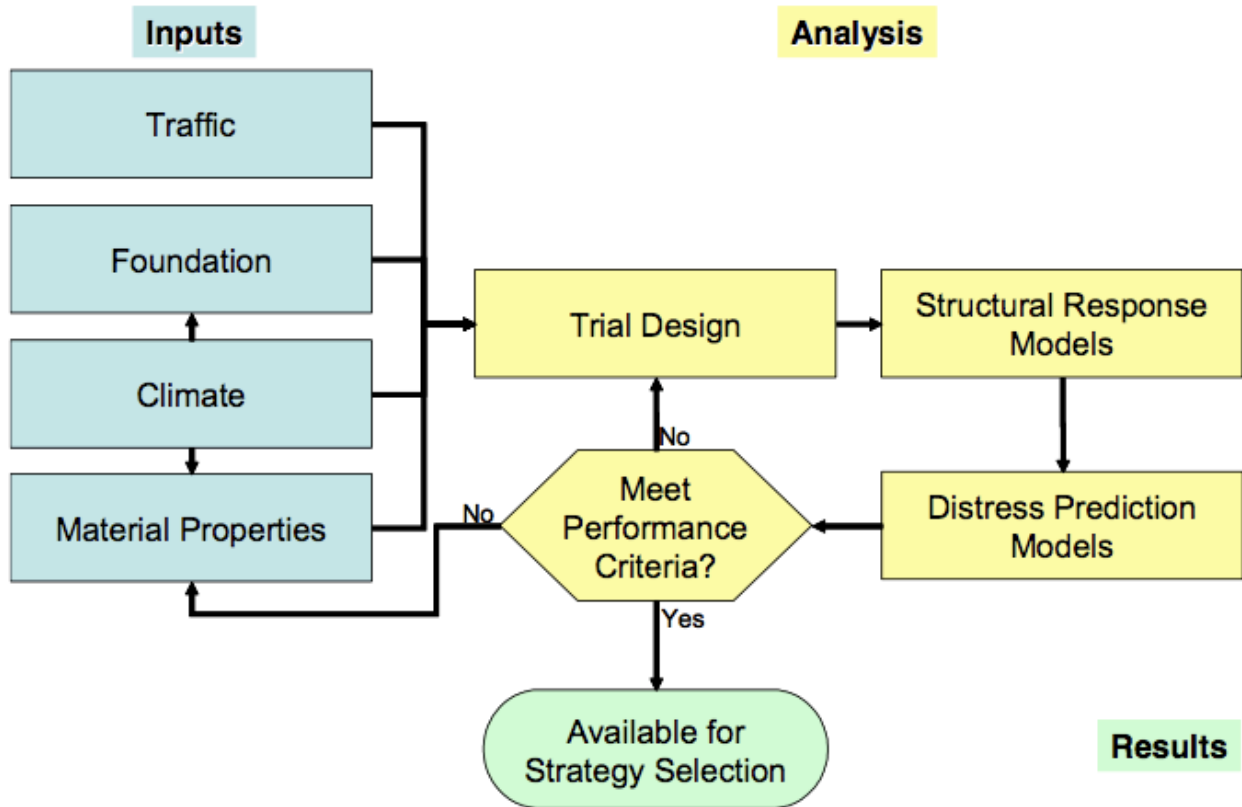


Figure 2.4. M-E flexible pavement design flow chart

The M-E PDG has a hierarchical approach for the design inputs, defined by the quality of data available and importance of the project. There are three levels:

- Level 1 – Laboratory measured material properties are required (e.g., dynamic modulus master curve for asphalt concrete, nonlinear resilient modulus for unbound materials). Project-specific traffic data is also required (e.g., vehicle class and load distributions);
- Level 2 – Inputs are obtained through empirical correlations with other parameters (e.g., resilient modulus estimated from CBR values);
- Level 3 – Inputs are selected from a database of national or regional default values according to the material type or highway class (e.g., soil classification to determine the range of resilient modulus, highway class to determine vehicle class distribution).

According to the NCHRP 1-37A report, level 1 is recommended for heavily trafficked highways where premature failure is economically undesirable. Level 2 can be used for intermediate projects, while level 3 is recommended for minor projects, usually low traffic roads. In addition, level 3 may be appropriate for pavement management programs widely implemented in highway state agencies.

The M-E PDG software uses the Multi Layer Linear Elastic Theory (MLET) to predict mechanistic responses in the pavement structure. When level 1 nonlinear stiffness inputs for unbound material are selected, MLET is not appropriate and a nonlinear Finite Element Method (FEM) is used instead.

Level 3 was used throughout this study because (a) at present there are rarely level 1 input data to be used on a consistent basis, and (b) the final version of the M-E PDG software was calibrated using level 3.

### **2.3.2.2 Design input**

The hierarchical level defines what type of input parameter is required. This section describes the input variables required for level 3.

#### *Design Criteria*

The design criteria are defined as the distress magnitudes at the minimum acceptable level of service. The design criteria are agency-defined inputs that may vary by roadway class, location, importance of the project, and economics.

The distresses considered for flexible pavements are: permanent deformation (rutting), “alligator” (bottom-up) fatigue cracking, “longitudinal” (top-down) cracking, thermal cracking, and roughness. The only functional distress predicted is roughness. Friction is not considered in the M-E PDG methodology. Among all these distresses, roughness is the only one not predicted entirely from mechanistic responses. Roughness predictions also include other non-structural distresses and site factors. Design criteria must be specified for each of these distresses predicted in the M-E PDG methodology.

#### *Traffic*

The M-E PDG uses the concept of load spectra for characterizing traffic. Each axle type (e.g., single, tandem) is divided in a series of load ranges. Vehicle class distributions, daily traffic volume, and axle load distributions define the number of repetitions of each axle load group at each load level. The specific traffic inputs consist of the following data:

- Traffic volume-base year information:
  - Two –way annual average daily truck traffic (AADTT)
  - Number of lanes in the design direction
  - Percent trucks in design direction
  - Percent trucks in design lane

- Vehicle (truck) operational speed
- Traffic volume adjustment factors:
  - Vehicle class distribution factors
  - Monthly truck distribution factors
  - Hourly truck distribution factors
  - Traffic growth factors
- Axle load distribution factors
- General traffic inputs:
  - Number axles/trucks
  - Axle configuration
  - Wheel base
  - Lateral traffic wander

Vehicle class is defined using the FHWA classification (FHWA, 2001). Automatic Vehicle Classification (AVC) and Weigh-in-Motion (WIM) stations can be used to provide data. The data must be sorted by axle type and vehicle class to be used in the M-E PDG. In case site-specific data are not available, default values are recommended in the procedure.

The use of load spectra enhances pavement design. It allows mixed traffic to be analyzed directly, avoiding the need for load equivalency factors. Additional advantages of the load spectra approach include: the possibility of special vehicle analyses, analysis of the impact on performance of overloaded trucks, and analysis of weight limits during critical climate conditions (e.g., spring thawing).

### *Environment*

The environmental conditions are predicted by the Enhanced Integrated Climatic Model (EICM).

The following data are required:

- Hourly air temperature
- Hourly precipitation
- Hourly wind speed
- Hourly percentage sunshine
- Hourly relative humidity

These parameters can be obtained from weather stations close to the project location. The M-E PDG software includes a library of weather data for approximately 800 weather stations throughout the U.S.

Additional environmental data are also required:

- Groundwater table depth
- Drainage/surface properties:
  - Surface shortwave absorptivity
  - Infiltration
  - Drainage path length
  - Cross slope

The climate inputs are used to predict moisture and temperature distributions inside the pavement structure. Asphalt concrete stiffness is sensitive to temperature variations and unbound material stiffness is sensitive to moisture variations.

*Material properties*

The M-E PDG requires a large set of material properties. Three components of the design process require material properties: the climate model, the pavement response models, and the distress models.

Climate-related properties are used to determine temperature and moisture variations inside the pavement structure. The pavement response models use material properties (corrected as appropriate for temperature and moisture effects) to compute the state of stress/strain at critical locations in the structure due to traffic loading and temperature changes. These structural responses are used by the distress models along with complementary material properties to predict pavement performance. Only flexible pavements were evaluated in this study and therefore only material properties for asphalt concrete and unbound materials are described. Table 2.8 summarizes the flexible pavement material properties required by the M-E PDG.

**Table 2.8. Material inputs requirement for flexible pavements.**

Material Category	Material inputs required		
	Climatic models	Response models	Distress models
Asphalt concrete	- <u>mixture</u> : surface shortwave absorptivity, thermal conductivity, and heat capacity - <u>asphalt binder</u> : viscosity (stiffness) characterization to account for aging - plasticity index - gradation parameters - effective grain sizes	- time-temperature dependent dynamic modulus (E*) of HMA mixture - Poisson’s ratio  - resilient modulus (Mr) at optimum density and moisture content	- tensile strength, - creep compliance - coefficient of thermal expansion
Unbound materials	- specific gravity - saturated hydraulic conductivity - optimum moisture content - parameters to define the soil-water characteristic curve	- Poisson’s ratio - unit weight - coefficient of lateral pressure	- gradation parameters

Two material properties required in the M-E PDG are considered innovative for pavement design methods, the dynamic modulus for asphalt concrete and the nonlinear stiffness model for unbound materials. Time- and temperature-dependency of asphalt mixtures is characterized by the dynamic modulus,  $|E^*|$ . The dynamic modulus master curve models the variation of asphalt concrete stiffness due to rate of loading and temperature variation (hardening with low temperature/high frequency and softening with high temperature/low frequency). The nonlinear elastic behavior of unbound granular materials is modeled by a stress-dependent resilient modulus included as level 1 input.

### Asphalt Concrete

The complex dynamic modulus  $|E^*|$  is the principal material property input for asphalt concrete. It is a function of mixture characteristics (binder, aggregate gradation, and volumetrics), rate of loading, temperature, and age. For level 1 inputs, the dynamic modulus master curve is constructed based on time-temperature superposition principles (Huang, 2004; Pellinen, 2004) by shifting laboratory frequency sweep test data. Binder viscosity measured using the dynamic shear rheometer (DSR) is also a required level 1 input. Aging effects on binder viscosity are simulated using the Global Aging System, which considers short term aging from mix/compaction and long term aging from oxidation (NCHRP, 2004).

For level 2 and 3 inputs, the dynamic modulus master curve is obtained via an empirical predictive equation. The  $|E^*|$  predictive equation is an empirical relationship between  $|E^*|$  and mixture properties:

$$\begin{aligned} \log E^* &= 3.750063 + 0.02932 \times \rho_{200} - 0.001767 \times (\rho_{200})^2 - 0.002841 \times \rho_4 - 0.058097 \times V_a \\ &- 0.802208 \times \left( \frac{V_{beff}}{V_{beff} + V_a} \right) \\ &+ \frac{3.871977 + 0.0021 \times \rho_4 + 0.003958 \times \rho_{38} - 0.000017 \times (\rho_{38})^2 + 0.005470 \times \rho_{34}}{1 + e^{(-0.603313 - 0.313351 \times \log f - 0.393532 \times \log \eta)}} \end{aligned}$$

Equation 2.14

in which:

$E^*$  = dynamic modulus, 10<sup>5</sup> psi

$\eta$  = binder viscosity, 10<sup>6</sup> Poise

$f$  = loading frequency, Hz

$V_a$  = air void content, %

$V_{\text{beff}}$  = effective binder content, % by volume

$\rho_{34}$  = cumulative % retained on the 19-mm sieve

$\rho_{38}$  = cumulative % retained on the 9.5-mm sieve

$\rho_4$  = cumulative % retained on the 4.75-mm sieve

$\rho_{200}$  = % passing the 0.075-mm sieve

The binder's viscosity at any temperature is given by the binder's viscosity-temperature relationship:

$$\log \log \eta = A + VTS \times \log T_R$$

**Equation 2.15**

in which:

$\eta$  = bitumen viscosity, cP

TR = temperature, Rankine ( $T_R = T_{\text{Fahrenheit}} + 460$ )

A = regression intercept

VTS = regression slope of viscosity temperature susceptibility

For level 2 asphalt concrete inputs, binder parameters A and VTS are determined from DSR testing. For level 3, default A and VTS values are based on the binder grading (e.g., Superpave performance grade, penetration grade, or viscosity grade).

Additional asphalt concrete material properties are required to predict thermal cracking: (1) tensile strength, (2) creep compliance, (3) coefficient of thermal expansion, (4) surface shortwave absorptivity, and (5) thermal conductivity and heat capacity. The last two properties are also required for the climatic model (EICM). Tensile strength and creep compliance are determined in the laboratory using the indirect tensile test for level 1 and 2 inputs. At level 3, these properties are correlated with other material parameters.

### *Unbound Materials*

Resilient modulus is the principal unbound material property required for the structural response model. Level 1 resilient modulus values are determined from laboratory test data as fitted to the stress-dependent stiffness model:

$$M_R = k_1 p_a \left( \frac{\theta}{p_a} \right)^{k_2} \left( \frac{\tau_{oct}}{p_a} \right)^{k_3}$$

**Equation 2.16**

in which:

$M_R$  = resilient modulus

$\theta$  = bulk stress =  $\sigma_1 + \sigma_2 + \sigma_3$

$\sigma_1$  = major principal stress

$\sigma_2$  = intermediate principal stress =  $\sigma_3$  for MR test on cylindrical specimens

$\sigma_3$  = minor principal stress/confining pressure

$\tau_{\text{oct}}$  = octahedral shear stress =  $\frac{1}{3}\sqrt{(\sigma_1 - \sigma_2)^2 + (\sigma_1 - \sigma_3)^2 + (\sigma_2 - \sigma_3)^2}$

$p_a$  = atmospheric pressure (used to normalize the equation)

$k_1, k_2, k_3$  = regression constants determined from the laboratory tests

At level 2 the resilient modulus is correlated with other parameters (e.g., California Bearing Ratio (CBR), R-value, AASHTO layer coefficient). At level 3 the resilient modulus can be selected from a range of default values that are typical for the material type and/or soil classification. The input resilient modulus data at all levels are assumed to be at optimum moisture content and density; this value is adjusted by the EICM for seasonal climate variations. There is also an option for direct entry of a best estimate for the seasonally-adjusted unbound resilient modulus, in which case the EICM is bypassed.

Poisson's ratio is also required for the structural response model. It can be determined from laboratory testing, correlations with other properties, or estimated from ranges of typical values. The Atterberg limits, gradation, hydraulic conductivity, maximum dry unit weight, specific gravity, optimum moisture, and degree of saturation are additional unbound material inputs used for determining the effect of seasonal climate variations on resilient modulus.

### **2.3.2.3 Pavement Response Models**

The M-E PDG utilizes three models to predict pavement structural responses (stresses, strains, and displacements). Multi-Layer Elastic Theory (MLET) and the Finite Element Model (FEM) are used to compute responses due to traffic loading and the Enhanced Integrated Climate Model (EICM) is used to predict temperature and moisture histories throughout the pavement structure. When non-linear behavior of unbound materials is desired-i.e, for level 1 inputs – the FEM is chosen; otherwise the load-related analysis is done with MLET.

The load-related structural responses are predicted at critical locations based on maximum damage. The response at each point is evaluated at various depths and afterward the most critical is used to predict pavement distress performance. Figure 4 shows in plan view the location of possible critical points for single, tandem, and tridem axles. If a single axle is being analyzed,

line Y1 of points is used; if tandem, lines Y2 and Y3; and if tridem, lines Y2, Y3, Y6 and Y7 (NCHRP, 2004).

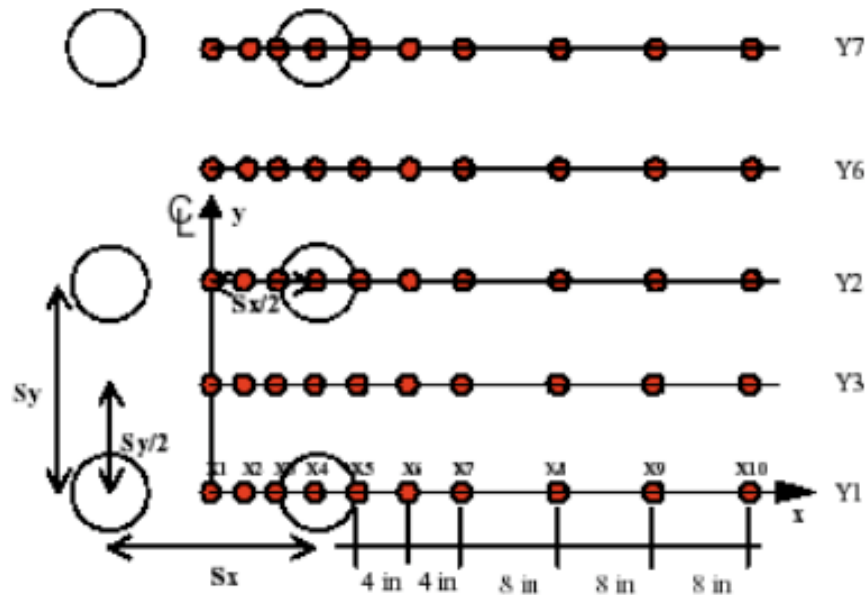


Figure 2.5. Summary of schematics for horizontal location of critical response predictions (NCHRP, 2004)

The depths at which the calculations are performed depend on the distress type:

- Fatigue cracking
  - At surface (top-down cracking)
  - 0.5 inches from the surface (top-down cracking)
  - at the bottom of the asphalt concrete layer (bottom-up cracking)
- Rutting
  - mid-depth of each layer/sublayer
  - top of subgrade
  - 6 inches below the top of subgrade

Each pavement layer is divided into thin sublayers so that properties varying in the vertical direction are represented better (e.g., asphalt concrete layer is divided and different dynamic moduli are assigned depending on the temperature in each sublayer). For flexible pavements, the sublayering is determined as follows:

- The first 1 inch of asphalt concrete (AC) is divided into two 0.5-inch sublayers. The remaining AC thickness is divided into 1-inch sublayers until 4 inches of total depth from the surface is achieved. The remaining thickness, if there is any, is considered the final AC sublayer.

- The unbound base is divided into  $a+nb$  sublayers, in which  $a$  has half the thickness of  $b$ . The number of remaining sublayers is determined by:  $n=int[(h_{base} - 2)/4]$ . Therefore, the total number of sublayers is  $n+1$ . This procedure is valid for base thickness exceeding 6 inches.
- The subgrade is divided into 3 sublayers of equal thickness until the total depth of the pavement structure reaches 8 feet. From this point on there is no more sublayering and the remaining subgrade is treated as an infinite layer.

### *Multi-layer Linear Elastic Theory*

The first attempt to calculate displacements due to loading on an elastic half-space, such as the surface of a homogeneous material with infinite area and depth, was made by Kelvin in 1868 (Croney and Croney, 1997). Later, Boussinesq's solution (1885) for a concentrated load became a fundamental tool to compute stress, strain and deflection. The solution could be integrated to obtain responses due to a general surface load, including a circular loaded area (Huang, 1993). The concept of multi-layer analysis has its roots in the Burmister two-layer and three-layer solutions (Burmister, 1945); charts and tables summarizing these solutions were developed later (Foster and Alvin, 1954; Burmister, 1958; Jones, 1962; Huang, 1969, and 1973).

Burmister's layered theory can be applied to a multi-layer system of linear elastic materials structured on top of a half space subgrade following the basic assumptions (Huang, 1994):

- Each layer is homogeneous, isotropic, and linearly elastic, characterized by Young's modulus of elasticity,  $E$ , and Poisson's ratio,  $\nu$ .
- The material is weightless and horizontally infinite.
- The thickness of each layer is finite, and the subgrade is considered as infinite layer.
- The load is uniformly applied on the surface over a circular area.
- Continuity conditions are satisfied at the layer interfaces.

In the M-E PDG, the MLET is implemented in a modified version of the JULEA algorithm (NCHRP, 2004). Using the principle of superposition, single wheels can be combined spatially into multi-wheel axles to simulate different axle configurations.

The small set of input parameters required by MLET facilitates its implementation and use. The only inputs required are the layer thicknesses, the elastic properties (Young's modulus of elasticity and Poisson's ratio) for each layer, the tire pressure and the tire contact area. The main disadvantage of MLET is its inability to consider nonlinearities often exhibited by pavement materials.

### Finite Element Method

The Finite Element Method (FEM) allows structural modeling of a multi-layer pavement section having material properties that can vary both vertically and horizontally throughout the profile. It is a versatile tool capable of considering three dimensional geometries, non-linear material behavior, large strain effects, dynamic loading and other features. It is well suitable for structural evaluation and response prediction of pavements. Although its robustness permits solving more complex problems, the longer computational time compared to MLET represents a significant disadvantage.

The general idea of finite element technique is the partitioning of the problem into small discrete elements (mesh), formulating an approximation to the stress and strain variations across each individual element, and then applying equilibrium requirements to combine the individual elements to get the formulation for the global problem in terms of a set of simultaneous linear equations. The solution is therefore a piecewise approximation to the true solution. In the M-E PDG, the FEM was implemented with the following features:

- Linearly elastic behavior for asphalt concrete
- Nonlinearly elastic behavior (stress-dependent stiffness model) with tension cut-off for unbound materials.
- Fully bonded, full slip, and intermediate interface conditions between layers.

The asphalt concrete layer is modeled as a linearly elastic material with stiffness given by the mixture dynamic modulus master curve. The stress dependence of unbound materials is expressed by the following stiffness model:

$$M_R = k_1 p_a \left( \frac{\theta}{p_a} \right)^{k_2} \left( \frac{\tau_{oct}}{p_a} \right)^{k_3}$$

**Equation 2.17**

In which the parameters are as previously described. The tension cut-off feature is triggered whenever tensile principal stresses are calculated in the unbound layers (the excess tensile stress is distributed over neighboring elements in an iterative process). The load is applied in small increments, and the stress/strain output each increment provides the initial condition for the next stage (NCHRP, 2004).

### *EICM Environmental Model*

EICM is a mechanistic model of one dimensional heat and moisture flow that simulates changes in the behavior and characteristics of pavement and subgrade materials induced by environmental factors (NCHRP, 2004). Daily and seasonal variations of temperature and moisture within the pavement structure are induced by the weather history at the project site. Different material types have different responses to climatic variations. Unbound materials are affected by moisture change and by freeze-thaw cycles during winter and spring seasons. Asphalt concrete responds to temperature variations, which affects directly the dynamic modulus of the mixture. Temperature is also the cause of thermal cracks, either from a single thermal or from repetitive cycles of warm/cool temperatures.

The EICM consists of three major components (NCHRP, 2004):

- The Climatic-Materials-Structural Model (CMS Model) originally developed at the University of Illinois.
- The CRREL Frost Heave and Thaw Settlement Model (CRREL Model) originally developed at the United States Army Cold Regions Research and Engineering Laboratory (CRREL).
- The Infiltration and Drainage Model (ID Model) originally developed at Texas A&M University.

In the case of flexible pavements, three major environmental effects are of particular interest:

- Temperature variations for the asphalt concrete. The dynamic modulus of concrete mixtures is very sensitive to temperature. Temperature distributions in asphalt concrete layers are predicted and then used to define the stiffness of the mixture throughout the sublayers. Temperature distributions are also used as inputs for the thermal cracking prediction model.
- Moisture variation for subgrade and unbound materials. The resilient modulus input of unbound materials is defined as being at optimum density and moisture content. A correction factor is defined to adjust the resilient modulus based on predicted moisture content.
- Freezing and thawing for subgrade and unbound materials. The resilient modulus of unbound materials located within the freezing zone increases during freezing periods and

decrease during thawing periods. The EICM predicts the formation of ice lenses and defines the freezing zone.

#### **2.3.2.4 Empirical Performance Models**

This section presents a description of empirical models for predicting performance of flexible pavements in the M-E PDG. The models described here are the following: “alligator” or bottom-up fatigue cracking, longitudinal or top down fatigue cracking, thermal cracking, rutting and roughness. The calibration of these models was done using the Long Term Pavement Performance (LTPP) database with sections distributed all over the U.S. This calibration effort is defined in the M-E PDG as the national calibration.

The national calibration was a task undertaken by the NCHRP 1-37A project team to determine calibration coefficients for the empirical distress models that would be representative of the wide range of materials available in the U.S. for pavement construction. The LTPP database was used as primary source of data for this purpose. Permanent deformation, longitudinal (top-down), alligator (bottom-up) and thermal cracking were calibrated for flexible pavement sections. According to the NCHRP 1-37A report, the roughness model was developed directly using the LTPP data and therefore required no additional calibration.

The importance of calibration is evident. Pavement structures behave in different ways and the current state-of-the-art mechanistic models are not capable of fully predicting the behavior of pavement structures. The empirical models are not sufficient to stand alone and capture the wide possibilities of failure mechanism. In addition, most of these models were developed from laboratory test data and laboratory-field shifting factors are required.

##### *Alligator Fatigue Cracking*

“Alligator” fatigue cracking develops from mechanical failure caused by tensile strains at the bottom of asphalt concrete layers and once developed propagates upwards. It is also known as bottom-up cracking. Stiffer mixtures or thin layers are more likely to exhibit bottom-up fatigue cracking problems, which makes it a problem often aggravated by cold weather. It is also noted that the supporting layers are important for the development of fatigue cracking. Soft layers placed immediately below the asphalt concrete layer increase the tensile strain magnitude at the bottom of the asphalt concrete and consequently increase the probability of fatigue crack development.

Fatigue cracking is evaluated by first predicting damage and then converting damage into cracked area. The model used in the M-E PDG was adopted from the Asphalt Institute (Asphalt Institute, 1991) and calibrated based on 82 LTPP section data in 24 states across the country (NCHRP, 2004). The number of repetitions to failure for a given load magnitude is computed as follows:

$$N_f = K_t [\beta_1 K_1 C (\varepsilon_t)^{-\beta_2 k_2} (E)^{-\beta_3 k_3}]$$

Equation 2.18

in which:

$N_f$  = number of repetitions of a given load to failure

$k_t$  = thickness correction factor

$\beta_1, \beta_2, \beta_3$  = field calibration coefficients

$k_1, k_2, k_3$  = material properties determined from regression analysis laboratory test data

$C$  = laboratory to field adjustment factor

$\varepsilon_t$  = tensile strain at the critical location within asphalt concrete layer

$E$  = asphalt concrete stiffness at given temperature

The calibration of the model using the LTPP database resulted in the following values:  $k_1 = 0.00432$ ,  $k_2 = 3.9492$ ,  $k_3 = 1.281$ . The bi field calibrations coefficients were assumed to be equal to 1 for this calibration. This set of calibration coefficients is referred to in the M-E PDG as the national calibration.

The thickness correction factor is determined as follows:

$$K_t = \frac{1}{0.000398 + \frac{0.003602}{1 + e^{(11.02 - 3.49 \times h_{AC})}}}$$

Equation 2.19

in which  $h_{AC}$  = total AC thickness. The laboratory-field adjustment factor is given by:

$$C = 10^M$$

$$M = 4.84 \left( \frac{V_{beff}}{V_a + V_{beff}} - 0.69 \right)$$

in which:

$V_{beff}$  = effective binder content

$V_a$  = air voids (%)

The damage resulted from a given load is then computed from the number of repetitions using Miner's Law:

$$D = \sum_{i=1}^T \frac{n_i}{N_{fi}}$$

Equation 2.20

in which:

D = damage

T = total number of seasonal periods

$n_i$  = actual traffic for period  $i$

$N_{fi}$  = traffic repetitions of a given loa to cause failure at period  $i$

The last step is to convert damage into cracked area as follows:

$$FC = \left( \frac{C_4}{1 + e^{(C_1 C_1' + C_2 C_2' \log(D \times 100))}} \right) \times \left( \frac{1}{60} \right)$$

Equation 2.21

in which:

$$C_2' = -2.40874 - 39.748(1 + h_{AC})^{-2.856}$$

$$C_1' = -2C_2'$$

FC = “alligator” fatigue cracking (% of lane area)

$C_1, C_2, C_4$  = constants

D = damage

$h_{AC}$  = total AC thickness

The calibration using the LTPP database resulted in the following values for the regression constants:  $C_1 = 1$ ,  $C_2 = 1$  and  $C_4 = 6000$ . Equation (2.21) is of a convenient sigmoidal form that models the two end-conditions of the damage-cracked area relationship. At 0% damage the percentage of cracked area is equal to zero. At the other end, at 100% damage, an assumption was adopted that only half of the area would be cracked. Therefore when damage is 100%, cracked area is equal to 50% or 3000 ft<sup>2</sup> over a 500 ft lane length (the total lane area considered in the M-E PDG is 12 ft x 500 ft = 6000 ft<sup>2</sup>). The statistics for “alligator” fatigue cracking model after calibration using 461 observations from the LTPP database standard error (Se) = 6.2%, and Se/Sy = 0.947.

### *Longitudinal Cracking*

Longitudinal cracking develops at the surface and propagates downward (top-down cracking). Longitudinal crack formation in flexible pavements is conceptually similar

to “alligator” fatigue cracking. Tensile strains at the top of the surface asphalt concrete layer induced by traffic loading cause the appearance of cracks.

The M-E PDG model for longitudinal cracking follows the same formulation as for alligator cracking. The difference is in the damage-crack relationship. Equation 2.18 is used to calculate the number of applications to failure for a given load. Damage is computed using Miner’s Law. Cracking, in units of foot/mile, is then given by:

$$FC = \left( \frac{C_4}{1 + e^{(C_1 - C_2 \log(D \times 100))}} \right) \times 10.56$$

**Equation 2.22**

in which:

FC = longitudinal cracking (foot/mile)

$C_1, C_2, C_4$  = calibration coefficients

D = damage

The calibration using the LTPP database resulted in the following values for the regression constants:  $C_1 = 7$ ,  $C_2 = 3.5$  and  $C_4 = 1000$ . The sigmoidal form model was used to model the damage-crack length relationship. The two end-conditions are satisfied. At 0% damage the model predicts no cracking, and at 100% damage, 500 ft of longitudinal cracking per 500 ft of pavement (assumed only 50% of the lane with cracks on both wheel paths: 2 x 250 ft). The statistics for the longitudinal cracking calibration based on 414 field measurements are  $Se = 1242.25$  feet/mile and  $Se/Sy = 0.977$ .

### *Thermal Cracking*

Thermal cracking is a consequence of heating/cooling cycles occurring in the asphalt concrete. The pavement surface cools down faster and with more intensity than the core of the pavement structure, which causes thermal cracking to occur at the surface of flexible pavements. Thermal cracks extend in the transverse direction across the full width of the pavement.

The thermal cracking model used in the M-E PDG is an enhanced version of the TCMODEL developed under the SHRP A-005 research contract. This model has a robust theoretical background and is the most fully mechanistic of the distress prediction components in the M-E PDG.

The main improvement from the SHRP A-005 model was the incorporation of an advanced analysis technique to convert data directly from the Superpave Indirect Tensile Test into viscoelastic properties, specifically the creep compliance function that is further converted to the relaxation modulus. The relaxation modulus is coupled with the temperature data from the EICM to predict thermal stresses. The growth behavior of the thermal crack is calculated from the thermal stresses.

The crack propagation is computed using Paris's law:

$$\Delta C = A \times \Delta K^n$$

**Equation 2.23**

in which:

$\Delta C$  = change in crack depth for each thermal cycle

$\Delta K$  = change in stress intensity factor during thermal cycle

A, n = fracture parameters for the asphalt concrete mixture

The master creep compliance function is expressed as a power law:

$$D(\xi) = D_0 + D_1 (\xi)^m$$

**Equation 2.24**

in which:

$\xi$  = reduced time

$D_0, D_1, m$  = compliance coefficients

Given the compliance function model expressed by Equation 2.23, the values of n and A can be calculated as follows:

$$n = 0.8 \left( 1 + \frac{1}{m} \right)$$

$$A = 10^{\beta(4.389 - 2.52 \log(E\sigma_m^n))}$$

in which:

m = power coefficient in the compliance function

$\beta$  = calibration coefficient

E = mixture stiffness

$\sigma_m$  = undamaged mixture tensile strength

The length of the thermal cracking is then predicted based on an assumed relationship between the crack depth and percentage of cracking in the pavement:

$$C_f = \beta_1 \times N\left(\frac{\log C/h_{ac}}{\sigma}\right)$$

Equation 2.25

in which:

$C_f$  = predicted thermal cracking, ft/500ft

$\beta_1$  = field calibration coefficient

$N()$  = standard normal distribution at ( )

$C$  = crack depth

$\sigma$  = standard deviation of the log of crack depth

$h_{ac}$  = asphalt concrete thickness

The calibration of the thermal cracking model was based on data from the LTPP database, the Canadian C-SHRP program, MnROAD, and one section in Peoria, IL. The value of the calibration coefficient  $b_1$  was found equal to 400.

### *Rutting*

Permanent deformation or rutting is a load-related distress caused by cumulative applications of loads at moderate to high temperatures, when the asphalt concrete mixture has the lowest stiffness. It can be divided into 3 stages. Primary rutting develops early in the service life and it is caused predominantly by densification of the mixture (compaction effort by passing traffic) and with decreasing rate of plastic deformations. In the secondary stage, rutting increments are smaller at a constant rate, and the mixture is mostly undergoing plastic shear deformations. The tertiary stage is when shear failure occurs, and the mixture flows to rupture. Usually the tertiary stage is not reached in in-service pavements – preventive maintenance and rehabilitation are required by agencies long before this stage is achieved.

Permanent deformation is predicted using empirical models. Only primary and secondary stages are modeled. For asphalt concrete materials the model is an enhanced version of Leahy's model (Leahy, 1989), modified by Ayres (1997) and then by Kaloush (2001). The model for unbound materials is based on Tseng and Lytton's, which was modified by Ayres and later on by El-Basyouny and Witeczak (NCHRP, 2004).

Total permanent deformation is the summation of rut depths from all layers:

$$RD_{total} = RD_{AC} + RD_{Base} + RD_{subgrade}$$

Equation 2.26

*Asphalt concrete model*

The asphalt concrete layer is subdivided into sublayers and the total predicted rut depth for the layer is given by:

$$RD_{AC} = \sum_{i=1}^N (\varepsilon_p) \Delta h_i$$

**Equation 2.27**

in which:

$RD_{AC}$  = rut depth at the asphalt concrete layer

$N$  = number of sublayers

$(\varepsilon_p)$  = vertical plastic strain at mid-thickness of layer  $i$

$\Delta h_i$  = thickness of sublayer  $i$

The vertical plastic strain ( $\varepsilon_p$ ) at each sublayer is calculated as:

$$\frac{\varepsilon_p}{\varepsilon_r} = \beta_{\sigma_3} [\beta_1 10^{k_1} T^{k_2} \beta_2 N^{k_3} \beta_3]$$

**Equation 2.28**

in which:

$\varepsilon_r$  = computed vertical resilient strain at mid-thickness of sublayer  $i$

$\beta_{\sigma_3}$  = depth correction factor

$k_1, k_2, k_3$  = regression coefficients derived from laboratory testing

$\beta_1, \beta_2, \beta_3$  = field calibration coefficients

$T$  = temperature

$N$  = number of repetitions for a given load

After the calibration using the national LTPP database, the regression coefficients are  $k_1 = -3.4488$ ,  $k_2 = 1.5606$ ,  $k_3 = 0.4791$ , and the assumed  $\beta_i$ 's are equal to 1. A total of 387 observed rut points from the LTPP sections were used in the calibration effort. The goodness-of-fit statistics for the calibration are  $R^2 = 0.643$ , standard error  $S_{e_3} = 0.055$  in for the wide range mixture types in the LTPP calibration sections.

### Unbound Materials

The M-E PDG divides all unbound granular materials into sublayers, and the total rutting for each layer is the summation of the permanent deformation of all sublayers. The permanent deformation at any given sublayer is computed as:

$$\delta_i = \beta_1 k_1 \left( \frac{\varepsilon_0}{\varepsilon_r} \right) e^{-\left(\frac{\rho}{N}\right)} \varepsilon_v h_i$$

**Equation 2.29**

in which:

$\delta_i$  = permanent deformation for sublayer i

$\beta_1$  = field calibration coefficient

$k_1$  = regression coefficient determined from laboratory permanent deformation test data

$\varepsilon_0/\varepsilon_r, \rho$  = material properties

$N$  = number of repetitions of a given load

$\varepsilon_v$  = computed vertical resilient strain at mid-thickness of sublayer i for a given load

$h_i$  = thickness of sublayer i

The model described in Equation 31 is a modification of the original Tseng and Lytton's model. The material properties  $\varepsilon_0/\varepsilon_r, b, \rho$  are derived from other properties.

The subgrade is modeled as a semi-infinite layer in the structural response models (MLET or FEM). An adjustment on the permanent deformation models is therefore required for computing the plastic strains in a semi-infinite layer. The plastic strain at different depths in the subgrade can be computed by:

$$\varepsilon_p(Z) = (\varepsilon_{p0}) e^{-\alpha Z}$$

**Equation 2.30**

in which :

$\varepsilon_p(z)$  = plastic vertical strain at depth z (measured from the top of the subgrade)

$\varepsilon_{p0}$  = plastic vertical strain at the top of the subgrade ( $z = 0$ )

$z$  = depth measured from the top of the subgrade

$\alpha$  = regression coefficient

#### 2.3.2.5 Reliability

Pavement design inputs have large uncertainties. The design is often based on the mean values of the input parameters. In the M-E PDG, the key outcomes are the individual distresses, considered

as the random variables of interest. The distress distribution is considered to be normal with a mean predicted value and a corresponding standard deviation. The standard deviation of the distribution is estimated based on the model's calibration error. The predicted distress considering reliability is given by the general formulation:

$$D_{\text{reliability}} = D_{\text{mean}} + S_D \times Z_R$$

**Equation 2.31**

in which  $D_{\text{reliability}}$  is the distress prediction with reliability,  $D_{\text{mean}}$  is the mean distress value from the performance model,  $S_D$  is the computed standard deviation for the distress type (D), and  $Z_R$  is the standard normal deviate from the normal distribution for the level of reliability selected. The formulation in Equation 33 for the M-E PDG models reliability in the same way as the general reliability factor in the 1993 AASHTO Guide. Recall in the 1993 AASHTO Guide, reliability is included in the design equation via the product of the overall standard deviation and the reliability factor ( $S_0 \times Z_R$ ).

The estimates of error are obtained from the calibration (predicted versus measured data). They include a combined input variability from the input uncertainties, construction variability, and model error. Therefore, the model's error becomes a key factor in the reliability – the smaller the error, the smaller is the gap between a design with a reliability factor (higher than 50%) and one at the mean value (reliability = 50%).

Based on the national calibration results, the default standard error ( $Se$ ) for permanent deformations is defined for each individual layer as follows:

$$Se_{AC} = 0.1587 \times RD_{AC}^{0.4579}$$

**Equation 2.32a**

$$Se_{GB} = 0.1169 \times RD_{GB}^{0.5303}$$

**Equation 2.32b**

$$Se_{SG} = 0.1724 \times RD_{SG}^{0.5516}$$

**Equation 2.32c**

in which AC represents asphalt concrete, GB, granular base, and SG, subgrade. RD is the rut depth at any given sublayer.

The standard error for alligator and longitudinal cracking are defined as follows:

$$(Se)_{alligator} = 0.5 + 12/(1 + e^{1.308-2.949 \log D})$$

Equation 2.33

$$(Se)_{longitudinal} = 200 + 2300/(1 + e^{1.072-2.1654 \log D})$$

Equation 2.34

in which D is a damage computed as the primary variable in the cracking model.

There were data available for all three input levels for the calibration of the mechanistic thermal cracking model. Standard error equations were developed for each input level as follows:

$$\text{Level 1: } Se_{\text{thermal-1}} = 0.2474 \times C_{\text{thermal}} + 10.619$$

$$\text{Level 2: } Se_{\text{thermal-2}} = 0.3371 \times C_{\text{thermal}} + 14.468$$

$$\text{Level 3: } Se_{\text{thermal-3}} = 0.6803 \times C_{\text{thermal}} + 29.197$$

It is important to notice the reduction in error estimate as input level goes from 3 to 1. Level 1 input requires more laboratory data to better characterize the material behavior which in turn reduces the predicted standard error.

The M-E approach for designing and evaluating flexible pavements represents a major step forward from purely empirical methods. Mechanistic models are employed for predicting pavement responses and climatic effects on material behavior. The pavement distresses are too complex to be modeled by mechanistic models only. Empirical models are employed to overcome these limitations of theory; the empirical models establish a connection between structural responses and performance prediction. Calibration of the empirical distress models is a critical requirement for quality performance predictions.

***CalME:  
California Mechanistic-Empirical  
design software***



## **3.1 Introduction to CalME and CalBack**

### **3.1.1 Overview**

Until 1900s, the California Department of Transportation (Caltrans) procedures for new pavements and for rehabilitation designs were based on the AASHTO guide; the approach used was empirical. While the Caltrans empirical procedures performed generally well, they are limited in their ability to benefit from the vast number of emerging new products, construction practices, and design innovations that optimize performance of the pavement system and the cost of maintenance and rehabilitation activities.

In order to realize the benefits of continuously emerging innovations in the pavement field, California started in 1996 an extensive research project for developing Mechanistic-Empirical (ME) design and analysis tools. These tools will help engineers in the state to incorporate the impact of new products, new construction technologies, increased traffic volumes and axle loading, various axle configurations, and variable climatic conditions.

As part of the development of new ME design procedures, Caltrans has been developing a suite of dedicated software. These programs support engineers in designing new structures and in rehabilitating existing flexible pavements. One major product of this suite is *CalME*, which is an ME design and analysis program for flexible pavements that parallels the NCHRP 1-37A product. *CalBack*, another product of this suite, is a sophisticated back-calculation program that contains specific features pertinent to California and is designed to work as a standalone or in concert with *CalME* (P. Ullidtz, J.T. Harvey, 2008).

### **3.1.2 CalME**

In 1990s the California Department of Transportation (Caltrans) recognized that future design procedures would be based on ME principles and approved an issue memo titled “Adoption of Mechanistic-Empirical (ME) Pavement Design Method”, which recommend for the adoption of ME pavement design methodology. The existing pavement design methods and in particular the “AASHTO Design Guide”, the primary document used to design new and rehabilitated highway pavements in the United States and in California based on empirical theories, should have been slowly replaced by ME design methods.

Caltrans has worked on the development of a ME flexible pavement design procedure, in addition to the ME procedure in the “Guide for Mechanistic-Empirical Design of new and rehabilitated pavement structures” by NCHRP and the final result was the first draft software program called CalME.

CalME has been developed, beginning in the late 1990s, to fill the following needs for an ME analysis tool for use in California:

- emphasis on rehabilitation and pavement preservation that account for more than 90 percent of Caltrans pavement program, rather than new pavements.
- emphasis on use of in-situ pavement testing data for existing pavements (FWD data) instead of laboratory testing.
- study of reflection cracking and rutting in modified asphalt mixtures, particularly rubber- and polymer-modified mixes.
- capacity of simulating damage and predicting pavement response (deflections, strains, stresses) throughout the pavement life and not only the initial and final conditions.
- compatibility with calibration using laboratory and in situ pavement testing data.
- ability to consider variability through Monte Carlo simulation with reasonable run times.

CalME development was continued by Caltrans in the 2000s when it was determined that the flexible pavement models in NCHRP “Mechanistic Empirical Pavement design Guide” did not fully meet these criteria. Caltrans ultimate goal is that *CalME*, its models and its ideas become part of multi-state or national long-term research and development programs (P. Ullidtz, 2010).

*CalME* software, for new flexible pavements as well as for rehabilitation of existing pavements, provides the user with three approaches for analysis and design. It includes:

1. “*Caltrans*” empirical design methods:

The *R-value method* for new flexible structures described in the Highway Design Manual (HDM) and based on resistance values (R-values) and Gravel factors.

The *Deflection reduction method* for rehabilitation of existing flexible pavements described in the Caltrans “Flexible Pavement Rehabilitation Manual”.

2. “*Classical*” Mechanistic-Empirical (ME) method:

Based largely on the Asphalt Institute Method which uses very simple model to characterize materials, climate, and traffic inputs.

In this Classical ME method the pavement response is only calculated for the initial pavement condition. Then using empirical relations it can be predicted the number of load to failure, through cracking, rutting or roughness.

3. “Incremental” ME method and “Incremental-recursive” ME method:

The “incremental design” sums the damage over all of the time increment during one year, without updating of the material’s properties through the life of the project, but using Miner’s law and considering the full axle load spectrum, the lateral wander of the wheels and the seasonal variation of the materials. This type of approach assumes a linear accumulation of damage to get to failure state.

In the “Incremental-Recursive” instead, the materials properties of the pavement, in terms of damage and aging are updated. The damage is calculated from damage functions and the output from one increment is used, recursively, as input to the next increment, allowing the effects of time and gradual damage to be considered (CalME Manual, 2012).

The “Caltrans” and the “Classical” methods are very fast in terms of computational time, and they are user-friendly. In *CalME* both of these options allow the designer to calculate and realize pavement structures that agree with the design requirements for the design traffic, materials, and climate. These two methods can be used to produce a group of potential pavement sections that certainly meet design requirements, then the Recursive method or the Incremental-Recursive procedure can be run to check the cheapest alternative in the group and select the final pavement section. In addition, the Incremental-Recursive output provides also a prediction of the pavement condition, of its distress and its performance across its entire life (P. Ullidtz et al.2010).

### 3.1.3 CalBack

Caltrans, as part of the development of new ME design procedures, has been developing a sophisticated back-calculation program that parallels CalME for flexible pavement design. *CalBack* (short for *California Back-calculation*) is a software tool developed under the ongoing ME research activities funded by Caltrans under contract with the University of California Pavement Research Center (UCPRC) (Davis and Berkeley), and the Dynatest Group. It is a unique and important addition to the existing knowledge base. It possesses multiple data input/output methods, several new analytical modeling methods, and numerous user performance options (Lu Qing, James

Signore, Ullidtz et al. 2008). The main purpose of CalBack is to provide layer moduli used for rehabilitation design with CalME. Deflections measured through a FWD can be used to determine pavement structural layer moduli and the sub-grade resilient modulus through back-calculation. Back-calculation, utilizing deflection data and the use of multilayer elastic analysis in an iterative procedure, permits to determine the most reasonable set of in situ moduli that will minimize the difference between measured and calculated deflections.

CalBack can be used to analyze flexible, rigid, and composite pavements with the ability to automatically import and analyze data from FWD output files. One of the most important features that makes it a unique and useful tool is expandable nature that allows for further growth of the materials library via inputs from real projects (Lu Qing, James Signore, Ullidtz et al. 2008).

When starting a new project, a CalBack database is created in Microsoft Access format and the FWD raw data are imported (measured deflections). For each layer in the pavement structure a standard material is imported from a CalME design database and a large number of material parameters, that will be needed for the flexible pavement rehabilitation design, such as the asphalt concrete master curve parameters, fatigue parameters and permanent deformations parameters are assigned for that material. The parameters can be edited from *CalBack*.

The layer temperature may be calculated from the measured surface temperature using the Bells equation (Baltzer and Jansen, 1994).

Pavement surface deflections are calculated using the response model. In CalBack are implemented three response models:

- Odemark–Boussinesq;
- WESLEA;
- LEAP.

All these response models have been modified to enable a nonlinear elastic sub-grade, an essential requirement on thin or weak pavement structures. The nonlinear sub-grade modulus model used in *CalBack* is as follows in Equation 3.1:

$$E = C x \left( \frac{\sigma_1}{pa} \right)^n$$

**Equation 3.1.** The nonlinear sub-grade modulus

where:

- E is the sub-grade modulus;

- $\sigma I$  is the major principal stress, positive for compression;
- $p_a$  is a reference stress (atmospheric pressure = 0.1 MPa);
- $C$  and  $n$  are constants ( $n$  being negative).

Based on the imported master curve parameters and Bells temperature, *CalBack* calculates the modulus at a reference temperature, as well as the modulus at the actual temperature of each pavement layer that minimize the difference between measured (FWD data) and calculated deflections (response model)(Lu Qing, James Signore, Ullidtz et al. 2008).

CalBack contains three search engines to determine material moduli:

- a gradient search;
- a Kalman filter;
- a genetic algorithm.

For the gradient search and the genetic algorithm, the minimization may be based on the root mean square (RMS) values of either the absolute or relative differences between measured deflections (with FWD) and calculated deflections (with the response models).

The Kalman filter is a set of mathematical equations that provides an efficient recursive means to estimate the state of a dynamic system from a series of incomplete and noisy measurements.

The results of the back-calculation are stored in the project database and the back-calculated moduli can be imported directly by CalME for use in rehabilitation design (Lu Qing, James Signore, Ullidtz et al. 2008).

## **3.2 CalME Design Methods: The “Caltrans” Empirical Design Methods**

### **3.2.1 R-Value Method for New Pavement**

The first approach used in the software CalME for the design of new flexible pavements is an empirical method named *R-value* design method. It is described in the “Highway Design Manual” (HDM), Chapter 600 and it is based on an empirical relationship, developed by Caltrans through research and field experimentation, between the *Gravel Equivalent* (GE) of the pavement structural materials, the *Traffic Index* (TI), and the *California R-value* (R) of the underlying material.

The procedure for design a Multiple Layered Flexible Pavement using the R-value methods is:

- 1) determination of *TI* to the nearest 0.5;
- 2) determination of the *California R-value* for the sub-grade;
- 3) definition of the *Gravel Factors* (GF) and *Gravel Equivalents* (GE) for all the pavement structural materials;
- 4) prediction of the thickness of each layer.

This method will be mainly explained in Chapter 4.

### **3.2.2 Deflection Reduction Method for Rehabilitation**

In a rehabilitation design of existing pavements the “Caltrans” empirical design approach used in *CalME* is based on the “Flexible Pavement Rehabilitation Manual”, 2001. The empirical method used is the “Deflection reduction method” where deflections are used for determining the thickness requirements for rehabilitation of asphalt concrete (AC) pavements when considering structural section adequacy.

To evaluate an existing flexible pavement structure, surface deflection measurement is a primary means adopted by pavement engineers. Deflection measurements can be used in back-calculation procedures to determine pavement structural layer moduli and the sub-grade resilient modulus. Moreover, an evaluation of pavement deflections versus pavement conditions, permits the establishment of the concept of "tolerable deflection" criteria for a variety of asphalt concrete (AC) structural sections (“Flexible Pavement Rehabilitation Manual”, 2001).

In 1960, California began using deflection data in conjunction with the tolerable deflection as the basis for rehabilitation overlay design. After many years of research into determining asphalt concrete pavement deflections and relating these deflections to pavement performance, the data collection and design procedures were formally adopted in 1969 in the California Test 356 “Methods of Test to Determine Flexible Pavement Rehabilitation Requirements By Pavement Deflection Measurements”.

There are different equipments used to obtain the pavement deflections. Since the early 1960’s, Caltrans research data have been based on deflections obtained by the “*California Traveling Deflectometer*” (CTD), in which a Benkelman Beam is used to measure the deflection at the site. Than from 1980’s it was no longer practical to use the CTD due to the age of its electronics and it has been used other deflection devices such as the Falling Weight Deflectometer and the Dynaflect (Figure 3.1). The CTD is currently used only to correlate other deflection devices (“*Flexible Pavement Rehabilitation Manual*”, 2001).

“California Test Method 356” should be consulted when pavement deflection measurements are obtained with different testing devices. The problem is that each FWD or Dynaflect for deflection measurements has a unique correlation curve. A correlation equation that relates deflection measurements obtained using any deflection device and the deflection measurements obtained using *California Traveling Deflectometer* (CTD) must be developed and used to obtain the equivalent CTD deflection value.

Caltrans investigated the relationship between the CTD deflections and deflections obtained using a special reference FWD (FWDref) able to provide 40 kN peak force and with a loading plate 30 cm in diameter (“*Flexible Pavement Rehabilitation Manual*”, 2001).



Figure 3.1. From left to right: California Traveling Deflectometer, Falling Weight Deflectometer and Dynaflect.

The relationship between deflections obtained using the two devices is expressed by the following Equation (3.2):

$$D(CTD) = 1.2 \times D(FWD_{ref})$$

**Equation 3.2.** Correlation between  $FWD_{ref}$  and CTD

Where  $D$  is deflection value at approximately  $21^{\circ}C$ , the coefficient of determination  $R^2$  for this equation is 0.93, and the number of data points used to derive it is equal to 439.

Therefore, if another deflection device other than the  $FWD_{ref}$ , such as a different FWD or a Dynaflect, is used for measuring deflections, then at first a correlation between that device and the  $FWD_{ref}$  is used and after through equation 2.8 the equivalent CTD deflections for use in the Caltrans flexible pavement rehabilitation design can be find.

By the use of the proper correlation equation, deflections produced by any type of loading device are converted to an equivalent  $CTD$  deflection.

Deflection measurements for each test section should be reviewed prior to compute the mean (3.3), the standard deviation (3.4), and 80th percentile deflection (3.5) (where 20% of the deflections are higher and 80% are lower than this level, and assuming normal probability distribution for the deflection data):

$$\bar{D} = \frac{\sum D_j}{n}$$

**Equation 3.3.** Mean of the  $CTD$  equivalent deflections

$$s_D = \sqrt{\frac{\sum (D_j - \bar{D})^2}{n - 1}}$$

**Equation 3.4.** Standard deviation of the  $CTD$  equivalent deflections

$$D_{80} = \bar{D} + 0.84 \times s_D$$

**Equation 3.5.** 80th percentile of the  $CTD$  equivalent deflections

where:

- $\bar{D}$  = Mean of the  $CTD$  equivalent deflections;
- $D_j$  = An individual (jth)  $CTD$  equivalent deflection;
- $n$  = Total number of deflection measurements;
- $D_{80}$  = 80th percentile of the  $CTD$  equivalent deflections;
- $s_D$  = Standard deviation of the  $CTD$  equivalent deflections.

### 3.3 CalME Design Methods: The “Classical” Mechanistic-Empirical Design Method

#### 3.3.1 Introduction

A Mechanistic-Empirical approach to pavement design consists of two steps. In the first step, through a mechanistic model, making use of fundamental physical properties and simplified assumptions, it predicts the pavement response, in terms of stresses, strains and deflections, caused by a load on the pavement. If the basic assumptions with respect to materials and boundary conditions are correct, this method is valid anywhere and may be used to correctly predict the response for any combination of loads, climatic effects and materials. In the second step, the calculated response (stresses, strains and deflections) is used to predict the pavement performance (cracking, rutting and roughness) using empirical relationship (Figure 3.2)

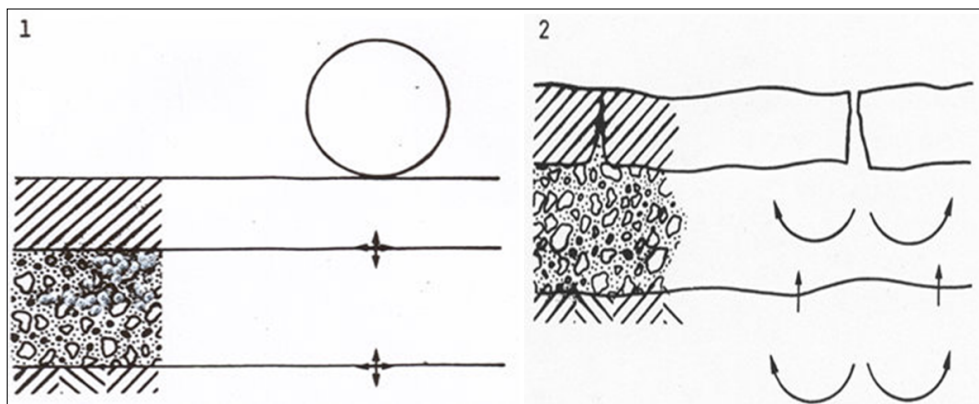


Figure 3.2. Calculation of pavement response (left), prediction of pavement performance (right).

In the CalME “Classical” Mechanistic-Empirical method the pavement response is only calculated from the initial pavement condition.

## 3.3.2 Pavement Response

### 3.3.2.1 Introduction

Mechanistic models predict pavement response in terms of stress, strain and deflection. There are a number of different types of models available today but the most commonly used are the *layered elastic models*. These models can easily be run on personal computers and only require data that can be realistically obtained.

The mechanistic model used in *CalME* to predict the stress, strain and deflection can be choose by the user between three different choices:

- Linear Elastic Theory (LET) based on Burmister's equations and limited to 5 layers;
- A simplified approach based on Odemark's transformations and Boussinesque's equation
- LEAP based on Burmister's equations but with unlimited number of layers.

All these *layered elastic models* provide stress, strain and deflection, resulting from the application of a surface load, at any point in a pavement structure. The main assumption is that each pavement structural layer is homogeneous, isotropic, and linearly elastic. In other words, it is the same everywhere and will rebound to its original form once the load is removed.

The origin of layered elastic theory is credited to V.J. Boussinesque and Burmister. Today, Boussinesque and Burmister's theories, even if are based on simplified assumptions, are still widely used in soil mechanics, foundation and pavement design.

The layered elastic approach works with relatively simple mathematical models and thus, requires some basic assumptions. These assumptions are:

- Pavement layers extend infinitely in the horizontal direction;
- The bottom layer (usually the subgrade) extends infinitely downward;
- Materials are not stressed beyond their elastic ranges (<http://pavementinteractive.org>).

A layered elastic model requires some inputs to adequately characterize a pavement structure and its response to loading. These *inputs* are (Figure 3.3):

- material elastic parameters of each layer: *Modulus of elasticity* (E), *Poisson's ratio* ( $\nu$ );
- layer thicknesses;
- loading conditions: *Magnitude*, *Geometry*, *Repetitions*.

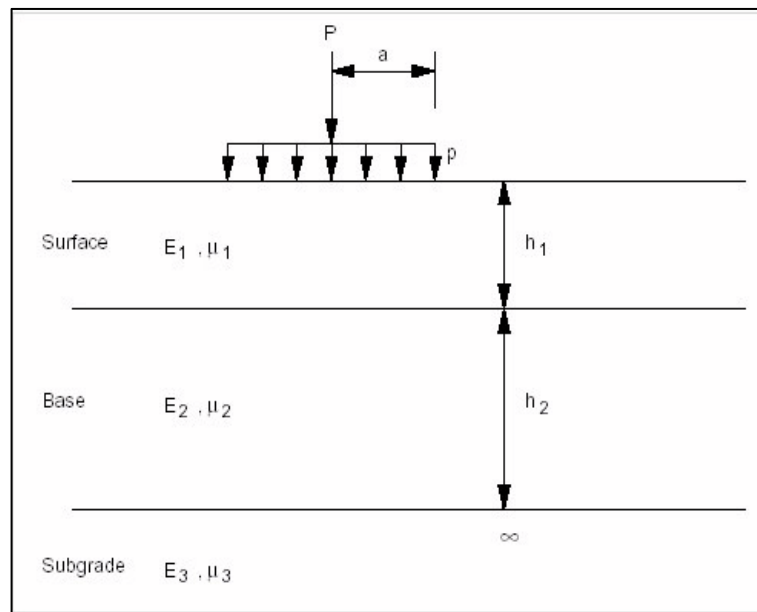


Figure 3.3. Layered elastic inputs

The *outputs* of a layered elastic model are the stress, strain, and deflection in any point of the pavement:

- *Stress*. The intensity of internally distributed forces experienced within the pavement structure at various points. Stress has units of force per unit area ( $\text{N/m}^2$ , Pa or psi).
- *Strain*. The unit displacement due to stress, usually expressed as a ratio of the change in dimension to the original dimension (mm/mm or in/in). Since the strains in pavements are very small, they are normally expressed in term of microstrain ( $10^{-6}$ ).
- *Deflection*. The linear change in a dimension. Deflection is expressed in units of length (mm or  $\mu\text{m}$  or inches or mils).

The use of a layered elastic analysis allows to calculate the theoretical stress, strain, and deflection anywhere in a pavement structure. However, there are a few critical locations that are often used in pavement analysis (Table 3.1, Figure 3.4):

**Table 3.1. Critical locations in a pavement structure.**

<i>Location</i>	<i>Response</i>	<i>Reason for Use</i>
<b>Pavement Surface</b>	Deflection	Used in imposing load restriction during spring thaw and overlay design (for example)
<b>Bottom of HMA layer</b>	Horizontal Tensile Strain	Use to predict fatigue in the HMA
<b>Top of intermediate layer (Base or Subbase)</b>	Vertical compressive strain	Use to predict rutting failure in the base or subbase
<b>Top of Subgrade</b>	Vertical compressive strain	Using to predict rutting failure in the subgrade

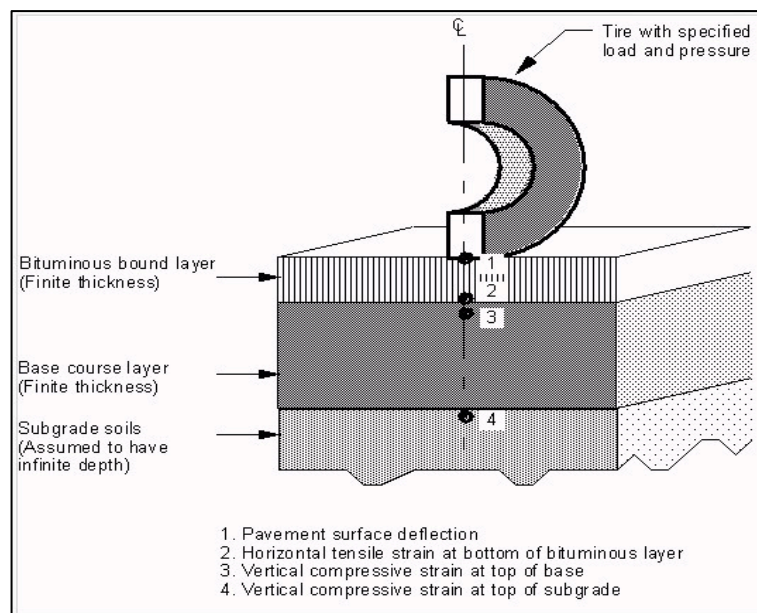


**Figure 3.4. Critical analysis locations in a pavement structure**

### 3.3.2.2 Boussinesque's equations

Boussinesque developed a set of equations to calculate the stress, strain and displacement conditions in a homogeneous, isotropic, linear elastic semi-infinite space under a point load. At the depth 'z' below the centre line of a uniform circular load ' $\sigma_0$ ' with radius 'a', the stress, strain and displacement are given by the following Equations (3.6, 3.7, 3.8, 3.9, 3.10, 3.11):

$$\sigma_z = \sigma_0 \times \left\{ 1 - \frac{1}{\left[ 1 + \left( \frac{a}{z} \right)^2 \right]^{\frac{3}{2}}} \right\}$$

Equation 3.6

$$\sigma_r = \sigma_t = \sigma_0 \times \left\{ \frac{(1 + 2\mu)}{2} - \frac{(1 + \mu)}{\left[ 1 + \left( \frac{a}{z} \right)^2 \right]^{1/2}} + \frac{\frac{1}{2}}{\left[ 1 + \left( \frac{a}{z} \right)^2 \right]^{3/2}} \right\}$$

Equation 3.7

$$\varepsilon_z = (1 + \mu) \times \frac{\sigma_0}{E} \times \left\{ \frac{\left( \frac{z}{a} \right)}{\left[ 1 + \left( \frac{z}{a} \right)^2 \right]^{\frac{3}{2}}} - (1 - 2\mu) \left\{ \frac{\left( \frac{z}{a} \right)}{\left[ 1 + \left( \frac{z}{a} \right)^2 \right]^{\frac{1}{2}}} - 1 \right\} \right\}$$

Equation 3.8

$$d_z = (1 + \mu) \times \sigma_0 \times \frac{a}{E} \times \left\{ \frac{1}{\left[ 1 + \left( \frac{z}{a} \right)^2 \right]^{\frac{1}{2}}} + (1 - 2\mu) \times \left\{ \left[ 1 + \left( \frac{z}{a} \right)^2 \right]^{\frac{1}{2}} - \frac{z}{a} \right\} \right\}$$

Equation 3.9

$$R = E \times \frac{a / [(1 - \mu^2) \times \sigma_0]}{\left\{ 1 + \left[ 1 + \frac{3}{\frac{2}{(1 - \mu)}} \right] \times \left( \frac{z}{a} \right)^2 \right\} \times \left[ 1 + \left( \frac{z}{a} \right)^2 \right]^{\frac{5}{2}}}$$

Equation 3.10

$$\varepsilon_r = \frac{z}{2R}$$

Equation 3.11

where:

-  $\sigma_z$  is the vertical stress;

- $\sigma_r$  is the radial stress;
- $\sigma_t$  is the tangential stress;
- $\epsilon_z$  is the vertical strain;
- $d_z$  is the vertical displacement;
- R is the radius of curvature;
- E is the modulus and
- $\mu$  is the Poisson ratio.

### **3.3.2.3 Burmister's Elastic Models**

Pavement systems typically have a layered structure with stronger/stiffer materials on top instead of a homogeneous mass as assumed in Boussinesque's theory. Therefore, a better theory is needed to analyze the behavior of pavement.

Burmister (1943) was the first to obtain the solution to calculate stress, strain and displacement in two-layered flexible pavement systems.

The basic assumptions for all Burmister's models include:

- The pavement system consists of several layers; each layer is homogeneous, isotropic, and linearly elastic with an elastic modulus and Poisson's ratio (Hooke's law).
- Each layer has a uniform thickness and infinite dimensions in all horizontal directions, resting on a semi-infinite elastic half-space.
- Before the application of external loads, the pavement system is free of stresses and deformations.
- All the layers are assumed to be weightless.
- The dynamic effects are assumed to be negligible.
- Either of the two cases of interface boundary conditions given below is satisfied:
  - 1) fully bonded: at the layer interfaces, the normal stresses, shear stresses, vertical displacements, and radial displacements are assumed to be the same.
  - 2) frictionless interface: the continuity of shear stress and radial displacement is replaced by zero shear stress at each side of the interface (Mohamed Hamdallah El-shaer).

Burmister derived the stress and displacement equations for two-layer pavement systems from the equations of elasticity for the three-dimensional problem solved by Love (1923) and Timoshenko (1934). To simplify the problem, Burmister assumed Poisson's ratio to be 0.5. He found the stress and deflection were dependent on the ratio of the modulus of subgrade to the modulus of the pavement ( $E_2/E_1$ ) as shown in Figure 3.5:

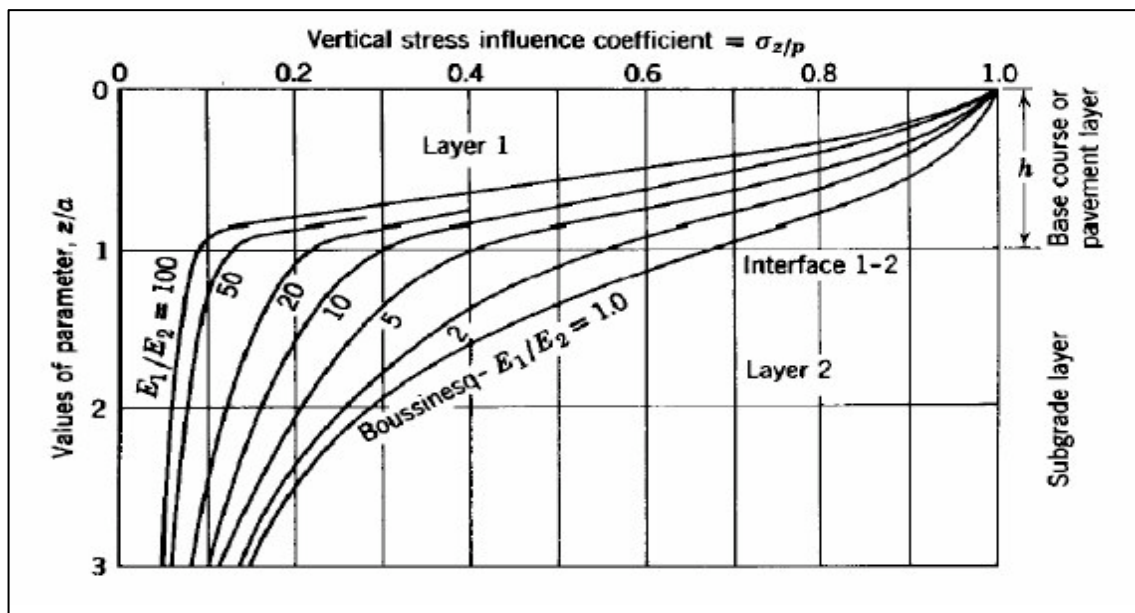


Figure 3.5: Vertical Stress in a Two-layer System

To attain a closer approximation of an actual pavement system, Burmister extended his solutions to a three-layer system (Burmister, 1945) and derived analytical expressions for the stress and displacement.

Then Schiffman (1962) completed Burmister work developing a general solution to the analysis of stress and displacement in a N-layer elastic system (Mohamed Hamdallah El-shaer).

His solution provides an analytical theory for the determination of stress and displacement of a multi-layer elastic system subjected to non-uniform normal surface loads, tangential surface loads, rigid, semi-rigid and slightly inclined plate bearing loads.

### **3.3.2.4 Odemark's Method of the Equivalent Thickness**

Boussinesque's equations are only applicable to a homogeneous layer. In practice, most pavement structures are not homogeneous but are layered systems. Odemark developed an approximate method to transform a system consisting of layers with different moduli into an equivalent system where the thicknesses of the layers are altered but all layers have the same

modulus. This is known as the *Method of Equivalent Thickness*. The transformation, expressed by the equation 3.12, assumes that the stiffness of the layer remains constant.

$$\frac{I \times E}{(1 - \mu^2)} = \text{const}$$

**Equation 3.12.** Constant stiffness of the layer

where:

- I = moment of inertia;
- E = layer modulus;
- $\mu$  = Poisson ratio.

Since I is a function of the cube of the layer thickness, the equivalent thickness transformation for a layer with thickness =  $h_1$ , modulus =  $E_1$ , and Poisson ratio  $\mu_1$  into a layer with equivalent thickness  $h_e$ , modulus  $E_2$ , and Poisson ratio  $\mu_2$  may be expressed as follows (Equation 3.13):

$$h_e = h_1 \times \left[ \frac{E_1}{E_2} \times \frac{(1 - \mu_2^2)}{(1 - \mu_1^2)} \right]^{\frac{1}{3}}$$

**Equation 3.13.** Odemark's transformation (Method of the equivalent thickness)

Since this is an approximate method, an adjustment factor ' $f$ ' is applied to the right hand side of the above equation to obtain a better agreement with elastic theory. The value of ' $f$ ' depends on the layer thicknesses, modular ratios, Poisson ratios and the number of layers in the pavement structure. Furthermore, the Poisson ratio for all pavement materials can be assumed to be the same, usually equal to 0.35. The equivalent thickness equation can therefore be expressed as (Equation 3.14):

$$h_e = f \times h_1 \times \left[ \frac{E_1}{E_2} \right]^{\frac{1}{3}}$$

**Equation 3.14.** Approximated Odemark's transformation (Method of the equivalent thickness)

To analyze a multi-layer pavement structure with known layer moduli, the layers can be transformed into an equivalent system with a homogeneous layer modulus equal to the modulus of the semi-infinite subgrade layer by applying Odemark's transformation.

Boussinesque's equations can then be applied to calculate the stress, strain and displacement conditions within the equivalent layered system ("*Guidance Notes on Back-calculation of layer moduli and estimation of residual life using falling weight Deflectometers test data*", 2000)

### 3.3.3 Pavement performance

#### 3.3.3.1 Design Criteria

After the prediction of the pavement response in terms of stress, strain and deflection through the mechanistic models, the second step in a ME design method is the simulation of the pavement performance (cracking, rutting and roughness) using empirical equations.

These empirical equations, derived from observing the performance of pavements and relating the type and extent of observed failure to an initial strain under various loads, are used to compute the number of loading cycles to failure. These equations define a *Design Criteria*.

Two types of failure criteria are mainly recognized, one relating to fatigue cracking and the other to rutting initiating in the subgrade. Since these failure criteria are empirically established, they must be calibrated to specific local conditions and are generally not applicable on a national and international scale. Many of these empirical equations have been developed to estimate the number of repetitions to failure in the fatigue and rutting mode for asphalt concrete (<http://pavementinteractive.org>).

The *Design Criteria*, used either for asphalt material (AC) or unbound material (UB), can be input in the format of Equation 3.15:

$$\text{Permissible response} = CA \times MN^{c\alpha} \times \left( \frac{E}{E_{ref}} \right)^{c\beta}$$

**Equation 3.15.** Format of the Design Criteria

where:

- MN is the number of loads in millions;
- E is the modulus of the material;

- $E_{ref}$  is a reference modulus (The reference modulus can be freely chosen, but it is practical to select a value that is typical for the material);
- CA,  $c\alpha$  and  $c\beta$  are constants;
- *Permissible response* may be either the vertical compressive strain or stress at the top of a layer or the maximum horizontal strain or stress at the bottom of a layer.

The “Classical” design is based on vertical or horizontal stresses or strains. In the database stresses are indicated by type “z” and strain by type “e”. Horizontal is indicated by “h”, vertical by “v”.

For structural deterioration (cracking) of a layer the permissible response is the horizontal tensile stress or strain (“zh”, “eh”) at the bottom of the layer.

Functional deterioration (rutting or roughness) is predicted from the vertical compressive stress or strain (“zv”, “ev”) on the top of the layer (*CalME Manual*). If the modulus and the response are known, the permissible number of load applications, in millions, may be found from Equation 3.16.

$$MNp = \left[ \frac{response}{CA} \times \left( \frac{E}{E_{ref}} \right)^{-c\beta} \right]^{\frac{1}{c\alpha}}$$

**Equation 3.16.** Number of load applications to failure

The permissible number of load applications (MNp) predicted with the Equation 3.16 should be compared with the number of load applications expected during the pavement design life.

Design criteria are often given in another format (Equation 3.17):

$$N = k_1 \times response^{k_2} \times E^{k_3}$$

**Equation 3.17.** Different format of the design criteria.

Many *Design Criteria* have been developed to estimate the number of repetitions to failure. In the table "*Criteria*" in the *CalME* database DesignData.mdb can be seen the different *Design Criteria* used in the *CalME* “Classical” methods and the value of the parameters CA,  $c\alpha$ ,  $c\beta$  and  $E_{ref}$  (Table 3.2).

Table 3.2. Types of criteria and corresponding parameters

Name	Material	CA	C $\alpha$	E <sub>ref</sub>	C $\beta$	Response
Kirk	AC	-195	-0.178	3000	0	eh
Ciannini & Camomilla	AC	-142	-0.234	3000	0	eh
South Africa gap graded	AC	-527	-0.137	3000	0	eh
South Africa continuous	AC	-279	-0.183	3000	0	eh
Nottingham hot rolled	AC	-209	-0.204	3000	0	eh
Nottingham DBM pen100	AC	-133	-0.285	3000	0	eh
Nottingham DBM pen200	AC	-94	-0.347	3000	0	eh
Shell 1978, 50%	AC	-538	-0.25	3000	0	eh
Shell 1978, 85%	AC	-403	-0.25	3000	0	eh
Shell 1978, 95%	AC	-344	-0.25	3000	0	eh
NCHRP 1-10b	AC	-240	-0.3039	3000	-0.26	eh
Corps of Engineers	AC	-214	-0.2	3000	-0.533	eh
Shell 1978, 50%	UB	885	-0.25	160	0	ev
Shell 1978, 85%	UB	664	-0.25	160	0	ev
Shell 1978, 95%	UB	567	-0.25	160	0	ev
Asphalt Institute	UB	482	-0.223	160	0	ev
Nottingham	UB	454	-0.28	160	0	ev
South Africa termianl psi=1.5	UB	1005	-0.1	160	0	ev
South Africa termianl psi=2.0	UB	728	-0.1	160	0	ev
South Africa termianl psi=2.5	UB	495	-0.088	160	0	ev
NAASRA	UB	1212	-0.141	160	0	ev
Kirk E<160 MPa, R=1.5	UB	0.145	-0.307	160	1.16	zv
Kirk E>160 MPa, R=1.5	UB	0.145	-0.307	160	1	zv
Asphalt Institute	AC	-240	-0.3039	3000	-0.26	eh
Ullidtz	AC	-246	-0.25	3000	-0.5	eh

### 3.3.3.2 Default Design Criteria in CalME

The *Asphalt Institute AC Criteria* is the default criteria in CalME for cracking of asphalt concrete. It is given in the format of Equation 3.18.

$$N = 18.4 \times 4.325 \times 10^{-3} \times 10^{4.48 \times \left( \frac{V_b}{V_b + V_v} - 0.69 \right)} \times \varepsilon_t^{-3.291} \times |E^*|^{-0.854}$$

**Equation 3.18.** Asphalt Institute AC Criteria

where:

- N is the permissible number of loads (to 45% fatigue cracking);
- $\varepsilon_t$  is the horizontal tensile strain at the bottom of the asphalt later in mm/mm (or inch/inch);
- $|E^*|$  is the (complex) modulus in psi;
- $V_b$  is the volume percent bitumen in the mix;
- $V_v$  is the volume percent of air voids;

It is assumed that the volume percent binder is 11,1 and the air void percent is 5. Equation 3.19 with this content of binder and air void becomes:

$$N = 0.07958 \times \varepsilon_t^{-3.291} \times |E^*|^{-0.854}$$

**Equation 3.19.** Asphalt Institute AC Criteria with  $V_b=11.1$  and  $V_v=5$

The *Asphalt Institute AC Criteria* for cracking of asphalt concrete in the format of Equation 3.15 is (Equation 3.20):

$$\text{Permissible strain} = 240 \mu\text{strain} \times MN^{-0.304} \times \left( \frac{E}{3000 \text{MPa}} \right)^{-0.259}$$

**Equation 3.20.** Asphalt Institute AC Criteria in an alternative format

Where the permissible strain is the horizontal tensile strain (“eh”) at the bottom of the asphalt layer. In CalME compression is positive and tension is negative, so the permissible strain in this case must be given as  $-240 \mu\text{strain}$ .

The *Asphalt Institute UB Criteria* is the default criteria in CalME for unbound materials, corresponding to 12.5 mm of rutting. It is given in the format of Equation 3.21:

$$\text{Permissible strain} = 482 \mu\text{strain} \times MN^{-0.223}$$

**Equation 3.21.** Asphalt Institute UB Criterion

Note that the constant  $c\beta$  is 0 for subgrade, so that the permissible strain, for a given number of load repetitions, is the same for all materials. The permissible response is the *vertical strain* (“ev”).

Alternatively, a stress criterion for unbound materials can be used. Equation 3.22 was derived from the *AASHTO Road Test* by J.M. Kirk:

$$\text{Permissible stress} = 0.137 \text{MPa} \times (MN \times R)^{-0.3067} \times \left( \frac{E}{160 \text{MPa}} \right)^{c\beta}$$

**Equation 3.22.** J.M. Kirk Criterion for unbound material

where R is the regional factor, and  $c\beta = 1.16$  for  $E < 160$  MPa, else  $c\beta = 1.0$ . The permissible response is the *vertical stress* (“zv”).

It should be noticed that the three criteria given above (Equations 3.20, 3.21 and 3.22) include a certain lateral wander of the wheels. If the wander is treated explicitly, for example by including a pass/coverage ratio, the criteria should be modified for the pass/coverage ratio for which they were developed. If, for example, the pass/coverage ratio was 2 when the criterion was developed, the constant CA should be multiplied by  $2^{c\alpha}$ . For the three criteria given above the constant CA would change as follow:

**Equation 3.23:**  $CA = -240 \mu\text{strain} * 2^{-0.34} = -194 \mu\text{strain};$

**Equation 3.23 :**  $CA = 482 \mu\text{strain} * 2^{-0.223} = 413 \mu\text{strain};$

**Equation 3.24:**  $CA = 0,137 \text{MPa} * 2^{-0.3067} = 0.111 \text{MPa}.$

## **3.4 CalME Design Methods: The “Incremental-Recursive” procedure**

### **3.4.1 Introduction**

The *Incremental-Recursive ME method (I-R)* is a procedure that works in increments of time and uses the output from one increment, recursively, as input to the next increment. The procedure, at each increment of time, predicts the pavement conditions, in terms of layer moduli, crack propagation, permanent deformation and roughness.

“*Classical*” and “*Caltrans*” methods are very fast in terms of computational time. They can be used to calculate and realize pavement structures that agree with the design requirements for the design traffic, materials, and climate. *I-R* procedure does not carry out an automatic design; the output of this procedure is not the layer thicknesses to achieve certain pavement conditions at the end of the design life. For this reason, “*Classical*” and “*Caltrans*” methods can be used to produce a group of potential pavement sections that meet design requirements, then the *I-R procedure* may be used to check these pavements.

The default duration of each increment is 30 days. The program will select the day in the middle of the first increment (10/12/2010 + 30/2 days) as being representative for the climatic conditions during that increment. The representative day is divided into periods. The default division is into 5 periods of 4, 4, 5, 5, and 6 hours, starting at 1 pm.

The program will select the hour corresponding to the middle of each time period during the representative day and will calculate the temperature and the modulus of the asphalt layers.

The temperature at the surface is read from the *EICM.mdb database*, that contains surface temperatures pre-calculated for each hour of a 30 years period for a number of Climate Zones and different pavement structures in California.

Then, using a *1-D Galerkin Finite Element* formulation, CalME will determine the temperature at one-third depth of each asphalt layer. The temperature at this depth has been found to correspond reasonably well to the “mean effective” temperature of the layer. If the temperature database (EICM.mdb) is not available, CalME will calculate the temperature from the Equations 3.26,3.27:

$$t_1 = t_{YearMean} + \frac{YearRange}{2} \times \left(1 - \frac{z}{1000}\right) \times \sin\left(\pi \cdot \frac{h}{4380} - \frac{\pi}{2} - \frac{\pi}{12}\right)$$

$$t = t_1 + \frac{DayRange}{2} \times \left(0.11 \cdot \left(\frac{z}{100}\right)^2 - 0.66 \cdot \frac{z}{100} + 1\right) \times \sin\left(\pi \cdot \frac{h}{12} - \frac{\pi}{2} - \frac{3\pi}{12}\right)$$

**Equation 3.26 and Equation 3.27.** Temperature at a particular depth (z)

where:

- $t_{YearMean}$  is the mean yearly surface temperature (°C);
- YearRange is the yearly range in surface temperature (°C);
- DayRange is the daily range in surface temperature (°C);
- z is the depth (mm);
- h is the hour counted from the start of the year.

The Yearly Mean, Yearly Range and Daily Range temperatures are stored in the “Climate zone” Table in the CalME database *DesignData.mdb*.

Due to determine the modulus of each asphalt layer, their master curves are used with the temperature at one third depth of each asphalt layer and the loading time, that depend on the vehicle speed and on the depth in the structure. The modulus may also be influenced by existing damage to the layer and by aging/hardening.

For the unbound materials the moduli are modified according to season. Moduli of the unbound materials may also be influenced by the stiffness of the pavement layers above the material and by the load level.

When the layers modulus have been determined for the first time period of the first increment using the hour corresponding to the middle of the period during the representative day, the response, in term of stresses and strains, at the center line of the wheel or of one of the wheels, in a dual-wheel, is calculated for each load of the load spectrum (WIM station), at each load position using a response model: LET, Boussinesque-Odemark, LEAP (no more used in 2012 CalME version).

If the calculation considers wheel wander, the passages of each load will be assumed to be normally distributed laterally, with an offset and standard deviation given in the “Wheels” table in CalME database *DesignData.mdb*. The number of wheel loads corresponding to each wheel position, are calculated from the normal distribution, and the damage is accumulated at an offset of 0.

The increase in fatigue damage and in permanent deformations during a period of the increment is calculated for each load and load position, for each layer using the fatigue and permanent deformation models and a particular procedure, named “*Time hardening*”.

Before proceeding to the next increment, the process must be repeated recursively, using output from each calculation as input to the next, for all loads at each position and for all the increment periods.

### 3.4.2 CalME Models used in the I-R procedure

#### 3.4.2.1 Asphalt Concrete Master Curve

Asphalt mixes stiffness is a fundamental material property, which can be measured using various test equipments and test methods.

Before talking about the asphalt concrete stiffness model (Master Curve) used in CalME it is important to recall the essential concepts of linear visco-elasticity of asphalt mixes. For the one-dimensional case of a sinusoidal loading (Figure 3.6), the following Equation (3.28) can represent the stress:

$$\sigma = \sigma_0 \cdot \sin(\omega t)$$

**Equation 3.28.** Sinusoidal loading.

where:

- $\sigma_0$  is the stress amplitude;
- $\omega$  is the angular velocity, related to the frequency  $f$ . ( $\omega = 2\pi f$ )

The resulting strain can be written as (Equation 3.29):

$$\varepsilon = \varepsilon_0 \cdot \sin(\omega t - \delta)$$

**Equation 3.29.** Resulting strain.

where:

- $\varepsilon_0$  is the strain amplitude;
- $\delta$  is the phase angle related to the time the strain lags the stress.

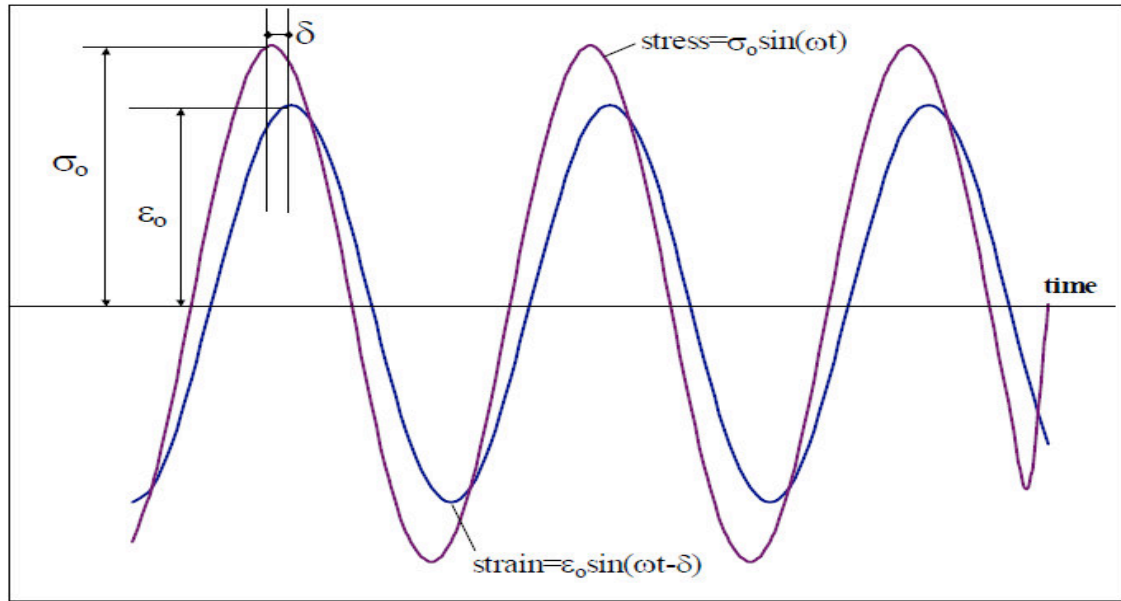


**Figure 3.6:** stress and strain in dynamic loading.

The Phase angle  $\delta$  is an indicator of the visco-elastic properties of the material. For a pure elastic material,  $\delta = 0^\circ$ , and for a pure viscous material,  $\delta = 90^\circ$ .

The absolute value of the dynamic modulus is defined as the ratio of the stress to strain amplitudes. We can define the *storage modulus (elastic)* (Equation 3.30):

$$E' = \frac{\sigma_0 \cos(\delta)}{\epsilon_0}$$

**Equation 3.30.** Elastic modulus.

and the *loss modulus (plastic)* (Equation 3.31):

$$E'' = \frac{\sigma_0 \sin(\delta)}{\epsilon_0}$$

**Equation 3.31.** Plastic modulus.

The stress and strain expressed in complex form can be seen in Equation 3.32 and 3.33:

$$\sigma^* = \sigma_0 e^{i\omega t}$$

**Equation 3.32.** Sinusoidal loading in complex form.

$$\varepsilon^* = \varepsilon_0 e^{i(\omega t - \delta)}$$

**Equation 3.33.** Strain in complex form.

From equations mentioned above the complex modulus,  $E^*(i\omega)$ , is defined as the complex quantity (Equation 3.34):

$$E^*(i\omega) = \frac{\sigma^*}{\varepsilon^*} = \frac{\sigma_0}{\varepsilon_0} \cdot e^{i\delta} = E' + iE''$$

**Equation 3.34.** Complex modulus.

The real part of the complex modulus is the *storage modulus (elastic)* and the imaginary part is the *loss modulus (plastic)*. The *Dynamic Complex modulus* is the absolute value of the complex modulus (Equation 3.35):

$$|E^*| = \frac{\sigma_0}{\varepsilon_0}$$

**Equation 3.35:** Dynamic Complex modulus.

The 2002 mechanistic–empirical pavement design guide developed in NCHRP Project 1-37A recommends the use of the complex modulus of asphalt mixes as a parameter in the design procedure. The modulus of asphalt materials changes with temperature, frequency/ loading time, age and damage. For this reason, its accurately determination over a wide range of temperatures and frequencies is an important priority.

For intact asphalt materials the variation of modulus with temperature and frequency/loading time is described through the *Master Curve*. The *Master Curve* of an asphalt mix allows comparisons to be made over extended ranges of frequencies or temperatures. *Master Curves* are generated using the time-temperature superposition principle. This principle allows for test data collected at different temperatures and frequencies to be shifted horizontally relative to a reference temperature or frequency, thereby aligning the various curves to form a single master curve. To accurately determine the complex modulus AASHTO recommends to test at least two replicate specimens at five temperatures between  $-10^\circ\text{C}$  and  $54.4^\circ\text{C}$  ( $14^\circ\text{F}$  and  $130^\circ\text{F}$ ) and six frequencies between 0.1 and 25 Hz.

The shift factor,  $\alpha(T)$ , defines the required shift at a given temperature. The actual *loading time* is divided by this shift factor to get a *reduced time* (Equations 3.36 and 3.37),  $t_r$ , for the master curve:

$$tr = \frac{t}{a(T)}$$

$$\log(tr) = \log(t) - \log(a(T))$$

**Equation 3.36 and Equation 3.37.** Reduced time as a function of the loading time and the shift factor.

The master curve for a material can be constructed using an arbitrarily selected reference temperature,  $T_R$ , to which all data are shifted. At the reference temperature, the shift factor is  $a(T)=1$ .

The *Asphalt Concrete Master Curve Model* used in the Incremental-Recursive procedure in CalME is the same model used in the report NCHRP 1-37A. The dynamic modulus can be represented by the Master Curve as a sigmoidal function (Equation 3.38):

$$\log(E^*) = \delta + \frac{\alpha}{a + \exp(\beta + \gamma \log(tr))}$$

**Equation 3.38.** Asphalt modulus versus reduced time

where:

- E is the modulus in MPa;
- $tr$  is reduced time in sec, the time of loading at the reference temperature;
- $\alpha, \delta, \beta, \gamma$  are fitting parameters describing the shape of the sigmoidal function.

The sigmoidal function describes the time dependency of the modulus at the reference temperature. The fitting parameters  $\alpha, \delta$  depend on aggregate gradation, binder content and air void content. The fitting parameters  $\beta, \gamma$  depend on the asphalt binder characteristics and on the magnitude of  $\alpha$  and  $\delta$ . Reduced time ( $tr$ ) in CalME is modeled as a function of temperature, of the loading time and of the viscosity (Equation 3.39).

$$tr = lt \times \left( \frac{visc_{ref}}{visc} \right)^{aT}$$

**Equation 3.39.** Reduced time as a function of loading time and viscosity

where:

- $lt$  is the loading time (in sec),

- $vis_{ref}$  is the binder viscosity at the reference temperature,
- $visc$  is the binder viscosity at the present temperature, and
- $aT$  is a constant.

Viscosity is found from Equation 3.40:

$$\log(\log(visc \text{ cPoise})) = A + VTS \times \log(t_R)$$

**Equation 3.40.** Binder viscosity, cPoise, as function of temperature

Where:

- $t_R$  is the temperature (in °Ranking);
- $A$  and  $VTS$  are constants;
- $visc$  indicates the viscosity;
- $cPoise$  indicates units of centipoises.

The values  $A$  and  $VTS$  depend on the asphalt penetration grade according to the NCHRP 1-37A Design Guide (Table 3.3). These parameters could be estimated from the *Dynamic Shear Rheometer Test* conducted in accordance with AASHTO T315 “*Determining the Rheological of Asphalt Binder Using a Dynamic Shear Rheometer (DSR)*”.

**Table 3.3. Dependence of A and VTS on Asphalt penetration grade given for temperature in °R**

Grade	$A$	$VTS$
40-50	10.5254	-3.5047
60-70	10.6508	-3.5537
85-100	11.8232	-3.6210
120-150	11.0897	-3.7252
200-300	11.8107	-4.0068

An example of CalME Master Curve can be seen in Figure 3.7:

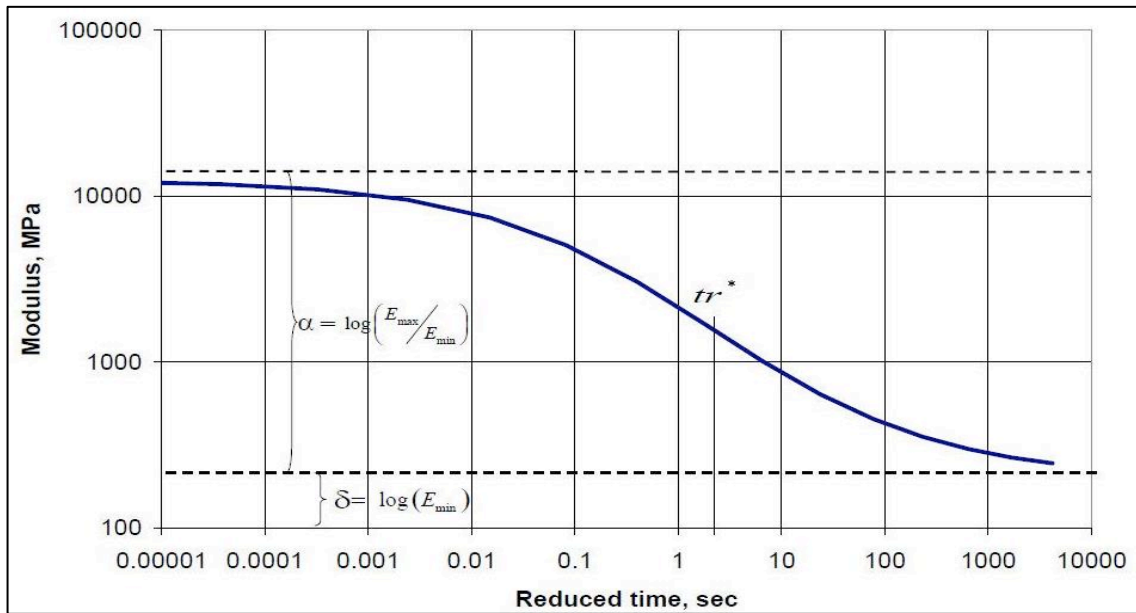


Figure 3.7. Example of modulus versus reduced time relationship

In a laboratory test, the loading time is the time between two following loading cycles and it is easy to identify. In the reality the loading time is a rather uncertain notion. It is determined from the speed of the wheel and from the depth at which the loading time is desired. The loading time ( $lt$ ) is calculated from Equation 3.41.

$$lt = \frac{200 + \frac{\text{layer depth (mm)}}{3}}{\text{wheel speed}(\frac{\text{mm}}{\text{s}})}$$

Equation 3.41. Loading time function of wheel speed and layer depth.

The complex modulus Master Curve can be obtained for a new layer from *Flexural Controlled-Deformation Frequency Sweep Tests* following the Modified AASHTO T-321 (*AASHTO T321*, 2007). For constructed layers, the Master Curve can be evaluated through back-calculation from *Falling Weight Deflectometer (FWD) Tests*.

The measured moduli can be fitted to the Master Curve model (Equation 3.38) minimizing the Root Mean Square (RMS) of the difference between the measured values and the calculated values through Equation 3.38. With this procedure the constants  $a$ ,  $\beta$ ,  $\gamma$ ,  $aT$  can be evaluated; all the remaining parameters, such as the constant  $\delta$ ,  $A$  or VTS are considered fixed.

It should be noted that usually  $\delta$  in the Master Curve model is typically fixed at 2.301, indicating a fixed value for a minimum stiffness of 200 MPa.

### **3.4.2.2 Aging of Asphalt Binder and Hardening of Asphalt Mixes**

For pavement design it is important to quantify the effects of changes in air-void content and asphalt properties on the aging characteristics of asphalt concrete. Aging affects both the stiffness and the fatigue characteristics of the asphalt mix.

Asphalt binder physical properties change with age. In general, as an asphalt binder ages, its viscosity increases and it becomes stiffer and more brittle. Asphalt binder aging is usually split up into two categories:

- *Short-term aging*: This occurs when asphalt binder is mixed with hot aggregates in an HMA.
- *Long-term aging*: This occurs after HMA pavement construction and is generally due to environmental exposure and loading.

It is a result of a number of factors:

- *Oxidation*. The reaction of oxygen with the asphalt binder.
- *Volatilization*. The evaporation of the lighter constituents of asphalt binder. It is primarily a function of temperature and occurs principally during HMA production.
- *Polymerization*. The combining of like molecules to form larger molecules. These larger molecules are thought to cause a progressive hardening.
- *Thixotropy*. The property of asphalt binder whereby it "sets" when unagitated. Thixotropy is thought to result from hydrophilic suspended particles that form a lattice structure throughout the asphalt binder. This causes an increase in viscosity and thus, hardening (Exxon, 1997). Thixotropic effects can be somewhat reversed by heat and agitation. HMA pavements with little or no traffic are generally associated with thixotropic hardening.
- *Syneresis*. The separation of less viscous liquids from the more viscous asphalt binder molecular network. The liquid loss hardens the asphalt and is caused by shrinkage or rearrangement of the asphalt binder structure due to either physical or chemical changes. Syneresis is a form of bleeding (Exxon, 1997).
- *Separation*. The removal of the oily constituents, resins or asphaltenes from the asphalt binder by selective absorption of some porous aggregates (Vallerga, Monismith and Grahthem, 1957).

Also the reduction in air void content caused by traffic, could increase the Asphalt mixes stiffness.

In *CalME*, a simple model is used to describe these two effects (Equation 3.42):

$$E(d1) = E(d0) \times \frac{AgeA \times \ln(d1) + AgeB}{AgeA \times \ln(d0) + AgeB}$$

**Equation 3.42.** Hardening model of asphalt mixes used in CalME

where:

- $E(d1)$  is the modulus after  $d1$  days;
- $d0$  is the initial age in days number;
- $E(d0)$  is the modulus at the initial age  $d0$  (the value given in the grid of the Structural form);
- $AgeA$  and  $AgeB$  are constants ( $AgeB$  may be fixed to 1).

### **3.4.2.3 Effect of seasonal variations on unbound materials**

The unbound materials moduli are affected by seasonal variations. Two types of seasonal effects on unbound materials may be considered:

- moisture content effect;
- thawing effect.

The *moisture content* effect on the modulus of the unbound materials is a sinusoidal variation with time during the year. The modulus at a given day, counted from January 1, is calculated using Equation 3.43.

$$E = E_{mean} \times \frac{1 + ERange}{2 \cdot \sin\left(\frac{2\pi(Day - MaxDay)}{365} + \frac{\pi}{2}\right)}$$

**Equation 3.43.** Moisture effect on the moduli of the unbound materials

where:

- $E_{mean}$  is the modulus given in the *Structural Form* (MPa);

- $ERange$  is the relative range in modulus during the year;
- $Day$  is the day number counted from the start of the year;
- $MaxDay$  is the day with maximum modulus.

Turning to the *thawing effect*, if a material was frozen and then thaws, the modulus is multiplied by a *Frost Reduction Factor* ( $R$ ) (Equation 3.44):

$$R = 1 - [(1 - R_0) \cdot \exp(A \cdot DaysFrost)]$$

**Equation 3.44.** Effect of thawing on moduli of unbound materials

where:

- $R_0$  is the maximum frost reduction;
- $A$  is the recovery rate;
- $DaysFrost$  are the days since frost.

#### **3.4.2.4 Effect of confinement and load level variations on unbound materials**

The modulus of unbound materials could vary with the stiffness of the above asphalt layers. This could happen both when the variation in stiffness was due to temperature variations and when it was due to the asphalt fatigue damage.

To describe this stiffness variation in the unbound layers due to *confinement effect*, it is used a relationship in which the unbound material modulus is a function of the combined bending resistance of the  $n-1$  layers above them (Equations 3.45, 3.46):

$$E_n = E_{nref} \times \left[ 1 - \left( 1 - \frac{S}{S_{ref}} \right) \times Stiffness\ factor \right]$$

$$S = \left( \sum_1^{n-1} h_i \cdot \sqrt[3]{E_i} \right)^3$$

**Equation 3.45 and Equation 3.46.** Modulus of an unbound material as a function of confinement.

where:

- $E_n$  is the modulus of the unbound material;

- $E_{nref}$  is the modulus of layer  $n$  at a bending stiffness  $S = S_{ref}$ ;
- $S$  is the bending stiffness;
- $h_i$  is the thickness of layer  $i$ ;
- $E_i$  is the modulus of the layer  $i$ ;
- $S_{ref}$  and *Stiffness factor* are constants that can be determined through calibration studies.

The stiffness of an unbound material is also a function of the *load level* (Equation 3.47). An higher load level increases the moduli for the granular layers and decreases the modulus for the subgrade.

$$E_p = \left( \frac{P}{40 \text{ KN}} \right)^\alpha \times E_{40\text{KN}}$$

**Equation 3.47.** Modulus of an unbound material as a function of the load level

where:

- $E_p$  is the modulus at wheel load  $P$  in KN;
- $P$  is the wheel load;
- $E_{40\text{KN}}$  is the modulus at a wheel load of 40 kN;
- $\alpha$  is a constant (positive for granular materials and negative for cohesive).

### **3.4.2.5 Damage functions and the Time-Hardening procedure**

In the ME design methods, through empirical equations the number of loading cycles to failure or permissible number of loads can be computed (Equation 3.48).

$$MNp = \left[ \frac{\text{response}}{CA} \times \left( \frac{E}{E_{ref}} \right)^{-c\beta} \right]^{\frac{1}{c\alpha}}$$

**Equation 3.48.** Number of loading applications to failure

There are *design criteria* for different failure conditions: fatigue cracking, rutting, roughness or crushing.

With the Asphalt Institutes AC criteria, for example, the pavement at failure has fatigue cracking over 20% or more of the total pavement area (Figure 3.8) (*CalME* manual). To pass from the

original condition to the failure condition, the pavement during its design life accumulates *damage* (fatigue or permanent deformation).

Originally, CalME used Miner's law to sum the damage over all of the time increments during one year. Miner's law assumes that the damage accumulates linearly with the number of loads (Figure 3.9).

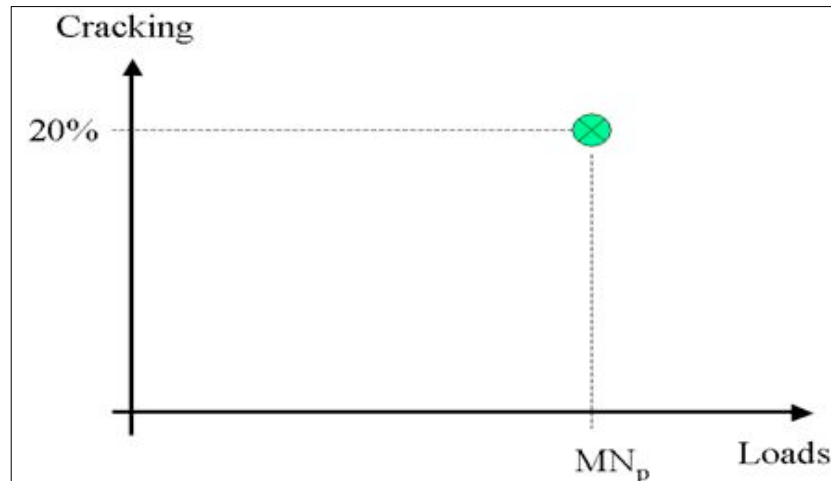


Figure 3.8. Asphalt Institute AC criteria for AC. (20% fatigue cracking as failure condition)

For each wheel load, at each position, the *damage* was calculated as (Equation 3.49):

$$Damage = \frac{MN}{MN_p}$$

Equation 3.49. Damage

The permissible number of loads ( $MN_p$ ) was determined from the calculated response and the design criteria chosen through Equation 3.48. Then the damage was added linearly using Miner's law without any influence of the existing damage. The failure condition was  $Damage = 1$  and the design life is the number of years required to reach a Damage of 1. There was no information on how the damage progresses from 0 to 1. It could be assumed that the development of damage could be described by Equation 3.50:

$$Damage = \left( \frac{MN}{MN_p} \right)^\alpha$$

Equation 3.50. Damage accumulation

with:

$\alpha = 1$  the progression would follow the straight line, in Figure 3.9, corresponding to Miner's law.

$\alpha < 1$  would correspond to the upper (red) curve.

$\alpha > 1$  to the lower (blue) curve.

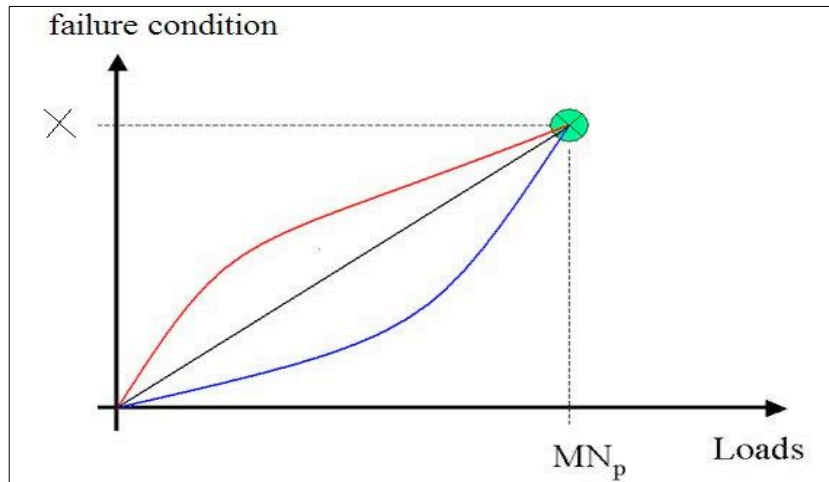


Figure 3.9: Assumed progression of damage

If the strain and the modulus remained constant throughout the life of the layer, a design criteria in the format of Equation 3.48 could be used directly to calculate  $MN_p$  and the Damage at any point in time as done in a Classic ME method. The problem is that strain and modulus do not remain constant throughout the life.

The *Incremental-Recursive procedure* overcome this problem through the use of the “*Time hardening*” procedure. The “*Time hardening*” procedure works in two steps:

- 1) at a new level of strain or modulus, the number of loads,  $MNo$  (in millions), that would have been required to reach the present condition, at the present level of strain and modulus, is calculated.  $MNo$  is calculated using the *damage functions* for the different failure conditions (fatigue, rutting or roughness) and the different material types (AC or unbound materials).
- 2) the new level of damage (fatigue damage, permanent deformation, roughness), is calculated from the same *damage functions* substituting  $MN$  by  $(MNo + dMN)$ , where  $dMN$  is the number of load applications (in millions) at the present level of strain and modulus during the increment that can be find out from the Load Spectra.

The process must be repeated recursively, using the output from each calculation as input to the next, for all loads at each position, before proceeding to the next time increment.

Damage functions are used for cracking of bound material, for permanent deformation and for crushing in lightly cemented materials. The general format of the *damage function* is represented by the Equation 3.51:

$$Damage = A \times MN^\alpha \times \left( \frac{resp}{resp_{ref}} \right) \times \left( \frac{E}{E_{ref}} \right)^\gamma$$

**Equation 3.51.** General format of the damage function

where:

- $MN$  is the number of load repetitions in millions;
- $resp$  is the response (stress or strain);
- $resp_{ref}$  is a reference response (can be related to strength);
- $E$  is the modulus of the material (adjusted for climate and damage);
- $E_{ref}$  is a reference modulus;
- $A$ ,  $\alpha$ ,  $\beta$  and  $\gamma$  are constants.

$A$ ,  $\alpha$ ,  $resp_{ref}$ ,  $\beta$ ,  $E_{ref}$  and  $\gamma$  are stored for each type of deterioration (rutting, fatigue cracking, crushing) for each material in the “*Material*” Table in Calme Database *DesignData.mdb*. In addition an “e” is stored if strain is to be used as the response, a “z” for stress or a “t” if shear deformation.

### **3.4.2.6 AC Fatigue damage model**

To evaluate the fatigue cracking performance in the bound layers, the damage may be defined as the decrease in modulus,  $dE$ , divided by the initial modulus,  $E_i$  ( $dE/E_i$ ). Early in the life of the layer, the decrease in modulus will primarily be due to microcracking which, much later, will develop into macrocracking. The process is complex and using the average modulus of the layer is a simplification.

Specifically, the *CalME* model for evaluate the *fatigue damage* ( $\omega$ ) of asphalt bound material is expressed by the following equations (3.52, 3.53, 3.54):

$$\omega = \left( \frac{MN}{MN_p} \right)^\alpha$$

Equation 3.52

$$\alpha = \exp \left( \alpha_0 + \alpha_1 + \frac{t}{1^\circ C} \right)$$

Equation 3.53

$$MN_p = A \times \left( \frac{\mu\varepsilon}{\mu\varepsilon_{ref}} \right)^\beta \times \left( \frac{E}{E_{ref}} \right)^\gamma \times \left( \frac{E_i}{E_{ref}} \right)^\delta$$

Equation 3.54

where:

- MN is the number of load applications in millions;
- $\mu\varepsilon$  is the horizontal tensile strain at bottom of asphalt layer;
- E is the damaged Modulus;
- $E_i$  is the intact Modulus;
- t is the temperature;
- $\mu\varepsilon_{ref}$  and  $E_{ref}$  are reference constants;
- A,  $\alpha_0, \alpha_1, \beta, \gamma, \delta_{Ei}, \delta_T$  are constant parameters.

The fatigue damage ( $\omega$ ) can be applied to the constant  $\alpha$  in the Master Curve model to evaluate the modulus of the damaged asphalt (Equation 3.55):

$$\log(E^*) = \delta + \frac{\alpha \cdot (1 - \omega)}{a + \exp(\beta + \gamma \log(tr))}$$

Equation 3.55. Modulus of damaged asphalt

where:

- $\omega$  is the fatigue damage  $dE/E_i$ .
- $\alpha$ ,  $\beta$  and  $\delta$  in the Master Curve model are not related with the constants of Equation 3.52, 3.53 and 3.54 (fatigue damage model).

The initial (intact) modulus,  $E_i$ , corresponds to a damage,  $\omega$ , of 0 and the minimum modulus,  $E_{min}=10^{\delta}$ , to a damage of 1.

The model parameters for Equations 3.52, 3.53 and 3.54 (*fatigue damage model*) can be determined from the four-point bending test, at controlled strain levels, minimizing the root mean square (RMS) of the difference between the measured modulus in the tests and the modulus calculated from Equation 3.55 with damage  $\omega$  calculated from Equation 3.52.

To predict in-situ damage from the laboratory test results, a shift factor, SF, is introduced as shown in Equation 3.56:

$$\omega = \left( \frac{MN}{SF \times MN_p} \right)^{\alpha}$$

**Equation 3.56.** Correlation between laboratory and in situ results

The Shift Factor is determined from the difference between laboratory fatigue tests and full scale testing (HVS and Wes-Track tests). The number of in situ load applications is divided by the Shift Factor to allow for differences between laboratory testing and in situ conditions.

### **3.4.2.7 AC fatigue cracking evaluation**

Based on calculated permanent fatigue damage (equation 3.53), the *amount of cracking* (Cr) in the pavement surface ( $m/m^2$ ) can be evaluated from Equation 3.57:

$$Cr = \frac{A}{1 + \left( \frac{\omega}{\omega_0} \right)^{\alpha}}$$

**Equation 3.57.** Amount of cracking in the pavement surface.

where:

- $\omega$  is the damage to the surfacing layer, and
- $A$  and  $\alpha$  are constants ( $A = 10$  and  $\alpha = -8$  as default for new pavements).
- $\omega_0$  is the damage to the surface layer at crack initiation (Equation 3.58).

$$\omega_0 = \frac{1}{1 + \left(\frac{h_{AC}}{h_{ref}}\right)^\alpha}$$

**Equation 3.58** Damage to the surface layer at crack initiation

where:

- $h_{AC}$  is the combined thickness of the asphalt layers;
- $\alpha$  and  $h_{ref}$  are constants (-2 and 250 mm as default for new pavements).

The amount of cracking at crack initiation must be assumed by the designer; the default is 0.5 m/m<sup>2</sup>.

### **3.4.2.8 Reflection cracking in an overlay asphalt layer**

Reflective cracking is a phenomenon that occurs in pavement overlays that are placed over a PCC layer (Portland Cement Concrete) or over an AC layer in poor condition (cracked). AC overlay over PCC or AC layer is one of the most common methods of rehabilitation and for this reason the reflection cracking phenomenon must be studied carefully.

In PCC pavement, the concrete layer expands and contracts as pavement temperature increases and decreases. As the joints open they induce tension at the bottom of the asphalt overlay.

The reflection cracking phenomenon is typical also in AC overlays over an AC layer already cracked. As the cracks open because of temperature variations, they induce tension the bottom of the asphalt overlay ([CalME Manual])

When the tensile stress exceeds the strength of the asphalt overlay, a crack is initiated in the asphalt layer at the PCC or AC interface.

In CalME, reflection cracking damage was calculated using the method developed by Wu (2005). In this method the tensile strain at the bottom of the overlay is estimated using a regression equation. The regression Equation (3.59) used to evaluate the tensile stain at the bottom of an AC overlay on a cracked AC pavement, is based on many finite element calculations, and assumes a dual wheel on a single axle:

$$\varepsilon = \alpha \times E_{an}^{\beta 1} \times E_{bn}^{\beta 2} \times (a1 + b1 \times \ln(LS_n)) \times \exp(b2 \times H_{an}) \times (1 + b3 \times H_{un}) \times (1 + b4 \times E_{un}) \times \sigma_n$$

**Equation 3.59.** Tensile strain at the bottom of an AC overlay on a cracked AC pavement

where:

$$E_{an} = \frac{E_a}{E_s}, \quad E_{bn} = \frac{E_b}{E_s}, \quad E_{un} = \frac{E_u}{E_s}, \quad \sigma_n = \frac{\sigma_o}{E_s}$$

$$LS_n = \frac{LS}{a}, \quad H_{an} = \frac{H_a}{a}, \quad H_{un} = \frac{H_u}{a}$$

- $E_a$  is the modulus of the overlay,
- $H_a$  is the thickness of the overlay,
- $E_u$  is the modulus of the underlayer,
- $H_u$  is the thickness of the underlayer,
- $E_b$  is the modulus of the base/sub-base,
- $E_s$  is the modulus of the subgrade,
- $LS_n$  is the crack spacing,
- $\sigma_o$  is the tire pressure, and
- $a$  is the radius of the loaded area for one wheel.

And with:

$$\alpha = 342650, \beta_1 = -0.73722, \beta_2 = -0.2645, \beta_3 = -1.16472, a_1 = 0.88432, b_1 = 0.15272, b_2 = -.21632, \\ b_3 = -0.061, b_4 = 0.018752.$$

The calculated tensile strain at the bottom of the overlay is used with the *fatigue damage model* for asphalt concrete layers (Equation 3.52) to evaluate the additional fatigue damage.

Reflection of cracking through an AC layer on a PCC support is also determined through a large number of finite element calculations. The equation and the parameters are similar to those used in Equations 3.59.

### **3.4.2.9 Fatigue damage to cemented materials**

For other cemented materials different from AC, the *damage function* can be written in the general format (Equation 3.51). The response used in the equation may be based on either the maximum tensile strain or stress at the bottom of the layer.

### **3.4.2.10 AC Permanent shear strain accumulation**

For an asphalt layer, the rutting performance is evaluated through a shear based approach developed by Jack Dean and Carl Monismith. In this approach, the performance of the asphalt layers in term of rutting is assumed to be controlled by shear deformation.

The permanent, or inelastic, shear strain,  $\gamma_i$ , is determined as a function of the shear stress,  $\tau$ , and of the elastic shear strain,  $\gamma^e$  evaluated with a response model at a depth of 50 mm beneath the edge of the tire. The laboratory test data are fitted either using a gamma function (Equation 3.60):

$$\gamma_i = \exp\left(A + \alpha \times \left[1 - \exp\left(\frac{-\ln(N)}{\gamma}\right) \times \left(1 + \frac{\ln(N)}{\gamma}\right)\right]\right) \times \exp\left(\frac{\beta \cdot \tau}{\tau_{ref}}\right) \times \gamma_e^\delta$$

**Equation 3.60.** Permanent shear strain damage (gamma equation)

where:

- $\gamma^e$  is the elastic shear strain at 50 mm depth (m/m);
- $\tau$  is the shear stress at 50 mm depth;
- $N$  is the number of load repetitions;
- $MN$  is the number of load repetitions in millions;
- $\tau_{ref}$  is a reference shear stress (0.1 MPa);
- $A, \alpha, \beta, \gamma$  and  $\delta$  are constants (different from constants of Master Curve and Fatigue Damage models).

The fitting of the parameters of Equation 3.60 can be done from laboratory tests (RSST-CH) minimizing the root mean square (RMS) of the difference between the permanent shear strains measured in the laboratory tests and the shear strains calculated. The permanent deformations in the asphalt concrete layers are calculated for the upper 100 mm of the AC layers. The shear stress is calculated at a depth of 50 mm beneath the edge of the tire. For each of the layers within 100 mm from the surface the elastic shear strain,  $\gamma_e$ , is calculated from equation 3.61:

$$\gamma_e = \frac{\tau \cdot (1 + \mu_i)}{E_i}$$

**Equation 3.61.** Elastic shear strain from the shear stress, modulus and Poisson's ratio

where:

- $E_i$  is the modulus of layer  $i$ ;
- $\nu_i$  is Poisson's ratio for layer  $i$ .

### **3.4.2.11 AC Rutting evaluation**

After the permanent shear strain of each layer,  $\gamma_i$ , is calculated from the Equation 3.60, the permanent deformation or rut depth is determined from Equation 3.62:

$$rut_{depth} = K \times \gamma_i \times h_i$$

**Equation 3.62:** vertical rut depth in the asphalt concrete.

where:

- $h_i$  is the thickness of layer  $i$  (above a depth of 100 mm);
- $K$  is a calibration constant.

### **3.4.2.12 Unbound materials Rutting evaluation**

Permanent deformation,  $dp$ , of unbound materials is based on the vertical elastic strain at the top of the layer,  $\mu\varepsilon$ , and on the modulus of the material,  $E$  (Equation 3.63):

$$dp (mm) = A \times MN^\alpha \times \left( \frac{\mu\varepsilon}{\mu\varepsilon_{ref}} \right)^\beta \times \left( \frac{E}{E_{ref}} \right)^\gamma$$

**Equation 3.63.** Permanent deformations of unbound materials.

where:

- $MN$  is the number of load applications in millions,
- $A$ ,  $\alpha$ ,  $\beta$ ,  $\gamma$ ,  $\mu\varepsilon_{ref}$  and  $E_{ref}$  are constants.

### **3.4.2.13 Crushing damage**

Some lightly cemented materials may crush from the top due to excessive compressive stress or strain. The damage due to crushing is calculated from the damage function in the general format (Equation 3.51) based on vertical stress or strain on top of layer. If the material is asphalt concrete or an unbound material, the crushing damage is not considered and the constant A is 0.



*Pavement  
Design*



## 4.1 Introduction

Pavement engineering involves the determination of the type and thickness of pavement surface course, base, and subbase layers that in combination are cost effective and structurally adequate for the projected traffic loading and specific project conditions. This combination of roadbed materials placed in layers above the subgrade (also known as basement soil) is referred to as the "pavement" or the "pavement structure" (Highway Design Manual, Chapter 600).

## 4.2 Pavement Structure Layers

Pavement structures are comprised of one or more layers of select materials placed above the subgrade. The basic pavement layers of the roadway are discussed below.

**Subgrade.** Also referred to as basement soil, the subgrade is that portion of the roadbed consisting of native or treated soil on which surface course, base, subbase, or a layer of any other material is placed. Subgrade may be composed of either in-place material that is exposed from excavation, or embankment material that is placed to elevate the roadway above the surrounding ground.

**Subbase.** Unbound or treated aggregate/granular material that is placed on the subgrade as a foundation or working platform for the base. It functions primarily as structural support but it can also minimize the intrusion of fines from the subgrade into the pavement structure, improve drainage, and minimize frost action damage. The subbase generally consists of lower quality materials than the base but better quality than the subgrade soils. Subbase may not be needed in areas with higher quality subgrade (California R-value > 40) or where it is more cost effective to build a thicker base layer.

**Base.** Select, processed, and/or treated aggregate material that is placed immediately below the surface course. It provides additional load distribution and contributes to drainage and frost resistance. Base may be one or multiple layers treated with cement, asphalt or other binder material, or may consist of untreated aggregate. In some cases, the base may include a drainage layer to drain water that seeps into the base. The aggregate in base is typically a higher quality material than that used in subbase.

Surface Course. This includes one or more layers of the pavement structure engineered to accommodate and distribute traffic loads, provide skid resistance, minimize disintegrating effects of climate, reduce tire/pavement noise, improve surface drainage, and minimize infiltration of surface water into the underlying base, subbase and subgrade. Sometimes referred to as the surface layer, the surface course may be composed of a single layer, constructed in one or more lifts of the same material, or multiple layers of different materials. Depending on the type of base or subbase layers, surface courses are used to characterize pavements into the following three categories:

(a) Flexible Pavements. These are pavements engineered to bend or flex when loaded. Flexible pavements transmit and distribute traffic loads to the underlying layers. The highest quality layer is the surface course, which typically consists of one or more layers of asphalt binder mixes and may or may not incorporate underlying layers of base and/or subbase. These types of pavements are called "flexible" because the total pavement structure bends (or flexes) to accommodate deflection bending under traffic loads.

(b) Rigid Pavements. These are pavements with a rigid surface course typically a slab of Portland cement concrete (or a variety of specialty hydraulic cement concrete mixes used for rapid strength concrete) over underlying layers of stabilized or unstabilized base or subbase materials. These types of pavements rely on the substantially higher stiffness of the concrete slab to distribute the traffic loads over a relatively wide area of underlying layers and the subgrade. Some rigid concrete slabs have reinforcing steel to help resist cracking due to temperature changes and repeated loading.

(c) Composite Pavements. These are pavements comprised of both flexible (asphalt binder mixes) and rigid (cement concrete) layers over underlying layers of stabilized or unstabilized base or subbase materials. Currently, for purposes of the procedures in this manual, only pavements with a flexible layer over a rigid surface layer are considered to be composite pavements. In California, such pavements consist mostly of existing rigid pavements (typically Portland cement concrete) that have had a flexible surface course overlay such as hot mix asphalt (HMA) (formerly known as asphalt concrete), open graded friction course (OGFC) (formerly known as open graded asphalt concrete), or rubberized hot mix asphalt (RHMA) (formerly known as rubberized asphalt concrete)(Highway Design Manual, Chapter 600).

## **4.3 Traffic Considerations**

Pavements are engineered to carry the truck traffic loads expected during the pavement design life. Truck traffic, which includes buses, trucks and truck-trailers, is the primary factor affecting pavement design life and its serviceability. Passenger cars and pickups are considered to have a negligible effect when determining traffic loads. Truck traffic information that is required for pavement engineering includes projected volume for each of four categories of truck and bus vehicle types by axle classification (2-, 3-, 4-, and 5-axles or more), axle configurations (single, tandem, tridem, and quad), axle loads, and number of load repetitions. This information is used to estimate anticipated traffic loading and performance of the pavement structure. The projected ESALs during the pavement design life are in turn converted into a Traffic Index (TI) that is used to determine minimum pavement thickness.

In order to determine expected traffic loads on a pavement it is first necessary to determine projected traffic volumes during the design life for the facility. Traffic volume and loading on State highways can come from vehicle counts and classification, weigh-in-motion (WIM) stations, or the Truck Traffic (Annual Average Daily Truck Traffic) on California State Highways published annually by Headquarters Division of Traffic Operations (Highway Design Manual, Chapter 610).

### **4.3.1 Traffic Index Calculation**

The Traffic Index (TI) is determined using the following procedures: (1) Determine the Projected Equivalent Single Axle Loads (ESALs). The information obtained from traffic projections and Truck Weight Studies is used to develop 80 kN Equivalent Single Axle Load (ESAL) constants that represent the estimated total accumulated traffic loading for each heavy vehicle (trucks and buses) and each of the four truck types during the pavement design life. Typically, buses are assumed to be included in the truck counts due to their relatively low number in comparison to trucks. However, for facilities with high percentage of buses such as high-occupancy vehicle (HOV) lanes and exclusive bus lanes, projected bus volumes need to be included in the projection used to determine ESALs. The ESAL constants are used as multipliers of the projected AADTT for each truck type to determine the total cumulative ESALs and in turn the Traffic Index (TI) during the design life for the pavement. The ESALs and the resulting TI are the same magnitude for both flexible, rigid, and composite pavement alternatives. The current

10-, 20-, 30-, and 40-year ESAL constants are shown in Table 4.1.

(2) Lane Distribution Factors. Truck/bus traffic on multilane highways normally varies by lanes with the lightest volumes generally in the median lanes and heaviest volumes in the outside lanes. Buses are also typically found in HOV lanes. For this reason, the distribution of truck/bus traffic by lanes must be considered in the engineering for all multilane facilities to ensure that traffic loads are appropriately distributed. Because of the uncertainties and the variability of lane distribution of trucks on multilane freeways and expressways, statewide lane distribution factors have been established for pavement engineering of highway facilities in California.

(3) Traffic Index (TI). The Traffic Index (TI) is a measure of the number of ESALs expected in the traffic lane over the pavement design life of the facility. The TI does not vary linearly with the ESALs but rather according to the following exponential formula and the values presented in Table 4.2. The TI is determined to the nearest 0.5.

$$TI = 9.0 \times \left( \frac{(ESAL \times LDF)}{10^6} \right)^{0.119}$$

Where:

TI = Traffic Index

ESAL = Total number of cumulative 80 kN Equivalent Single Axle Loads

LDF = Lane Distribution Factor (see Table 4.1)

**Table 4.1: Lane Distribution Factors for Multilane Highways.**

Number of Mixed Flow Lanes in One Direction	Factors to be Applied to Projected Annual Average Daily Truck Traffic (AADTT)			
	Mixed Flow Lanes (see Notes 1, 2, 3 & 4)			
	Lane 1	Lane 2	Lane 3	Lane 4
One	1.0	-	-	-
Two	1.0	1.0	-	-
Three	0.2	0.8	0.8	-
Four	0.2	0.2	0.8	0.8

NOTES:

- Lane 1 is next to the centerline or median.
- For more than four lanes in one direction, use a factor of 0.8 for the outer two lanes plus any auxiliary/collector lanes, use a factor of 0.2 for other mixed flow through lanes.
- For HOV lanes, use a factor of 0.2; however, the TI should be no less than 10 for a 20-year, or 11 for a 40-year pavement design life.
- For lanes devoted exclusively to buses and/or trucks, use a factor of 1.0 based on projected AADTT of mixed-flow lanes for auxiliary and truck lanes, and a separate AADTT based on expected bus traffic for exclusive bus lanes.

**Table 4.2: Conversion of ESAL to Traffic Index.**

ESAL <sup>(1)</sup>	TI <sup>(2)</sup>	ESAL <sup>(1)</sup>	TI <sup>(2)</sup>
4710		6 600 000	
	5.0		11.5
10 900		9 490 000	
	5.5		12.0
23 500		13 500 000	
	6.0		12.5
47 300		18 900 000	
	6.5		13.0
89 800		26 100 000	
	7.0		13.5
164 000		35 600 000	
	7.5		14.0
288 000		48 100 000	
	8.0		14.5
487 000		64 300 000	
	8.5		15.0
798 000		84 700 000	
	9.0		15.5
1 270 000		112 000 000	
	9.5		16.0
1 980 000		144 000 000	
	10.0		16.5
3 020 000		186 000 000	
	10.5		17.0
4 500 000		238 000 000	
	11.0		17.5 <sup>(3)</sup>
6 600 000		303 000 000	

Notes:

- (1) For ESALs less than 5000 or greater than 300 million, use the TI equation to calculate design TI, see Index 613.3(3).
- (2) The determination of the TI closer than 0.5 is not justified. No interpolations should be made.
- (3) For TI's greater than 17.5, use the TI equation, see Index 613.3(3).

## 4.4 Soil Characteristics

### 4.4.1 California R-Value

The California R-value is the measure of resistance to deformation of the soils under wheel loading and saturated soil conditions. It is used to determine the bearing value of the subgrade. Determination of R-value for subgrade is provided under California Test Method (CTM) 301. Typical R-values range from 5 for very soft material to 80 for treated base material (Highway Design Manual, Chapter 610).

The California R-value is determined based on the following separate measurements under CTM 301:

- The exudation pressure test determines the thickness of cover or pavement structure required to prevent plastic deformation of the soil under imposed wheel loads.
- The expansion pressure test determines the pavement thickness or weight of cover required to withstand the expansion pressure of the soil.

Because some soils, such as coarse grained gravel and sands, may exhibit a higher California R-value test result than would normally be required for pavement design, the California R-value for subgrade soils used for pavement design should be limited to no more than 50 unless agreed to otherwise by the District Materials Engineer. Local experience with these soils should govern in assigning R-value on subgrade. The California R-value of subgrade within a project may vary substantially but cost and constructability should be considered in specifying one or several California R-value(s) for the project. Engineering judgment should be exercised in selecting appropriate California R-values for the project to assure a reasonably "balanced design" which will avoid excessive costs resulting from over conservatism. The following should be considered when selecting California R-values for a project:

- If the measured California R-values are in a narrow range with some scattered higher values, the lowest California R-value should be selected for the pavement design.
- If there are a few exceptionally low California R-values and they represent a relatively small volume of subgrade or they are concentrated in a small area, it may be more cost effective to remove or treat these materials.
- Where changing geological formations and soil types are encountered along the length of a project, it may be cost-effective to design more than one pavement structure to accommodate major differences in R-values that extend over a considerable length. Care should be exercised to avoid many variations in the pavement structure that may result in increased construction costs that exceed potential materials cost savings.

## **4.5 Engineering Procedures for New Projects**

### **4.5.1 Empirical Method**

The data needed to engineer a flexible pavement are the California R-value of the subgrade and the TI for the pavement design life. Engineering of the flexible pavement is based on a relationship between the gravel equivalent (GE) of the pavement structural materials, the TI, and the California R-value of the underlying material. The relationship was developed by the Department of Caltrans through research and field experimentation (Highway Design Manual, Chapter 630). The procedures and rules governing flexible pavement engineering are as follows:

### Procedures for Engineering Multiple Layered Flexible Pavement.

- The TI is determined to the nearest 0.5 per Index 4.3.1, and the California R-value is established per Index 4.4.1.
- The gravel equivalent (GE) is defined as the required gravel thickness needed to carry a load compared to a different material's ability to carry the same load.

The following equation is applied to calculate the GE requirement of the entire flexible pavement or each layer and is calculated using the following equation:

$$GE = 0.975 \times (TI) \times (100 - R)$$

where:

GE = gravel equivalent in mm

TI = Traffic Index

R = California R-value of the material below the layer or layers for which the GE is being calculated.

The GE to be provided by each type of material in the pavement is determined for each layer, starting with the surface layer and proceeding downward. For pavements that include base and/or subbase, a safety factor of 60 mm is added to the GE requirement for the surface layer to compensate for construction tolerances allowed by the contract specifications. Since the safety factor is not intended to increase the GE of the overall pavement, a compensating thickness is subtracted from the subbase layer (or base layer if there is no subbase). For pavements that are full depth asphalt, a safety factor of 30 mm is added to the required GE of the flexible pavement. When determining the appropriate safety factor to be added, Hot Mix Asphalt Base (HMAB) and Asphalt Treated Permeable Base (ATPB) should be considered as part of the surface layer.

- The gravel factor (Gf) is the relative strength of a material to gravel. Gravel factors for HMA decrease as TI increases, and also increase with HMA thickness greater than 150 mm; while Gf for base and subbase materials are only dependent on the material type. The Gf of HMA varies with layer thickness (t) for any given TI as follows:

$t \leq 150 \text{ mm:}$	$G_f = \frac{5.67}{(TI)^{1/2}}$
$t > 150 \text{ mm:}$	$G_f = (1.04) \frac{(t)^{1/3}}{(TI)^{1/2}}$

These equations are valid for TIs ranging from 5 to 15. For TIs greater than 15, use a rigid or composite pavement or contact the Office of Pavement Design (OPD) for experimental options. For TIs less than 5, use a TI=5.

- The thickness of each material layer is calculated by dividing the GE by the appropriate gravel factor, or from Table 4.3. Typical gravel factors for HMA of thickness equal to or less 150 mm, and various types of base and subbase materials, are provided in Table 4.3. This table also shows the limit thickness for placing HMA for each TI, and the limit thickness for each type of base and subbase materials. Additional information on Gf for base and subbase materials are provided in Table 4.4

$$\text{Thickness } (t) = \frac{GE}{G_f}$$

Minimum thickness of any asphalt layer should not be less than twice the maximum aggregate size. When selecting the layer thickness, the value is rounded to the nearest 15 mm. A value midway between 15 mm increments is rounded to the next higher value. The surface course should have a minimum thickness of 45 mm. Base and subbase materials should each have a minimum thickness of 105 mm. When the calculated thickness of base or subbase material is less than the desired 105 mm minimum thickness, either (a) increase the thickness to the minimum without changing the thickness of the overlying layers or (b) eliminate the layer and increase the thickness of the overlying layers to compensate for the reduction in GE. Generally, the layer thickness of Lime Treated Subbase (LTS) should be limited, with 200 mm as the minimum and 600 mm as the maximum. A surface layer placed directly on the LTS should have a thickness of at least 75 mm.

The thicknesses determined by the procedure provided by this equation are not intended to prohibit other combinations and thickness of materials. Adjustments to the thickness of the various materials may be made to accommodate construction restrictions or practices, and minimize costs, provided the minimum thicknesses, maximum thicknesses, and minimum GE

requirements (including safety factors), of the subgrade and each layer in the pavement are satisfied.

**Table 4.3. Gravel Equivalents (GE) and Thickness of structural layers (mm)**

Actual Layer Thickness (mm) <sup>(3)</sup>	HMA <sup>(1), (2)</sup>											Base and Subbase <sup>(3)</sup>				
	Traffic Index (TI)											TI is not a factor				
	5.0 & below	5.5	6.5	7.5	8.5	9.5	10.5	11.5	12.5	13.5	14.5	CTPB;				
	6.0	7.0	8.0	9.0	10.0	11.0	12.0	13.0	14.0	15.0	HMAB	CTB	CTB		AS	
	G <sub>F</sub> (For HMA thickness equal to or less than 150 mm, G <sub>F</sub> decreases with TI) <sup>(4)</sup>											LCB	(CL.A)	ATPB	(CL.B)	AB
G <sub>F</sub> (constant for any base or subbase material irrespective of TI or thickness)											G <sub>F</sub> (constant for any base or subbase material irrespective of TI or thickness)					
GE for HMA layer (mm)											GE for Base or Subbase layer (mm)					
2.54	2.32	2.14	2.01	1.89	1.79	1.71	1.64	1.57	1.52	1.46	1.9	1.7	1.4	1.2	1.1	1.0
GE for HMA layer (mm)											GE for Base or Subbase layer (mm)					
45	114	104	96	90	85	81	77	74	71	68	66	--	--	--	--	--
60	152	139	128	121	113	107	103	98	94	91	88	--	--	--	--	--
75	191	174	161	151	142	134	128	123	118	114	110	--	--	105	--	--
90	229	209	193	181	170	161	154	148	141	137	131	--	--	126	--	--
105	267	244	225	211	198	188	180	172	165	160	153	200	180	147	126	116
120	305	278	257	241	227	215	205	197	188	182	175	228	204	168	144	132
135	343	313	289	271	255	242	231	221	212	205	197	257	230	189	162	149
150	381	348	321	302	284	269	257	246	236	228	219	285	255	210	180	165
165	421	392	362	338	318	301	287	275	264	254	247	314	281	231	198	182
180	473	441	407	380	357	338	322	308	296	285	278	342	306	252	216	198
195	526	490	453	422	397	377	359	343	329	317	309	371	332	273	234	215
210	--	541	500	466	439	416	396	379	363	350	341	399	357	--	252	231
225	--	593	548	511	481	456	434	415	399	384	374	428	383	--	270	248
240	--	647	597	557	524	497	473	452	434	418	407	456	408	--	288	264
255	--	--	647	604	568	538	513	491	471	453	442	485	434	--	306	281
270	--	--	698	652	613	581	553	529	508	489	477	513	459	--	324	297
285	--	--	--	701	659	625	595	569	546	526	512	542	485	--	342	314
300	--	--	--	750	706	669	637	609	585	563	548	570	510	--	360	330
315	--	--	--	801	753	714	680	650	624	601	585	599	536	--	378	347
330	--	--	--	--	802	759	723	692	664	639	623	--	--	--	--	330
345	--	--	--	--	851	806	767	734	705	679	661	--	--	--	--	345
360	--	--	--	--	900	853	812	777	746	718	699	--	--	--	--	360
375	--	--	--	--	--	901	858	820	787	758	738	--	--	--	--	375
390	--	--	--	--	--	949	904	864	830	799	778	--	--	--	--	390
405	--	--	--	--	--	998	950	909	873	840	818	--	--	--	--	--
420	--	--	--	--	--	--	997	954	916	882	859	--	--	--	--	--
435	--	--	--	--	--	--	1045	1000	960	924	900	--	--	--	--	--
450	--	--	--	--	--	--	1094	1046	1004	967	942	--	--	--	--	--
465	--	--	--	--	--	--	--	1093	1049	1010	984	--	--	--	--	--
480	--	--	--	--	--	--	--	1140	1094	1054	1026	--	--	--	--	--
495	--	--	--	--	--	--	--	1188	1140	1098	1069	--	--	--	--	--
510	--	--	--	--	--	--	--	--	1187	1143	1113	--	--	--	--	--
525	--	--	--	--	--	--	--	--	1233	1188	1156	--	--	--	--	--
540	--	--	--	--	--	--	--	--	1280	1233	1201	--	--	--	--	--
555	--	--	--	--	--	--	--	--	--	1279	1245	--	--	--	--	--
570	--	--	--	--	--	--	--	--	--	1325	1290	--	--	--	--	--
585	--	--	--	--	--	--	--	--	--	1372	1336	--	--	--	--	--
600	--	--	--	--	--	--	--	--	--	--	1382	--	--	--	--	--

Table 4.4 Gravel factor and California R-Values for Bases and Subbases

Type of Material	Abbreviation	California R-value	Gravel Factor ( $G_f$ )
Aggregate Subbase	AS-Class 1	60	1.0
	AS-Class 2	50	1.0
	AS-Class 3	40	1.0
	AS-Class 4	specify	1.0
	AS-Class 5	specify	1.0
Aggregate Base	AB-Class 2	78	1.1
	AB-Class 3	specify	1.1 <sup>(1)</sup>
Asphalt Treated Permeable Base	ATPB	NA	1.4
Cement Treated Base	CTB-Class A	NA	1.7
	CTB-Class B	80	1.2
Cement Treated Permeable Base	CTPB	NA	1.7
Lean Concrete Base	LCB	NA	1.9
Hot Mix Asphalt Base	HMAB	NA	<sup>(2)</sup>
Lime Treated Subbase	LTS	NA	0.9+UCS/6.9

## 4.6 Pavement design through Caltrans Highway Design Manual

### Pavement Structure 1 (HMA/CTB-B/AS-Class 3/CH) Design

Determine the total pavement structure GE over the subgrade, using the standard design formula and the California R-value of the subgrade. An inorganic clay of high plasticity (CH) is selected with a California R-value of 6. A TI (traffic index) of 10.0 is assigned based on the traffic forecasts for trucks.

1. Thus the total required GE is:

$$GE_{\text{Total}} = 0.975 (TI) (100 - R_{\text{Subgrade}}) = 0.975 (10) (100 - 6) = 917 \text{ mm}$$

2. Determine the GE of the HMA surface layer using the standard formula. In this case, R is the California R-Value of the Cement Treated Base Class B (CTB-B) layer.

$$GE_{\text{HMA}} = 0.975 (TI) (100 - R) = 0.975 (10) (100 - 80) = 195 \text{ mm}$$

3. Add the required 60 mm safety factor to the total GE of HMA.

$$\text{Final } GE_{\text{HMA}} = GE_{\text{HMA}} + \text{safety factor} = 195 + 60 = 255 \text{ mm}$$

4. Use Table 4.3 to determine the GE and thickness of the HMA surface layer. With a TI of 10 the closest GE from Table 4.3 is 242, for which the required HMA thickness is 135 mm. Although the thickness is chosen for the GE of 242 as nearest to the calculated value, in subsequent calculations for the remaining layers, the calculated value of 255 will be used in lieu of 242.

5. Determine the required GE of the combined HMA and CTB-B layers using the standard design formula. In this case, R is the California R-Value of the AS layer. The aggregate subbase is a Class 3 which has a specified minimum California R-value of 40 (see Table 4.4)

$$GE_{\text{HMA+CTB-B}} = 0.975 (TI) (100 - R) = 0.975 (10) (60) = 585 \text{ mm}$$

6. Add the required 60 mm safety factor to this value to determine the GE of the combined HMA and CTB-B

$$\text{Final } GE_{\text{HMA+CTB-B}} = GE_{\text{HMA+CTB-B}} + \text{safety factor} = 585 + 60 = 645 \text{ mm}$$

7. Subtract the GE of the HMA (step 4) from the combined GE of the HMA and CTB-B to determine the required GE of the CTB-B.

$$GE_{\text{CTB-B}} = GE_{\text{HMA+CTB-B}} - GE_{\text{HMA}} = 645 - 255 = 390 \text{ mm}$$

Table 4.3 shows a value of 378 as the closest value to the calculated 390 mm for the CTB-B layer. The corresponding CTB-B thickness for the tabular value of 378 is 315 mm.

8. Subtract the GE of the HMA and CTB-B layers, from the GE of the total pavement structure (step 1) to determine the GE of AS:

$$917 - 255(\text{HMA}) - 390(\text{CTB-B}) = 272 \text{ mm (Round to 270 mm)}$$

Since AS has a  $G_f$  of 1.0, the actual thickness and the GE are equal.

9. Thus the structural layer thicknesses for pavement 1 are:

<b>LAYER</b>	<b>THICKNESS (mm)</b>
HMA	135
CTB-B	315
AS-Class 3	270

Pavement Structure 2 (HMA/HMAB/AS-Class 3/CH) Design

Following the procedure outlined above, the structural layer thicknesses for pavement 2 are:

<b>LAYER</b>	<b>THICKNESS (mm)</b>
HMA	90
HMAB	165
AS-Class 3	315

***Pavement Simulations using the  
Incremental-Recursive procedure of the  
Mechanistic-Empirical software CalME***



## 5.1 Pavement structure definition, Traffic and Climate

In this chapter based on experimental work the two pavements designed (a flexible and a semi-rigid) are compared, as function of different climate conditions, different traffic index and different maintenance interventions.

A cement bounded base and a hot mix asphalt base were selected. The surface layer is a normal hot mix asphalt, the sub-base and subgrade are unbounded materials that are aggregate base and fat clay subgrade (high plasticity clay) respectively.

The two research pavement structures are hereby presented (Figure 5.1).

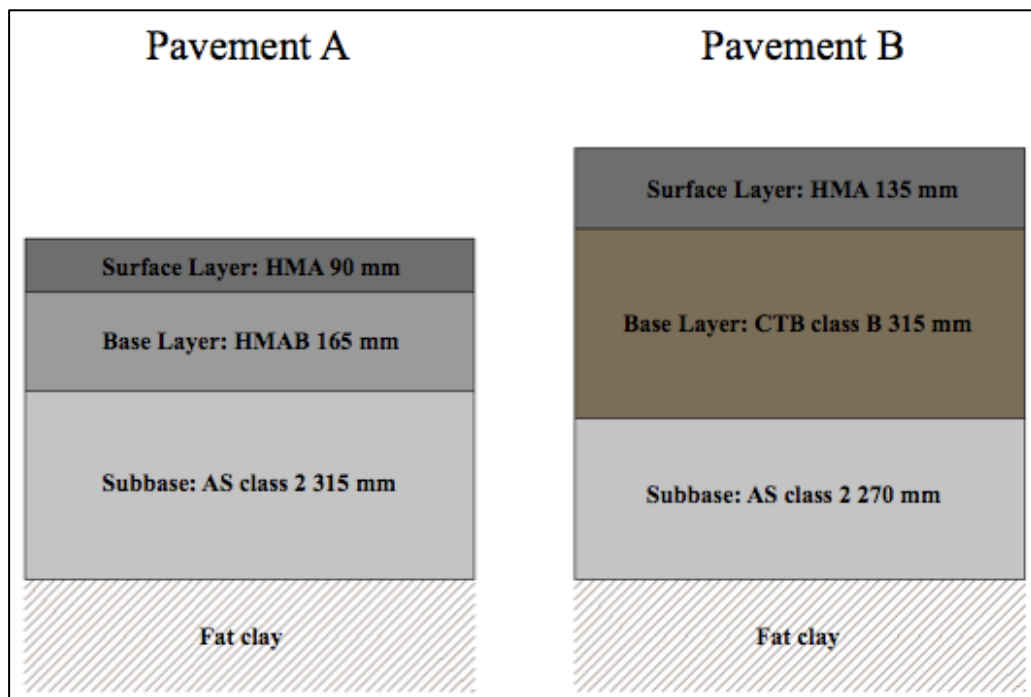


Figure 5.1. Pavement structure A and B

Concerning the traffic inputs, the Load Distribution of the WIM station 1b was chosen. Three different traffic levels were adopted:  $TI = 10$  (the traffic index used to design the pavement structure through the Caltrans Highway Design Manual),  $TI = 11.5$  and  $TI = 13$ . A traffic index of 10 is characterized by 338,750 axle/lane per year that can be converted to 2.424 million ESALs per year. The traffic indexes of 11.5 and 13 correspond to 7.845 and 21.980 million ESALs per year respectively. A growth rate of 3% was selected in all three cases.

Another input necessary for the performance simulations on CalME was the environmental aspect. Two climate zones were selected: the Central Coast and the Desert. The yearly mean

temperature is sufficiently different, but the largest difference can be seen in the yearly range. Therefore the Central Coast has a mild climate and the Desert a severe climate (Table 5.1)

**Table 5.1. Climate Zone studied.**

<b>Climate Zone</b>	<b>Site</b>	<b>Mean Yearly surface temperature (°C)</b>	<b>Range Yearly surface temperature (°C)</b>	<b>Range Daily surface temperature (°C)</b>
Desert	Dogget	26.3	28	22
Central Coast	San Francisco	19	14	20

Based on all defined inputs and the considered variables, it was proposed to run one simulation for each pavement structures. The objective of the simulations was to compare fatigue damage and rut depth of the bound layers, total surface cracking and total rut depth. The limit criteria for cracking and rutting were set to 0.5 m/m<sup>2</sup> and 10 mm respectively.

## 5.2 Performance simulation results

### 5.2.1 Central Coast Conditions

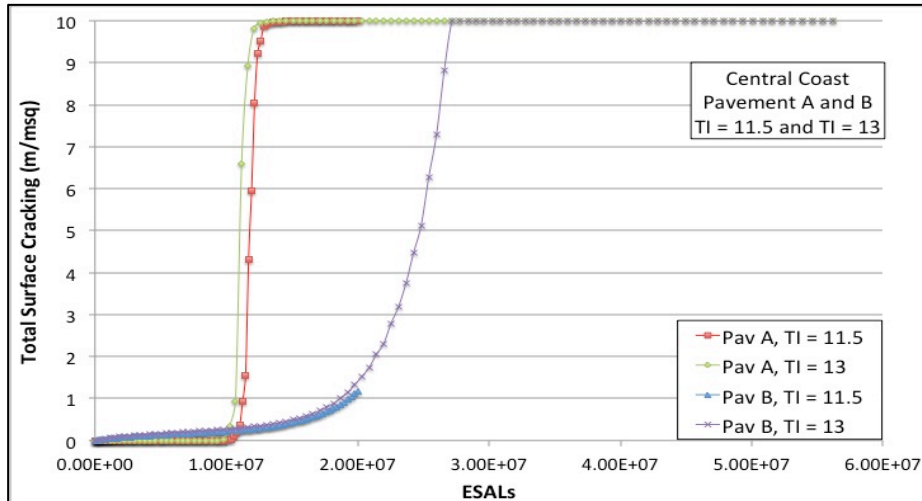


Figure 5.1. Total surface cracking in Central Coast

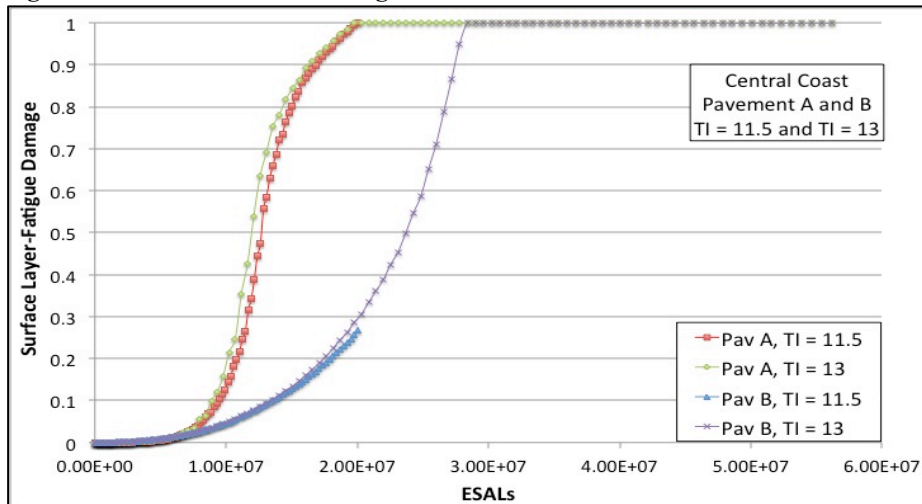


Figure 5.2. Fatigue damage in surface layer in Central Coast

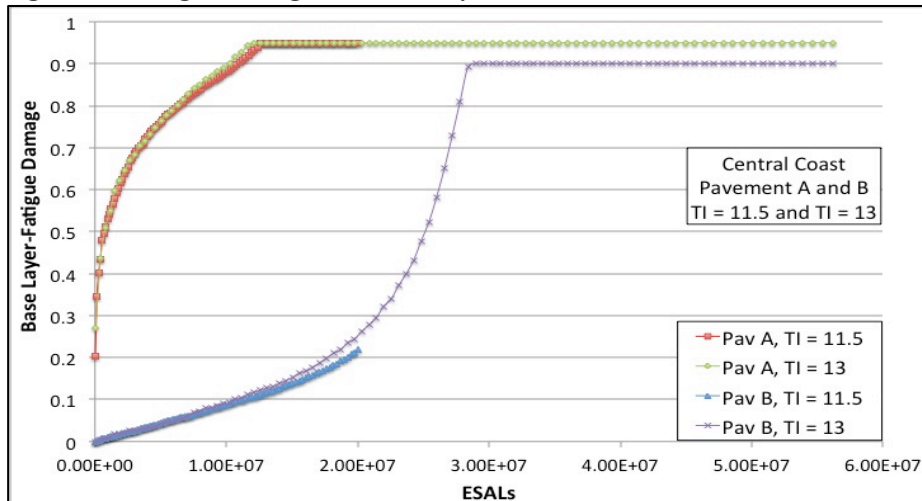


Figure 5.3. Fatigue damage in base layer in Central Coast

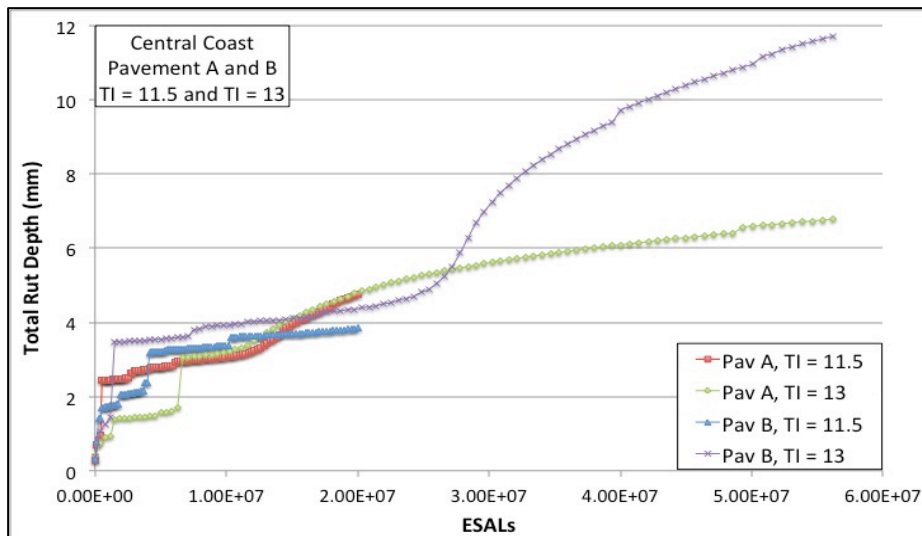


Figure 5.4. Total rut depth in Central Coast

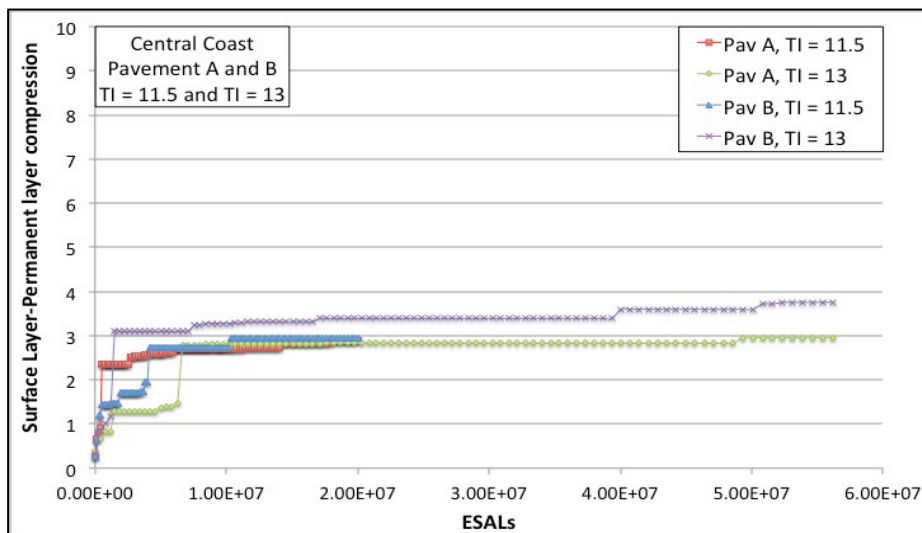


Figure 5.5. Permanent layer deformation in surface layer in Central Coast

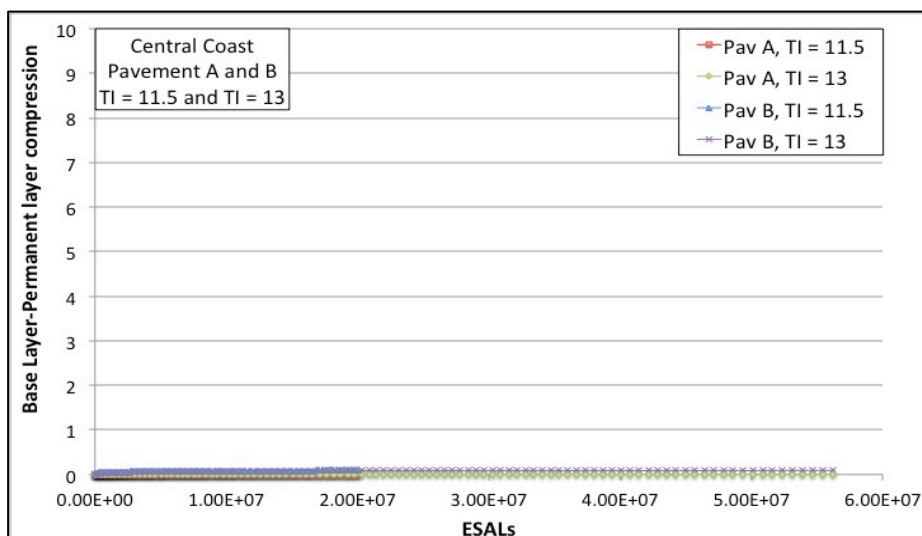


Figure 5.6. Permanent layer compression in base layer in Central Coast

In general the trend of the analyzed indicators, relative to the same pavement at different levels of traffic, is similar. Nevertheless greater damage is noted when the TI is equal to 13, despite the indicators being analyzed as a function of the number of ESALs and not of time. With regards to ESALs, the results found should be equal, this, however is not observed, fundamentally due to two factors:

- 1) ESAL is only one aspect of loading. The other is temperature. Applying the same ESAL under different climate conditions (climate conditions vary during the year) will lead to different damage;
- 2) With TI = 13, more ESALs are applied at the beginning, which is when the damage rate is faster.

Referring to the pavement structure A (base layer in hot mix asphalt) and to the pavement structure B (base layer in cement treated class B), the total cracking and the total rut depth obtained with the two different traffic index levels are summarized in Figures 5.1 and 5.4. Pavement B is the first mix to show surface cracking, although it is pavement A to reach first the limit criteria of  $0.5 \text{ m/m}^2$  and to achieve the limit value of  $10 \text{ m/m}^2$  faster. In terms of rutting performance, pavement B (TI=13) has the lower resistance with  $4.21 \cdot 10^7$  ESALs at the rutting limit, whereas the best performance is demonstrated by pavement A (TI=11.5) as it does not go over 4.77 mm of rutting at the highest level of ESALs ( $2.0 \cdot 10^7$  ESALs).

Upon analyzing the behavior of the asphalt bound layers and cement bound layer, it can be established that (from Figures 5.2 and 5.3) the fatigue damage in pavement A starts in the base layer and it then propagates to the surface layer. However, in terms of fatigue damage, the best performances are found in pavement B as the surface cracking analysis could suggest.

Viewing Figures 5.6 and 5.7 the rut depth enlargement for each mix is considered. The permanent layer compression of the surface layer reflects the trend of the total rut depth until  $2 \cdot 10^7$  ESALs. The base layer demonstrates a different behavior. Effectively in pavement A the base layer shows a rut depth of 0, as a matter of fact the software CalME assumes the rut depth in a cement-bounded layer is insignificant. Nevertheless for pavement B the influence of the base layer to the total rutting is minimal.

Table 5.2 summarizes the results for both pavement structure A and B and for both Traffic Index in Central Coast conditions. In the second part of the table, cracking and rutting performance were normalized to provide an easier way to interpret the behavior of the pavements.

**Table 5.2. ESALs for Cracking and Rutting limits in Central Coast**

Pavement	Traffic Index	Cracking Limit	Rutting Limit	
A	11.5	1.10E+07	2.0E+07	ESALS
	13	1.02E+07	6.5E+07	
B	11.5	1.61E+07	2.0E+07	
	13	1.51E+07	4.21E+07	
A	11.5	0.55	1	NORM.
	13	0.17	1	
B	11.5	0.805	1	
	13	0.25	0.70	
TI 11.5 normalized by 2.00E+07; TI 13 normalized by 6.50E+07				

## 5.2.2 Desert Conditions

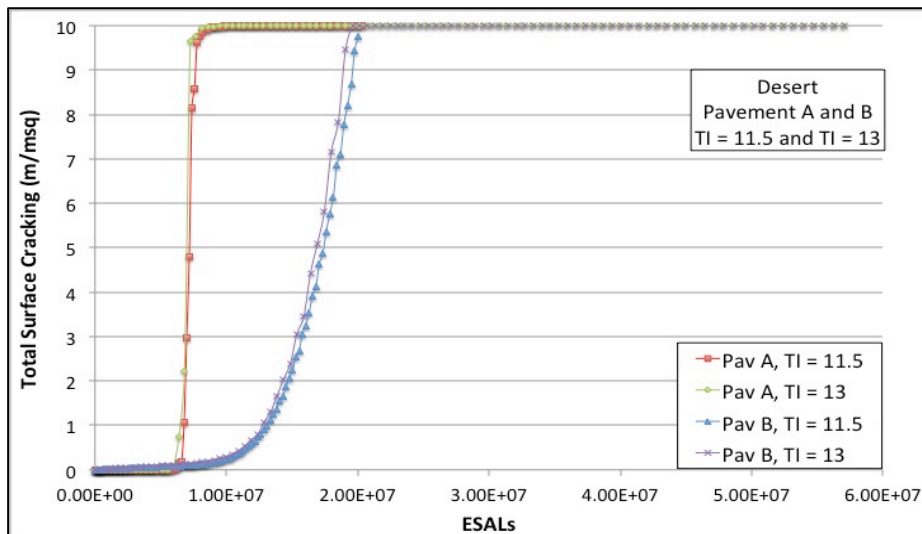


Figure 5.7. Total surface cracking in Desert

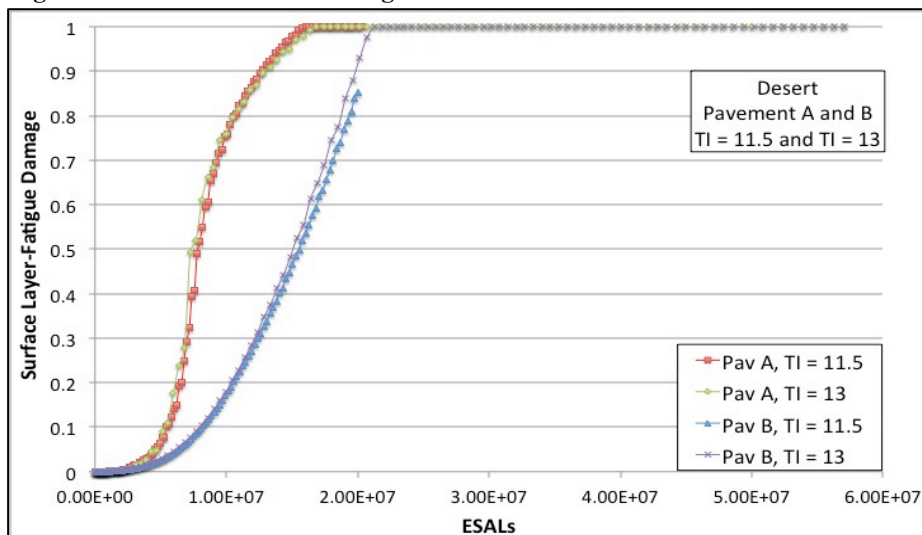


Figure 5.8. Fatigue damage in surface layer in Desert

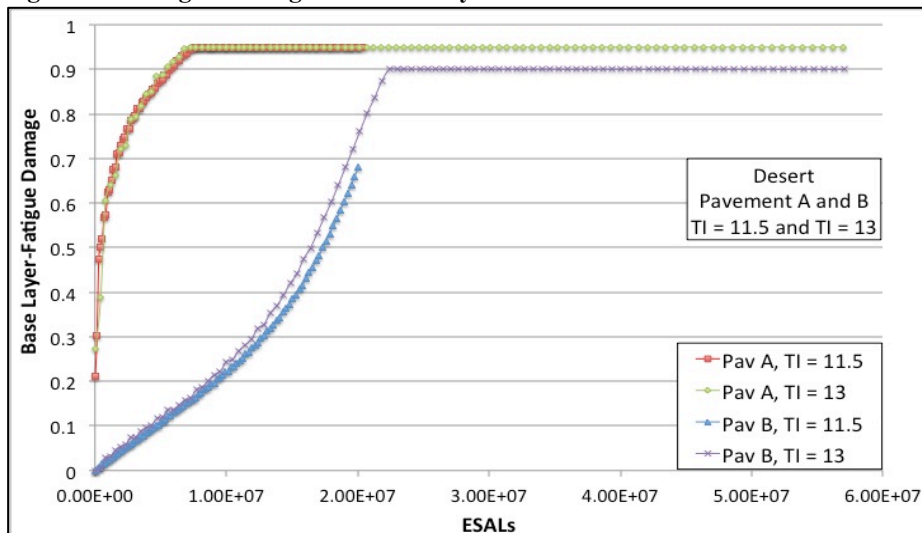


Figure 5.9. Fatigue damage in base layer in Desert

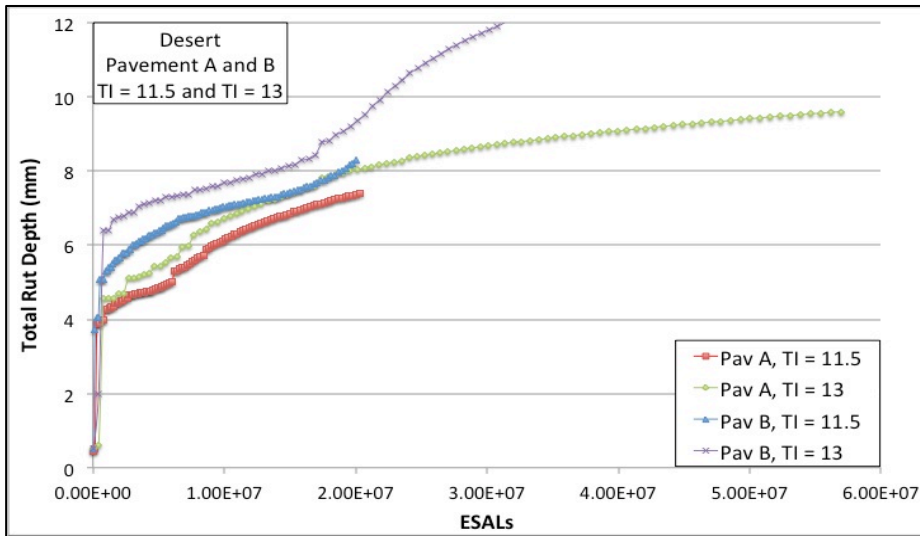


Figure 1.10. Total rut depth in Desert

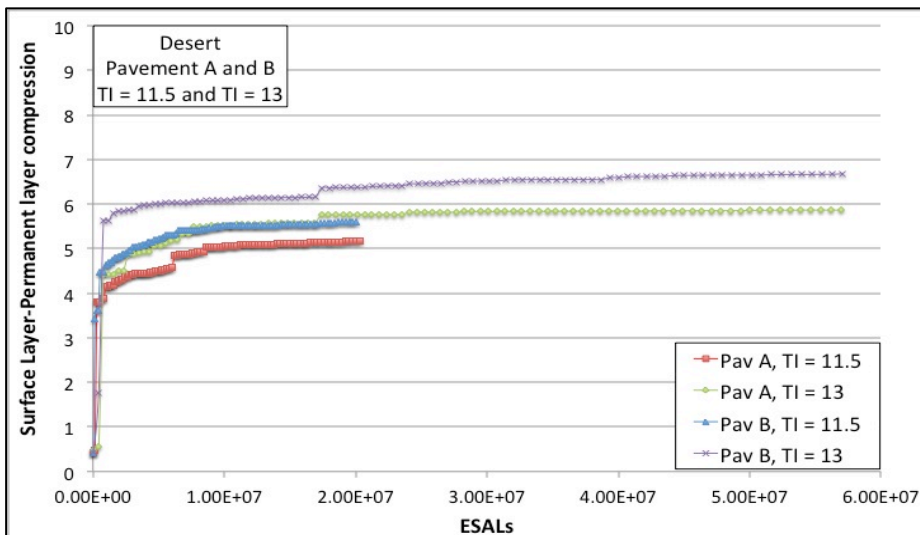


Figure 5.11. Permanent layer deformation in surface layer in Desert

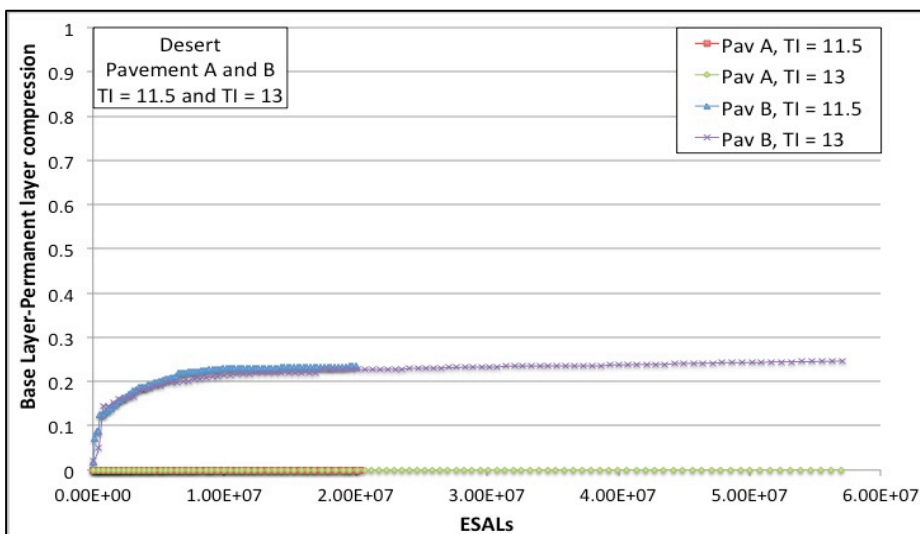


Figure 5.12. Permanent layer deformation in base layer in Desert

The desert environment with larger yearly temperature ranges tends to affect the pavement behavior.

Figure 5.7 and 5.10 respectively present the evolution curves of surface cracking and rutting for each pavement structures. The cracking trend is similar to the trend in Central Condition, though the Cracking limit is reached quicker (after  $6.39 \times 10^6$  ESALs for pavement A and after  $1.14 \times 10^7$  ESALs for pavement B). Compared with the Central Coast conditions both pavements have more total rut depth. Pavement A ratifies to have better resistance, while Pavement B due to its high asphalt content, suffer in particular with this kind of stress.

Figure 5.8 and 5.9 represent respectively the fatigue damage curves of the surface and base layers. The fatigue damage is higher in CTB base, which confirms what has been noted in the cracked surface. Relatively to pavement B, fatigue damage in the surface layer is greater compared to the fatigue damage in the base layer, as found in the Central Coast climate. Moreover the fatigue damage in the second layer of pavement A (Figure 5.9) increases quickly during the first 3 million ESAL application. The calculated rut depth in the surface layer demonstrates that the CTB base has the best resistance to shear stress (Figure 5.11). While as in the Central Coast climate the rut depth of the base layer is 0 in pavement A and nearly negligible in pavement B (Figure 5.12).

Table 5.3 summarizes the results for both pavement structure A and B and for both Traffic Index and in Desert conditions. In the second part of the table cracking and rutting performance were normalized to provide an easier way to interpret the behavior of the pavements.

**Table 5.3. ESALs for Cracking and Rutting limits in Desert**

Pavement	Traffic Index	Cracking Limit	Rutting Limit	
A	11.5	6.79E+06	2.0E+07	ESALs
	13	6.39E+06	6.5E+07	
B	11.5	1.17E+07	2.0E+07	
	13	1.14E+07	2.24E+07	
A	11.5	0.34	1	NORM.
	13	0.11	1	
B	11.5	0.59	1	
	13	0.19	0.37	
TI 11.5 normalized by 2.00E+07; TI 13 normalized by 6.50E+07				

Following that it was decided to consider the number of ESALs in which each pavement simulation achieved a total cracking surface of  $0.2 \text{ m}^2$  (Table 5.4).

**Table 5.4. ESALs corresponding to 0.2 m/m<sup>2</sup> of cracking surface**

Pavement Structure	Climate Zone	TI	ESALs corresponding to 0.2 m/m <sup>2</sup> cracking surface	Years
A	Central Coast	11.5	10138463	24
A	Central Coast	13	8872043	9
A	Desert	11.5	6107054	15
A	Desert	13	5121215	5
B	Central Coast	11.5	8047460	20
B	Central Coast	13	6688004	7
B	Desert	11.5	9074850	22
B	Desert	13	8167877	8

Another group of simulations was run applying different overlays (as maintenance interventions) to both pavement structures. It was decided to start the overlay application at the year corresponding to ESALs below considered. Two different materials were chosen:

- PGGWMA,
- MB4,

Two different thicknesses were adopted:

- 30 mm
- 45mm

The following table sums up the different overlays.

**Table 5.5. Overlay structures.**

Overlay	Material	Thickness (mm)
1	MB4	30
2	MB4	45
3	PGGWMA	30
4	PGGWMA	45

Based on these considerations one simulation for both pavement structures was completed, for each overlay. The main objective was to analyze the improvement resulting from the overlay application, in terms of fatigue damage and rut depth of bound materials, total surface cracking and total rut depth.

### 5.3 Performance simulation results, overlay applications

#### 5.3.1 Central Coast Condition

##### 5.3.1.1 Pavement Structure A and TI=11.5

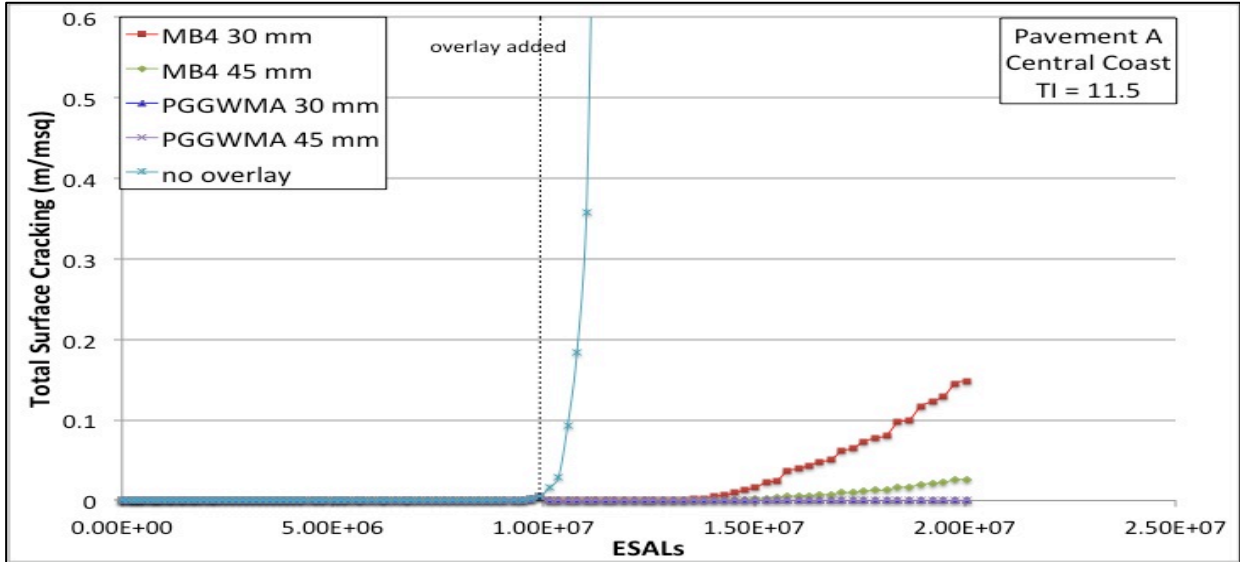


Figure 5.13. Total surface cracking in Central Coast

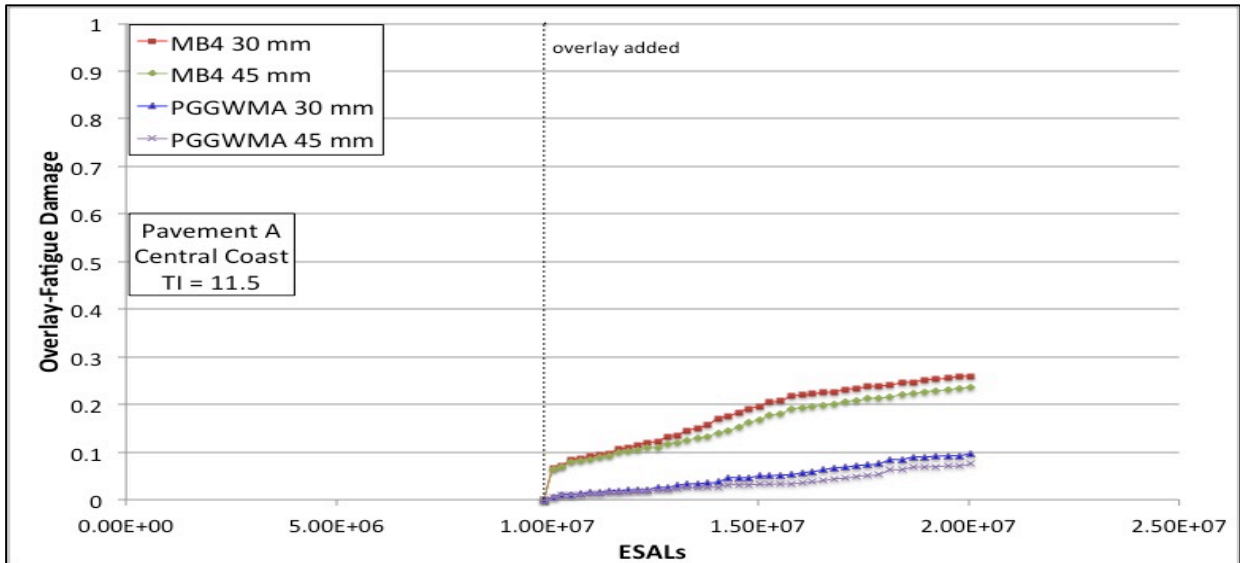


Figure 5.14. Fatigue damage in overlay in Central Coast

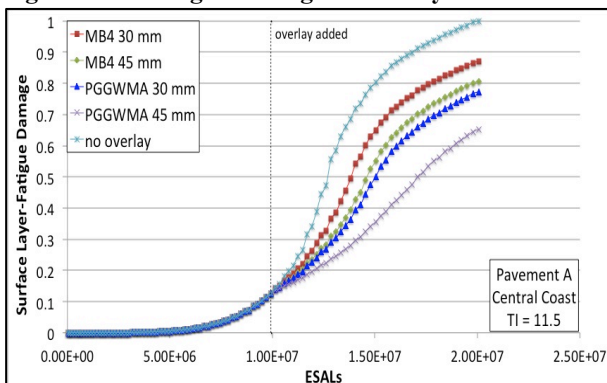


Figure 5.15. Fat. dam. surface layer in Central Coast

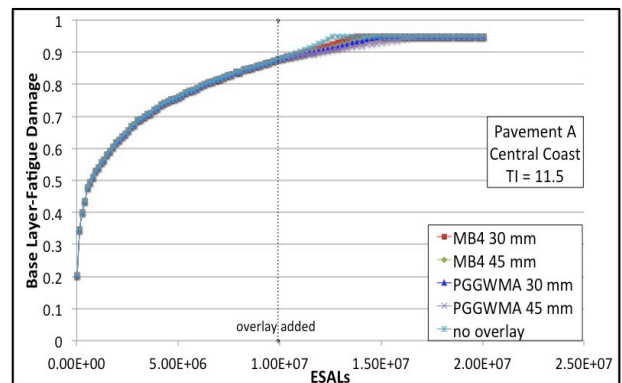


Figure 5.16. Fat. dam. base layer in Central Coast

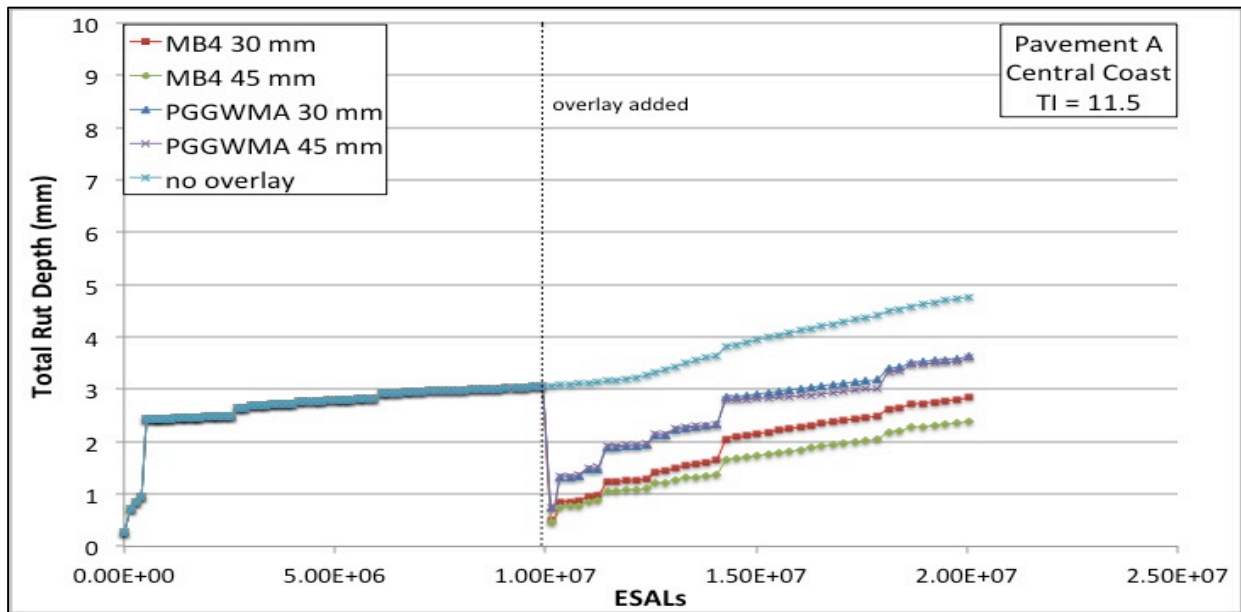


Figure 5.17. Total rut depth in Central Coast

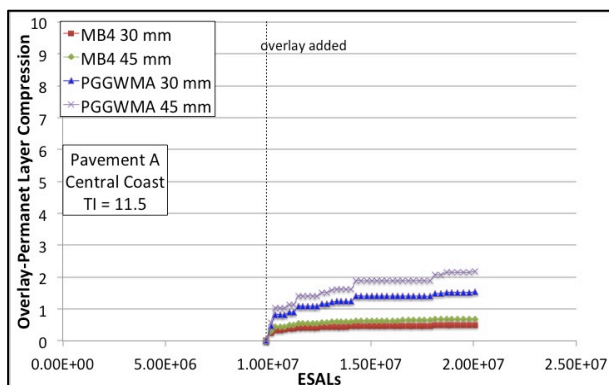


Figure 5.18. Rut depth overlay in Central Coast

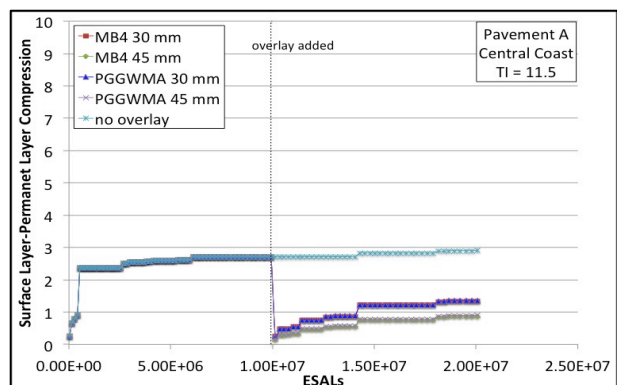


Figure 5.19. Rut depth surface layer in Central Coast

The total cracking obtained with the four different overlays is summarized in Figure 5.13. In general the overlay application exhibits a big improvement in terms of surface cracking: none of the overlay applications reach the limit criteria of  $0.5 \text{ m/m}^2$ . MB4 30 mm is the first mix to show surface cracking followed by MB4 45 mm while the PGGWMA (both thicknesses) does not show this kind of damage. Analyzing the overlay fatigue damage confirms the previous results. The materials rather than the thickness, mainly condition the behavior of the overlay and with the PGGWMA there are better performances (Figure 5.14). Also the fatigue damage in the surface layer confirms the results. Otherwise the base layer was too damaged when the overlay was applied and the fatigue damage does not improve in performance (Figure 5.16).

According to Figure 5.17, the total rut depth is under the limit criteria for all the overlays. MB4 shows better behavior (less rutting with a thickness of 45 mm) in comparison with the PGGWMA, which is not conditioned by the thickness. Beyond the rutting resistance of the

overlay, Figure 5.18 confirms that PGGWMA is weaker than MB4 from this point of view. Instead the rutting in the surface layer seems to be only affected from the overlay thickness. A thicker overlay leads to better outcomes.

Table 5.6 summarizes the results for any overlay applied, relatively to 5 indicators:

- Total Surface Cracking
- Fatigue Damage surface layer
- Fatigue Damage base layer
- Total Rut Depth
- Rut depth surface layer

Each result is compared to the performance obtained simulating the pavement without overlay. It is chosen to verify the improvement after  $5 \cdot 10^6$  ESALs and  $10 \cdot 10^6$  ESALs from the overlay application. For each outcome the enhancement is represented through the ratio in % between the result reached with the overlay and the result achieved without.

	Overlay	After 5*10 <sup>6</sup> ESALs	%	After 1*10 <sup>7</sup> ESALs	%
Total Surface Cracking	No Overlay	9.99	100	10	100
	MB4 30	0.016	0.16	0.149	1.49
	MB4 45	0.0018	0.02	0.026	0.26
	PGGWMA 30	2.7E-07	0.00	5.6E-05	0.00
	PGGWMA 45	3.5E-09	0.00	2.9E-06	0.00
Fatigue Damage Surface Layer	No Overlay	0.802	100	1	100
	MB4 30	0.649	80.94	0.871	87.11
	MB4 45	0.550	68.55	0.807	80.69
	PGGWMA 30	0.500	62.36	0.773	77.32
	PGGWMA 45	0.356	44.38	0.653	65.25
Fatigue Damage Base Layer	No Overlay	0.95	100.0	0.95	100.0
	MB4 30	0.95	100.0	0.95	100.0
	MB4 45	0.95	100.0	0.95	100.0
	PGGWMA 30	0.95	100.0	0.95	100.0
	PGGWMA 45	0.93	97.93	0.95	100.0
Total Rut Depth	No Overlay	3.95	100.0	4.77	100.0
	MB4 30	2.16	54.60	2.84	59.63
	MB4 45	1.73	43.90	2.39	50.13
	PGGWMA 30	2.92	73.86	3.64	76.23
	PGGWMA 45	2.83	71.58	3.60	75.48
Rut Depth Surface Layer	No Overlay	2.83	100.0	2.9	100.0
	MB4 30	1.22	43.00	1.34	46.24
	MB4 45	0.76	26.71	0.87	29.96
	PGGWMA 30	1.23	43.28	1.37	47.07
	PGGWMA 45	0.77	27.13	0.9	31.03

Table 5.6. Simulation Results

5.3.1.2 Pavement Structure A and TI=13

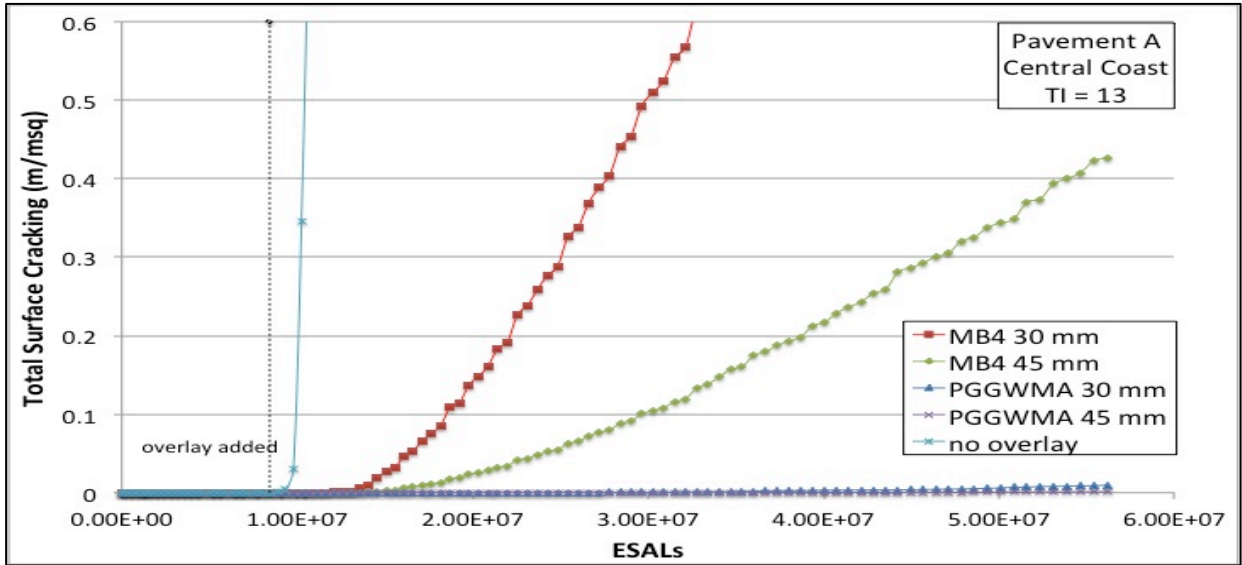


Figure 5.20. Total surface cracking in Central Coast

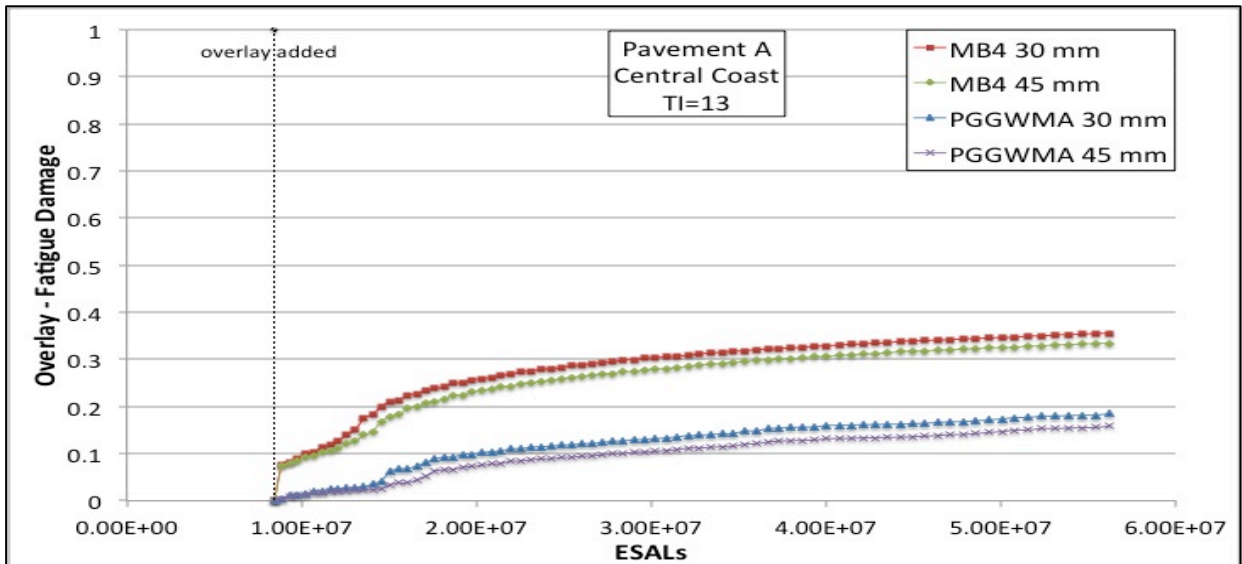


Figure 5.21. Fatigue damage in overlay in Central Coast

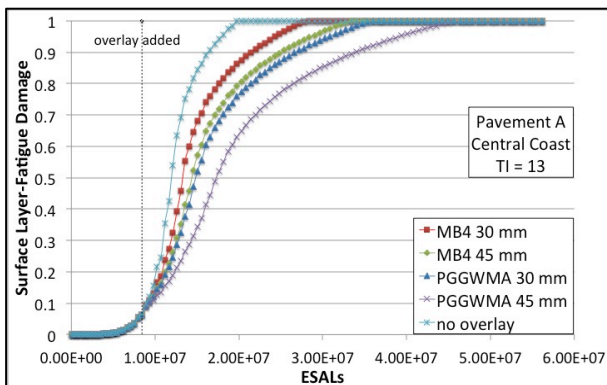


Figure 5.22. Fat. dam. surface layer in Central Coast

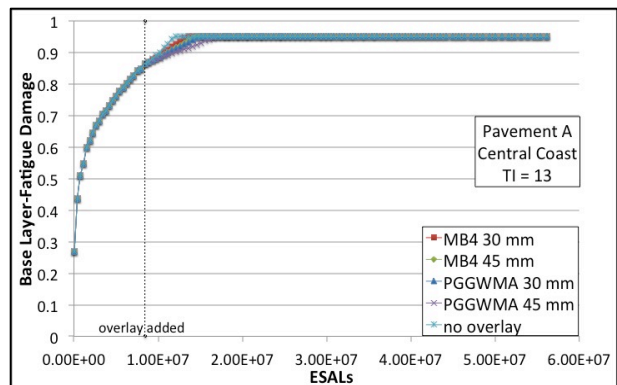


Figure 5.23. Fat. dam. base layer in Central Coast

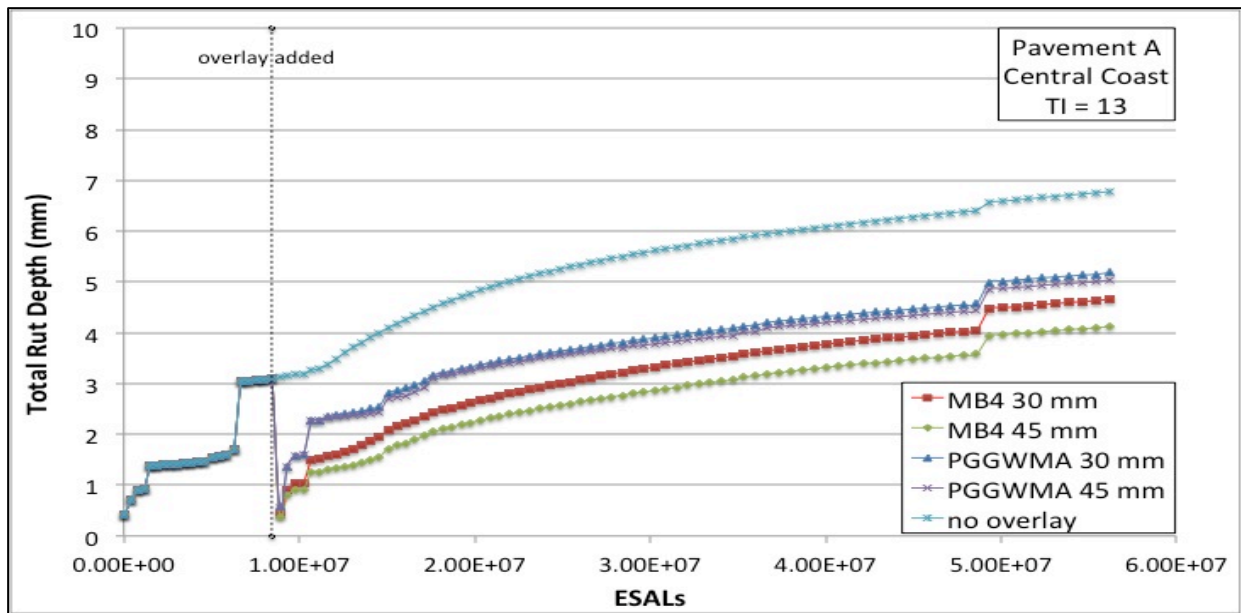


Figure 5.24. Total rut depth in Central Coast

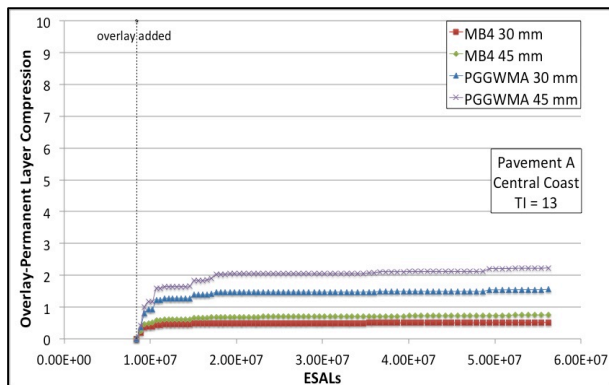


Figure 5.25. Rut depth overlay in Central Coast

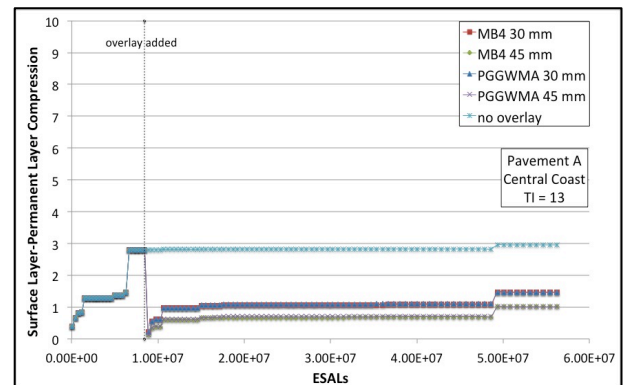


Figure 5.26. Rut depth surface layer in Central Coast

Analyzing the plots relating to  $TI = 13$  (in Central Coast with base in CTB class B), the results obtained are similar to the previous case with  $TI$  equal to 11.5. In general, however, higher values are reached both for the cracking and for the rutting. In fact the MB4 exceeds the limit criteria of the total surface cracking and all the overlays arrive at the maximum value of the fatigue damage in the surface layer (from Figure 5.20 to Figure 5.26).

Table 5.7 summarizes the results for any overlay applied, relative to 5 indicators:

- Total Surface Cracking
- Fatigue Damage surface layer
- Fatigue Damage base layer
- Total Rut Depth
- Rut depth surface layer

Each result is compared to the performance obtained simulating the pavement without overlay. It is chosen to verify the improvement after  $5 \cdot 10^6$  ESALs,  $10 \cdot 10^6$  ESALs and  $15 \cdot 10^6$  ESALs from

the overlay application. For each outcome the enhancement is represented through the ratio in % between the result reached with the overlay and the result achieved without.

Table 5.7. Simulation Results

	Overlay	After 5*10 <sup>6</sup> ESALs	%	After 1*10 <sup>7</sup> ESALs	%	After 1.5*10 <sup>7</sup> ESALs	%
Total Surface Cracking	No Overlay	9.99	100.0	10	100.0	10	100.0
	MB4 30	0.007	0.07	0.108	1.08	0.258	2.58
	MB4 45	0.0004	0.00	0.0175	0.17	0.0481	0.48
	PGGWMA 30	4.20E-09	0.00	4.13E-05	0.00	0.0002	0.00
	PGGWMA 45	1.44E-10	0.00	1.07E-05	0.00	1.07E-05	0.00
Fatigue Damage Surface Layer	No Overlay	0.75	100.0	0.97	100.0	1	100.0
	MB4 30	0.55	73.60	0.84	85.82	0.94	94.05
	MB4 45	0.41	55.00	0.76	78.24	0.88	87.78
	PGGWMA 30	0.38	50.12	0.73	74.57	0.85	84.91
	PGGWMA 45	0.26	35.21	0.58	60.04	0.74	74.39
Fatigue Damage Base Layer	No Overlay	0.95	100.0	0.95	100.0	0.95	100.0
	MB4 30	0.95	100.0	0.95	100.0	0.95	100.0
	MB4 45	0.94	98.58	0.95	100.0	0.95	100.0
	PGGWMA 30	0.93	98.11	0.95	100.0	0.95	100.0
	PGGWMA 45	0.91	96.17	0.95	100.0	0.95	100.0
Total Rut Depth	No Overlay	3.81	100.0	4.64	100.0	5.16	100.0
	MB4 30	1.79	46.87	2.52	54.42	2.92	56.61
	MB4 45	1.43	37.63	2.14	46.09	2.50	48.48
	PGGWMA 30	2.46	64.59	3.25	70.03	3.58	69.27
	PGGWMA 45	2.39	62.82	2.39	68.77	3.50	67.71
Rut Depth Surface Layer	No Overlay	2.82	100.0	2.83	100.0	2.83	100.0
	MB4 30	0.97	34.60	1.06	37.63	1.06	37.63
	MB4 45	0.60	21.20	0.67	23.84	0.67	23.84
	PGGWMA 30	0.98	34.88	1.10	38.79	1.10	38.79
	PGGWMA 45	0.62	21.91	0.70	24.72	0.70	24.72

5.3.1.3 Pavement Structure B and TI=11.5

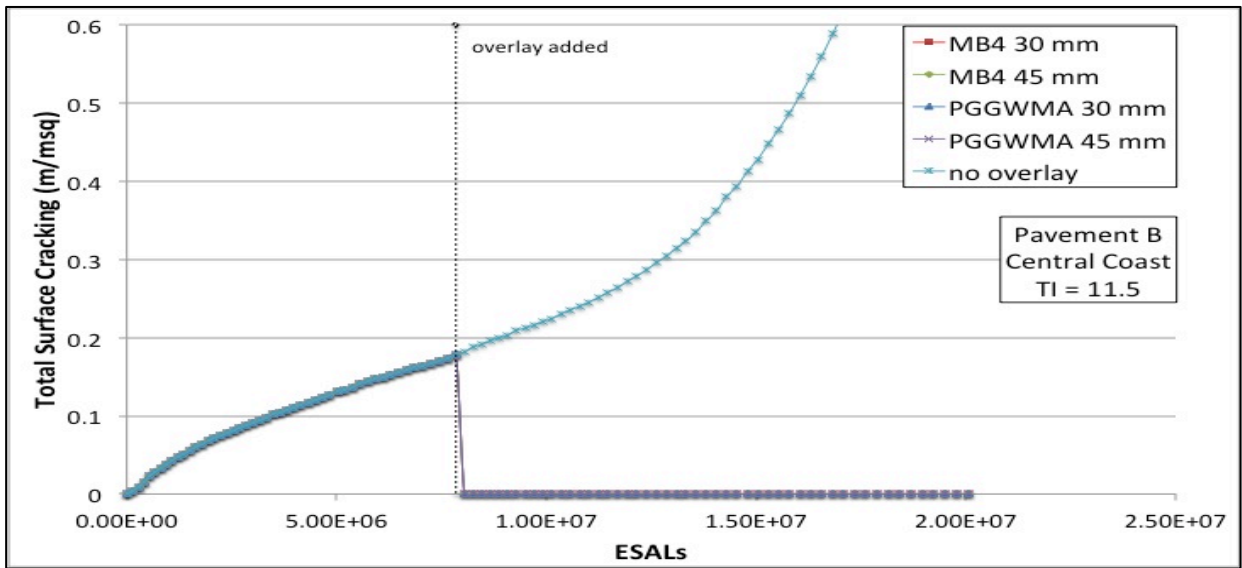


Figure 5.27. Total surface cracking in Central Coast.

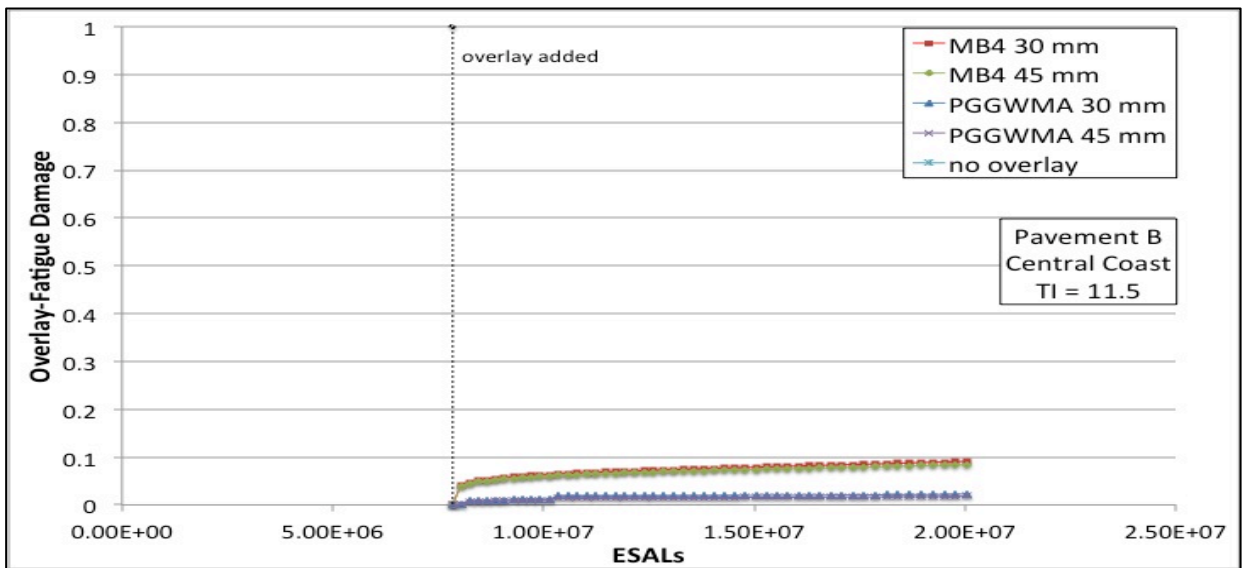


Figure 5.28. Fatigue damage in overlay in Central Coast

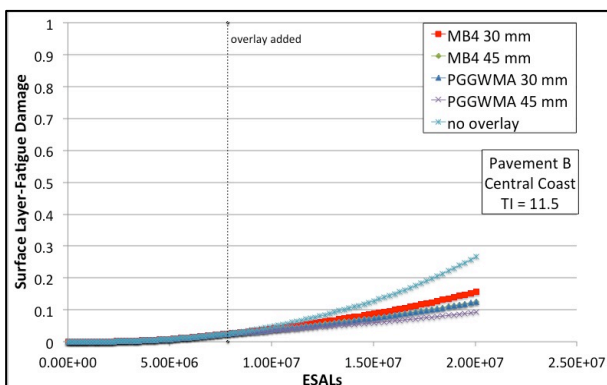


Figure 5.29. Fat. dam. surface layer in Central Coast

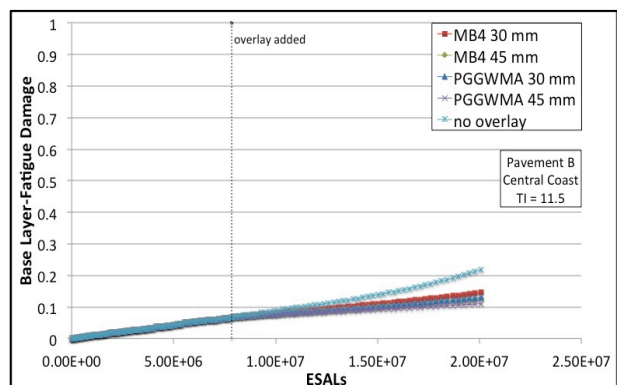


Figure 5.30. Fat. dam. base layer in Central Coast

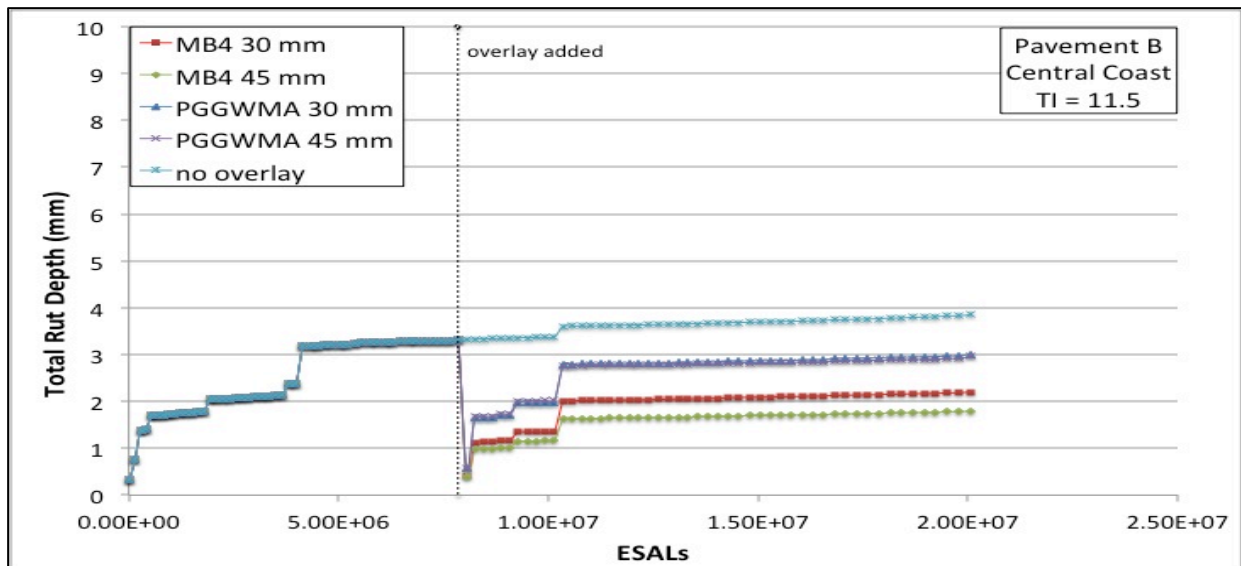


Figure 5.31. Total rut depth in Central Coast

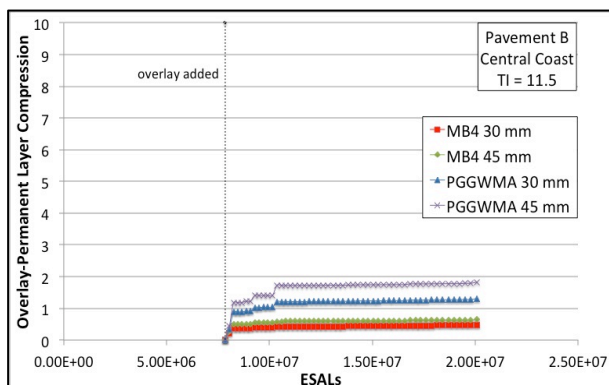


Figure 5.32. Rut depth overlay in Central Coast

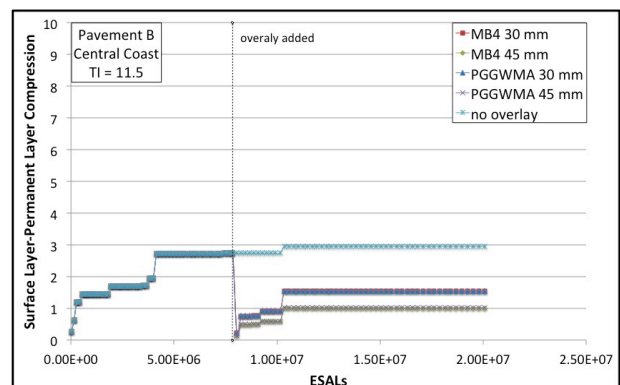


Figure 5.33. Rut depth surface layer in Central Coast

All the overlays applied do not show total surface cracking (Figure 5.27) when examining pavement B in Central Coast conditions and TI equal to 11.5. The fatigue damage of the PGGWMA overlay is quite close to 0 and in addition the MB4 overlay illustrates very low values (less than 0.1). In both situations the influence of the thickness is nearly insignificant. The fatigue damage in the second and first layer is similar for all the overlay applications (Figure 5.29 and Figure 5.30). As far as the rutting is concerned the results are similar to those found for pavement A. The main difference is related to the total rut depth in which, after a quick increase, the values become stable.

Table 5.8 summarizes the results for any overlay applied, relative to 5 indicators: total surface cracking, fatigue damage surface layer, fatigue damage base layer, total rut depth and rut depth surface layer.

	Overlay	After 5*10 <sup>6</sup> ESALs	%	After 1*10 <sup>7</sup> ESALs	%
Total Surface Cracking	No Overlay	0.314	100.0	0.761	100.0
	MB4 30	4.33E-08	0.00	1.53E-07	0.00
	MB4 45	1.89E-08	0.00	5.94E-08	0.00
	PGGWMA 30	8.11E-13	0.00	2.12E-12	0.00
	PGGWMA 45	9.92E-14	0.00	2.53E-13	0.00
Fatigue Damage Surface Layer	No Overlay	0.092	100.0	0.206	100.0
	MB4 30	0.067	73.29	0.128	62.17
	MB4 45	0.059	64.00	0.104	50.60
	PGGWMA 30	0.059	64.00	0.104	50.60
	PGGWMA 45	0.049	53.46	0.079	38.44
Fatigue Damage Base Layer	No Overlay	0.117	100.0	0.183	100.0
	MB4 30	0.098	83.70	0.131	71.82
	MB4 45	0.091	78.16	0.116	63.48
	PGGWMA 30	0.093	79.45	0.119	65.11
	PGGWMA 45	0.086	73.33	0.103	56.46
Total Rut Depth	No Overlay	3.65	100.0	3.78	100.0
	MB4 30	2.05	56.20	2.15	57.02
	MB4 45	1.66	45.52	1.75	46.40
	PGGWMA 30	2.83	77.47	2.94	77.82
	PGGWMA 45	2.79	76.54	2.89	76.43
Rut Depth Surface Layer	No Overlay	2.95	100.0	2.95	100.0
	MB4 30	1.54	52.30	1.54	52.30
	MB4 45	1.00	34.01	1.00	34.01
	PGGWMA 30	1.55	52.37	1.55	52.37
	PGGWMA 45	1.02	34.44	1.02	34.44

Table 5.8. Simulation Results

5.3.1.4 Pavement Structure B and TI=13

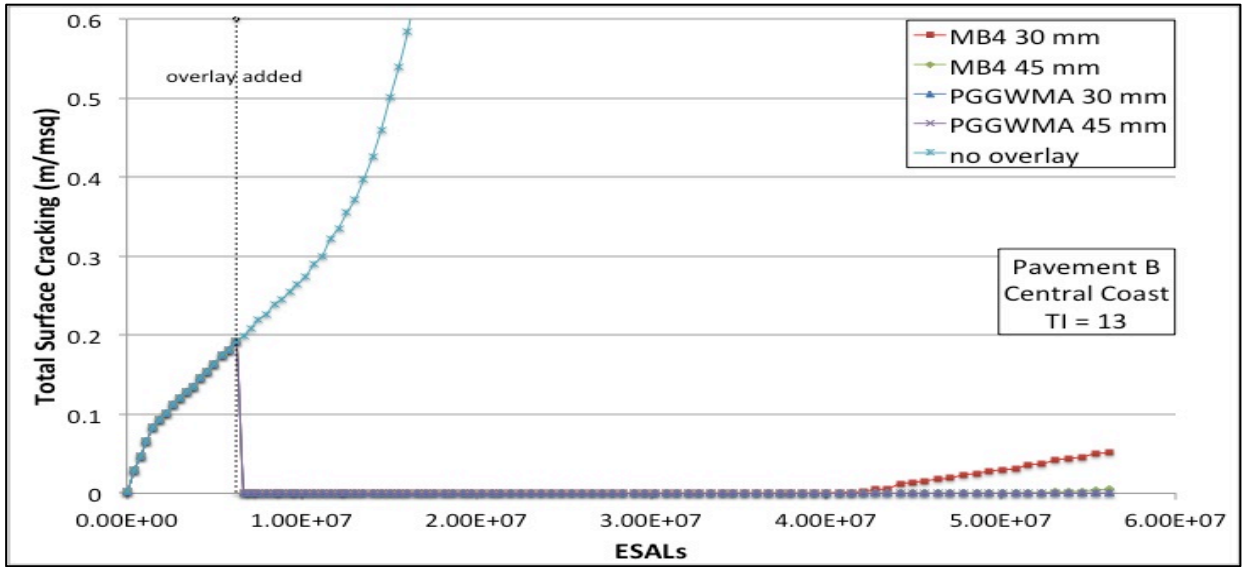


Figure 5.34. Total surface cracking in Central Coast

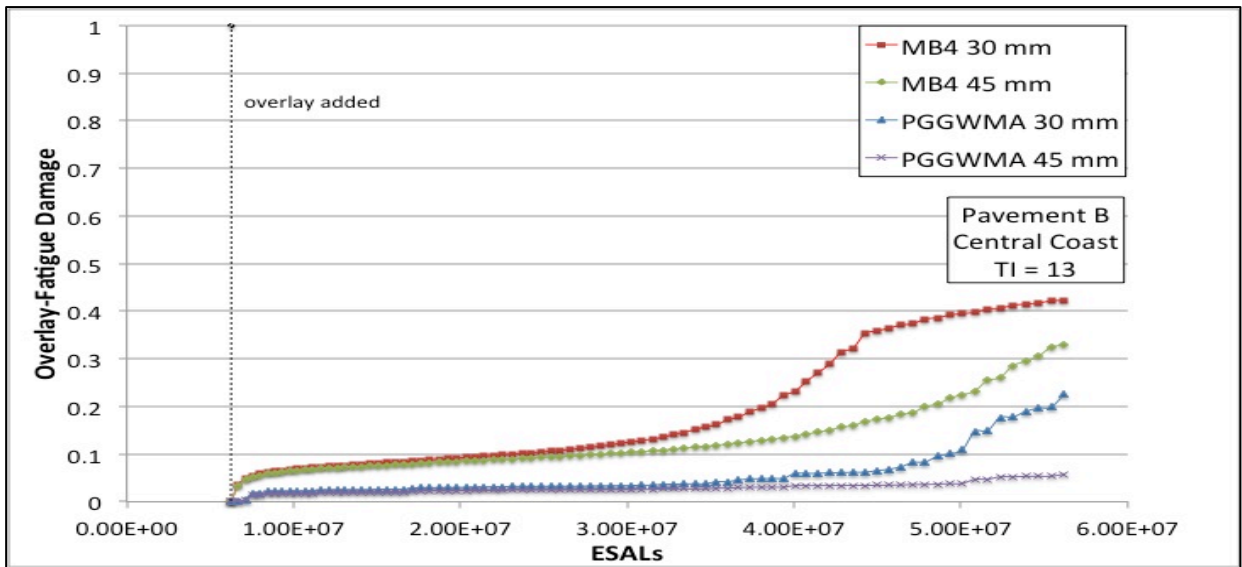


Figure 5.35. Fatigue damage in overlay in Central Coast

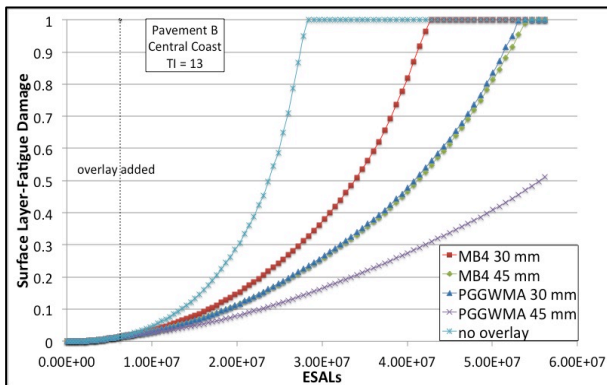


Figure 5.36. Fat. dam. surface layer in Central Coast

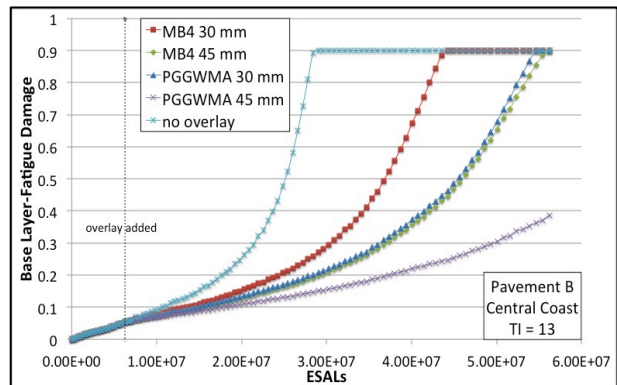


Figure 5.37. Fat. dam. base layer in Central Coast

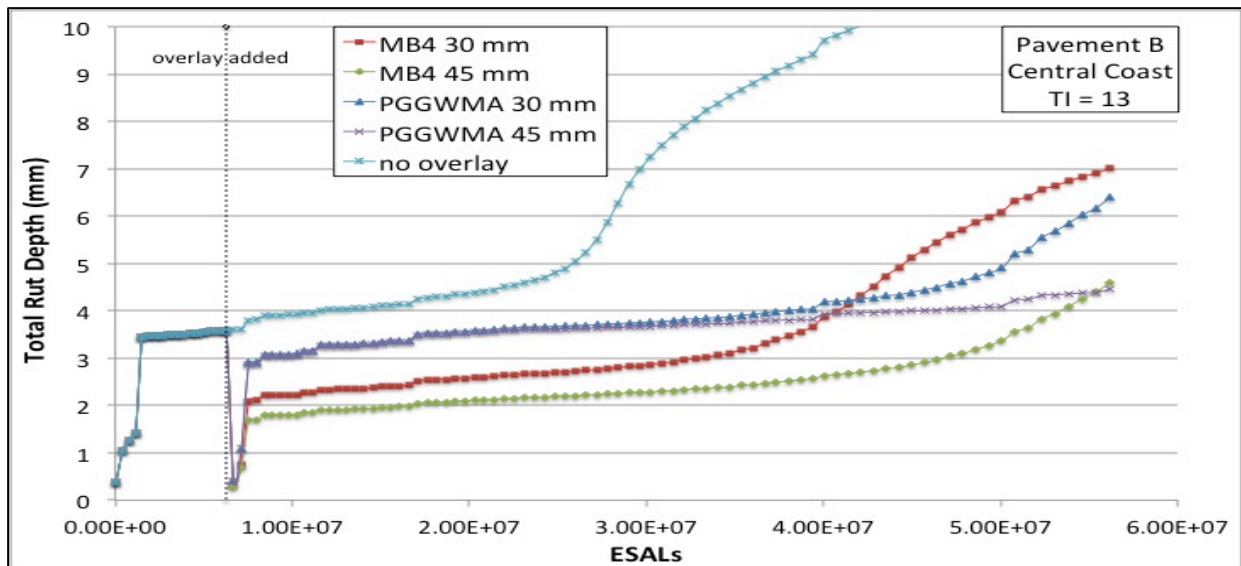


Figure 5.38. Total rut depth in Central Coast

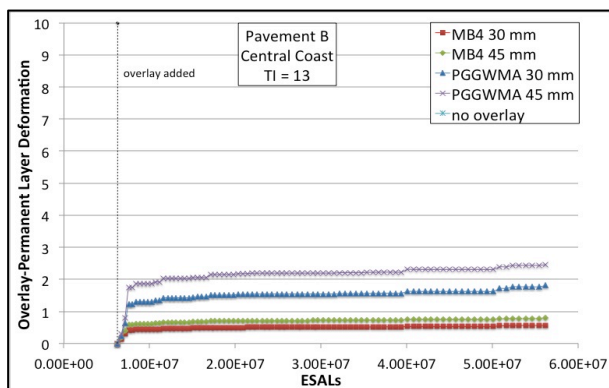


Figure 5.39. Rut depth overlay in Central Coast

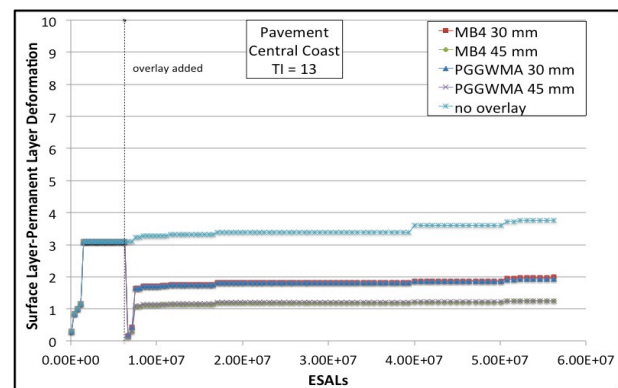


Figure 5.40. Rut depth surface layer in Central Coast

With a traffic index of 13, the pavements with an overlay, in terms of surface cracking, keep on improving. Only with MB4 30 mm, as overlay, few cracks are visible (less than  $0.1 \text{ m}^2$  after  $4 \cdot 10^7$  ESALs). The overlay fatigue damage grows slowly until  $3.5 \cdot 10^7$ , then for each overlay it starts to accelerate its growth (except for the PGGWMA 45). Figure 5.36 and Figure 5.37 confirm better performance in terms of fatigue damage with PGGWMA 45 mm (the only overlay that does not reach the limit of 1 for the surface layer and of 0.9 for the base layer) although the worst results are shown by MB4 30 mm. Until  $4 \cdot 10^7$  ESALs also in terms of rutting the previous results are confirmed (better performance with MB4), but after that load, on equal terms of thickness, PGGWMA becomes more suitable (Figure 5.38).

Table 5.9 summarizes the results for any overlay applied, relative to 5 indicators: total surface cracking, fatigue damage surface layer, fatigue damage base layer, total rut depth and rut depth surface layer.

	Overlay	After $5 \cdot 10^6$ ESALs	%	After $1 \cdot 10^7$ ESALs	%	After $1.5 \cdot 10^7$ ESALs	%
Total Surface Cracking	No Overlay	0.321	100.0	0.641	100.0	2.305	100.0
	MB4 30	4.24E-08	0.00	1.26E-07	0.00	3.94E-07	0.00
	MB4 45	1.82E-08	0.00	4.95E-08	0.00	1.26E-08	0.00
	PGGWMA 30	6.00E-12	0.00	1.17E-11	0.00	4.95E-11	0.00
	PGGWMA 45	7.09E-13	0.00	1.34E-12	0.00	4.51E-12	0.00
Fatigue Damage Surface Layer	No Overlay	0.068	100.0	0.174	100.0	0.387	100.0
	MB4 30	0.047	69.26	0.099	56.98	0.185	47.63
	MB4 45	0.040	59.26	0.078	44.83	0.137	35.28
	PGGWMA 30	0.041	59.61	0.079	45.36	0.140	36.04
	PGGWMA 45	0.033	48.86	0.058	33.11	0.094	24.26
Fatigue Damage Base Layer	No Overlay	0.112	100.0	0.177	100.0	0.322	100.0
	MB4 30	0.089	79.39	0.122	69.06	0.174	54.18
	MB4 45	0.081	72.63	0.106	59.97	0.142	44.05
	PGGWMA 30	0.084	74.91	0.110	62.38	0.149	46.28
	PGGWMA 45	0.076	67.55	0.093	52.90	0.118	36.62
Total Rut Depth	No Overlay	4.02	100.0	4.15	100.0	4.51	100.0
	MB4 30	2.33	58.08	2.43	58.58	2.64	58.66
	MB4 45	1.90	47.24	1.98	47.74	2.15	47.66
	PGGWMA 30	3.28	81.53	3.37	81.37	3.63	80.50
	PGGWMA 45	3.26	81.05	3.35	80.72	3.59	79.62
Rut Depth Surface Layer	No Overlay	3.31	100.0	3.32	100.0	3.39	100.0
	MB4 30	1.75	52.82	1.76	52.96	1.83	53.88
	MB4 45	1.14	34.45	1.14	34.54	1.19	35.04
	PGGWMA 30	1.75	52.85	1.76	53.00	1.83	53.91
	PGGWMA 45	1.16	34.88	1.16	34.98	1.20	35.47

Table 5.9. Simulation Results

### 5.3.2 Desert Condition

#### 5.3.2.1 Pavement Structure A and TI=11.5

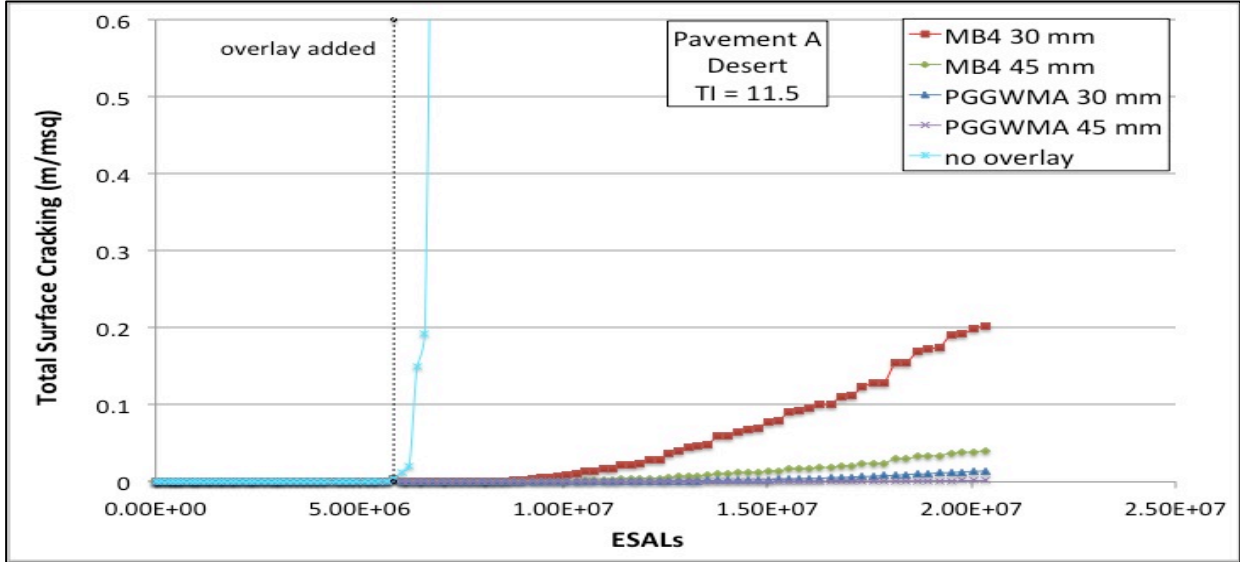


Figure 5.41. Total surface cracking in Desert

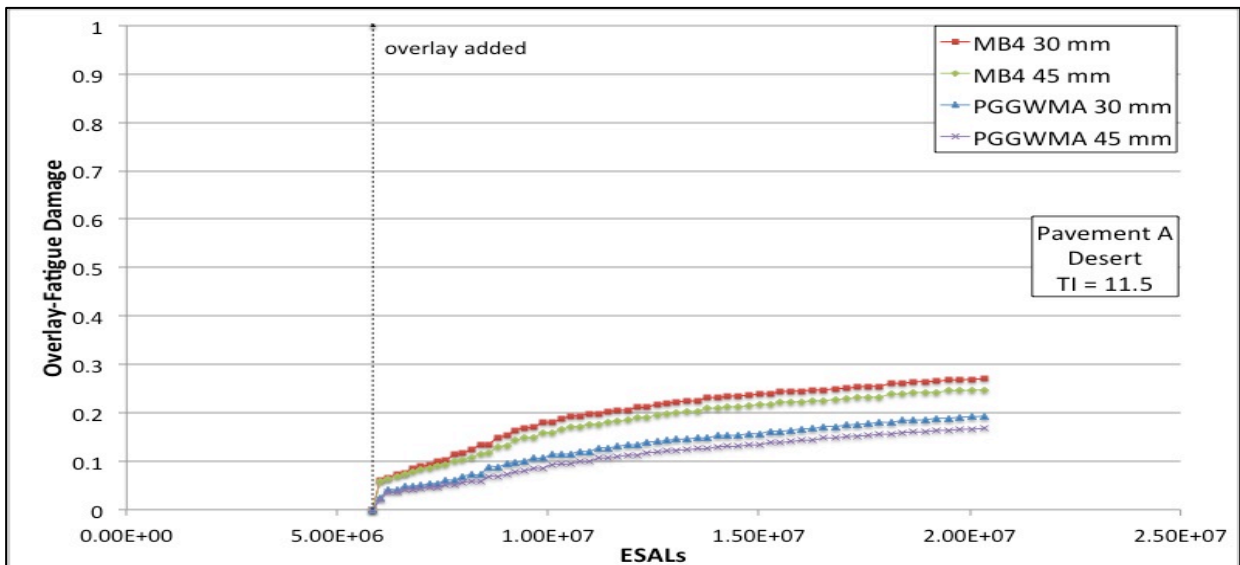


Figure 5.42. Fatigue damage in overlay in Desert

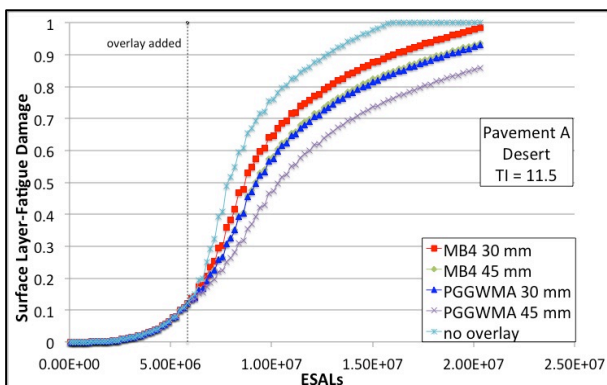


Figure 5.43. Fat. dam. surface layer in Desert

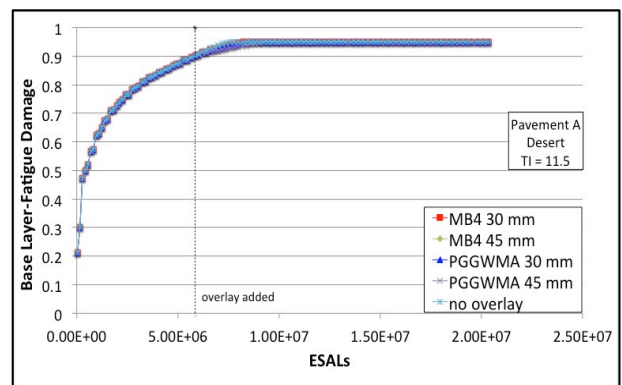


Figure 5.44. Fat. dam. base layer in Desert

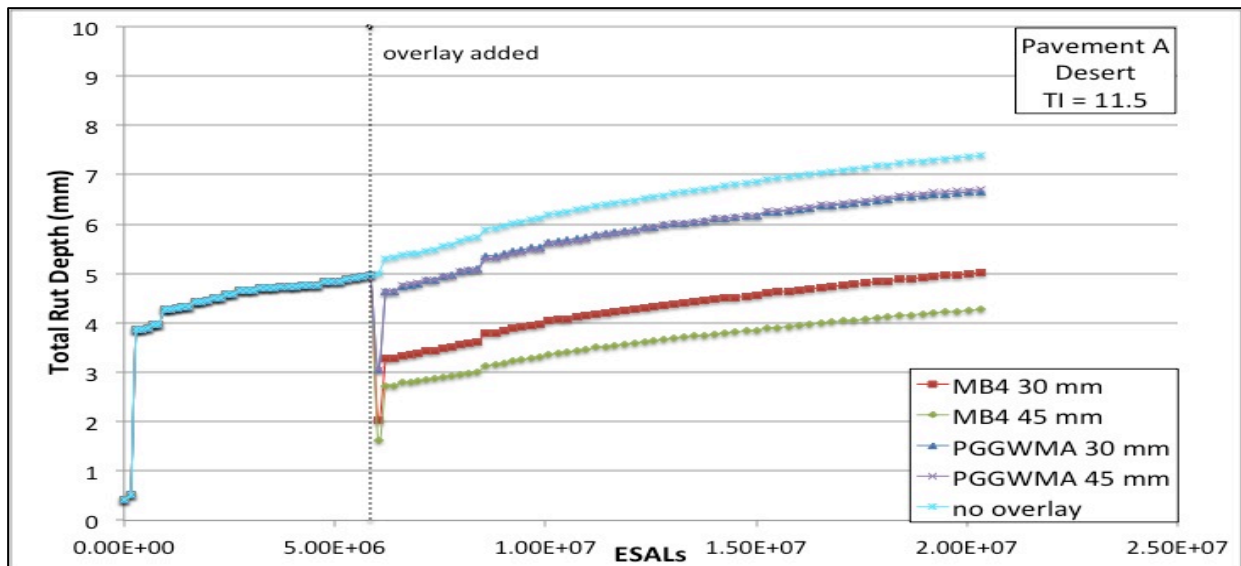


Figure 5.45. Total rut depth in Desert

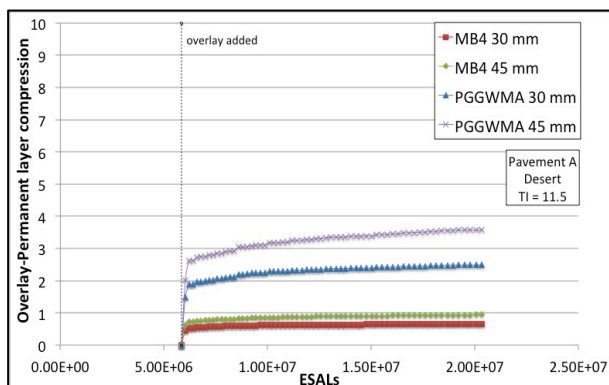


Figure 5.46. Rut depth overlay in Desert

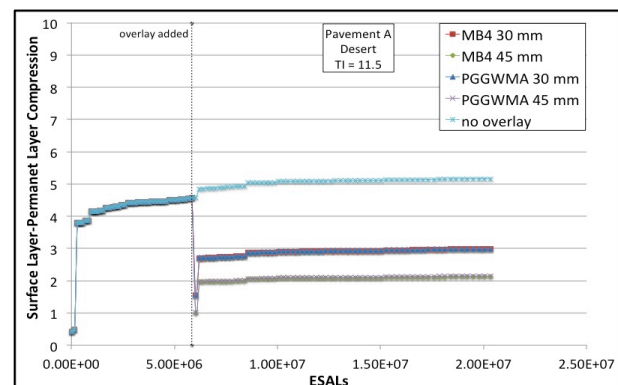


Figure 5.47. Rut depth surface layer in Desert

Considering Figure 5.41, the pavements with PGGWMA as overlay ascertain a better performance in terms of surface cracking also in Desert conditions. The worst overlay as usual is MB4 30 mm. On equal terms of pavement structure and traffic index the damage is higher compared with results obtained in Central Coast Climate. The fatigue damage in the overlay and in the first layer, verify the results observed in total surface cracking. As always, for pavement A, the base was too damaged at the time of the overlay application no overlay leads to a significant improvement in the fatigue damage of this layer. In terms of rutting, the severe climate has a negative influence on the behavior of the pavements that reach higher levels of total rut depth, permanent overlay compression and permanent surface layer compression. As usual best performances in total rut depth are obtained with MB4 45 mm followed by MB4 30 mm (Figure 5.45). Table 5.10 summarizes the results for any overlay applied, relative to 5 indicators: total surface cracking, fatigue damage surface layer, fatigue damage base layer, total rut depth and rut depth surface layer.

	Overlay	After 5*10 <sup>6</sup> ESALs	%	After 1*10 <sup>7</sup> ESALs	%
Total Surface Cracking	No Overlay	10	100.0	10	100.0
	MB4 30	0.017	0.17	0.095	0.95
	MB4 45	0.003	0.03	0.018	0.18
	PGGWMA 30	3.2E-04	0.00	0.004	0.04
	PGGWMA 45	2.8E-05	0.00	0.0005	0.01
Fatigue Damage Surface Layer	No Overlay	0.82	100.0	1.00	100.0
	MB4 30	0.72	86.83	0.90	89.89
	MB4 45	0.66	79.51	0.85	84.81
	PGGWMA 30	0.65	78.45	0.84	83.99
	PGGWMA 45	0.55	66.85	0.76	76.27
Fatigue Damage Base Layer	No Overlay	0.95	100.0	0.95	100.0
	MB4 30	0.95	100.0	0.95	100.0
	MB4 45	0.95	100.0	0.95	100.0
	PGGWMA 30	0.95	100.0	0.95	100.0
	PGGWMA 45	0.95	100.0	0.95	100.0
Total Rut Depth	No Overlay	6.32	100.0	6.98	100.0
	MB4 30	4.14	65.54	4.67	66.88
	MB4 45	3.45	54.68	3.95	56.59
	PGGWMA 30	5.72	90.61	6.30	90.28
	PGGWMA 45	5.68	89.93	6.32	90.56
Rut Depth Surface Layer	No Overlay	5.08	100.0	5.13	100.0
	MB4 30	2.91	57.30	2.95	57.49
	MB4 45	2.07	40.82	2.10	40.89
	PGGWMA 30	2.92	57.56	2.96	57.80
	PGGWMA 45	2.09	41.23	2.12	41.35

Table 5.10. Simulation Results

5.3.2.2 Pavement Structure A and TI=13

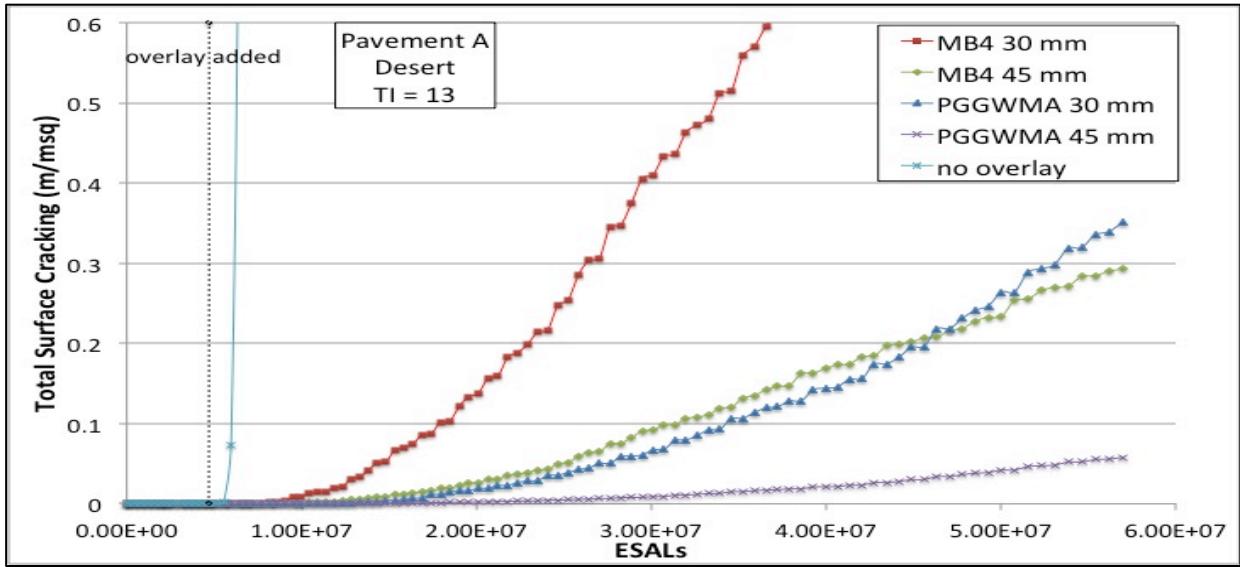


Figure 5.48. Total surface cracking in Desert

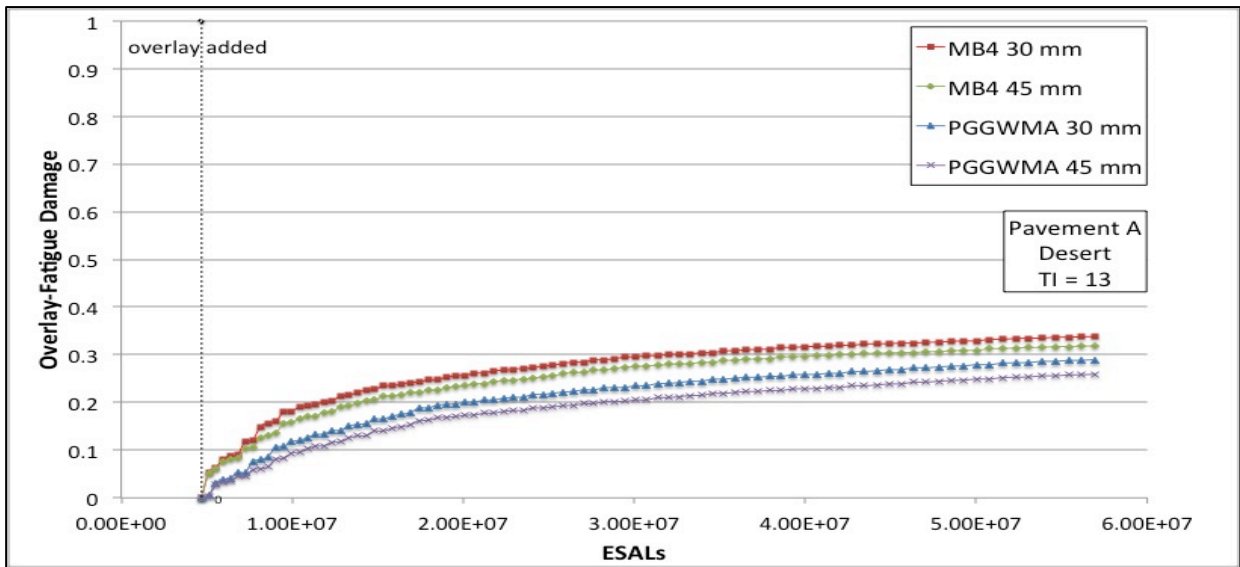


Figure 5.49. Fatigue damage in overlay in Desert

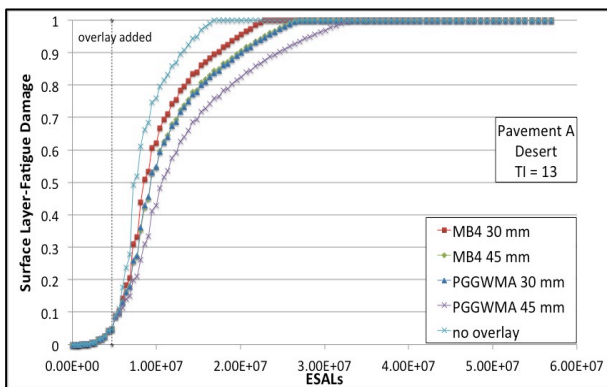


Figure 5.50. Fat. dam. surface layer in Desert

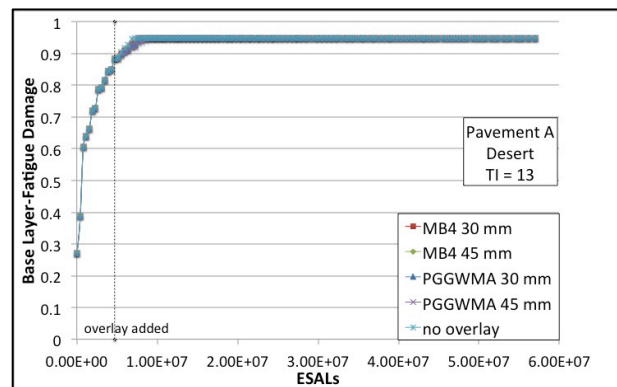


Figure 5.51. Fat. dam. base layer in Desert

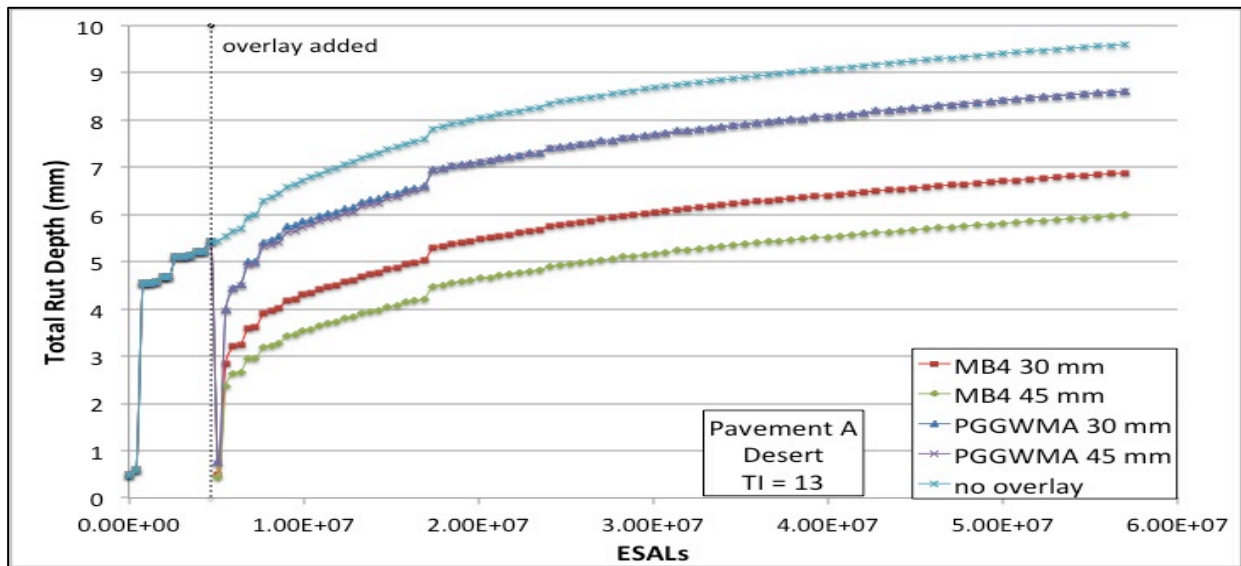


Figure 5.52. Total rut depth in Desert

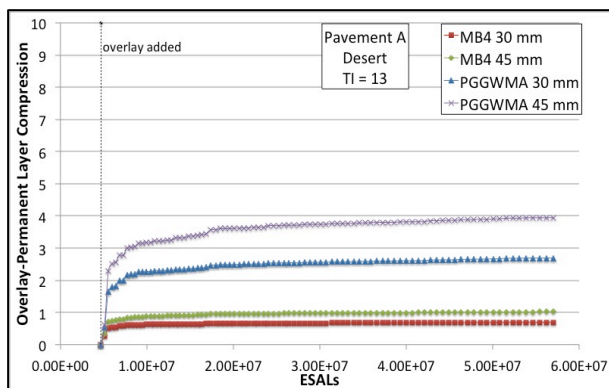


Figure 5.53. Rut depth overlay in Desert

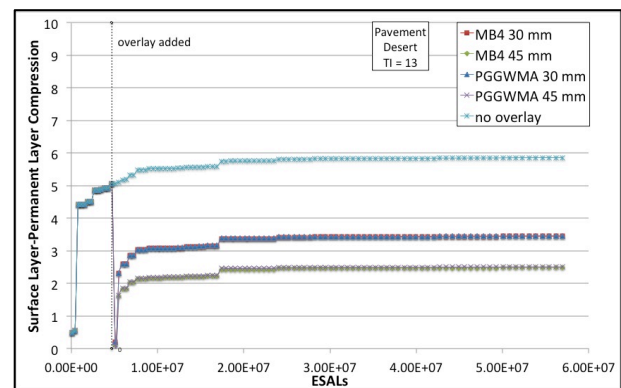


Figure 5.54. Rut depth surface layer in Desert

Analyzing the simulations with a traffic index of 13, a higher level of damage is reached both for cracking and rutting. The MB4 30 mm has the worst performance in terms of surface cracking and exceeds the  $0.5 \text{ m/m}^2$  at  $3.5 \times 10^7$  ESALs. Furthermore after  $5 \times 10^7$  ESALs the MB4 45 mm offers better outcomes than the PGGWMA 30 mm. The overlay fatigue damage is very similar for all the overlays. The fatigue damage of layer 1 and layer 2 follow the results obtained in the previous simulation. Concerning Figures 5.52, 5.53 and 5.54 the trend is similar to that obtained with the same pavement at the traffic index of 11.5, however with considerably higher values. Table 5.11 summarizes the results for any overlay applied, relative to 5 indicators: total surface cracking, fatigue damage surface layer, fatigue damage base layer, total rut depth and rut depth surface layer.

	Overlay	After $5 \times 10^6$ ESALs	%	After $1 \times 10^7$ ESALs	%	After $1.5 \times 10^7$ ESALs	%
Total Surface Cracking	No Overlay	9.99	100.0	10.0	100.0	10	100.0
	MB4 30	0.009	0.09	0.067	0.67	0.157	1.57
	MB4 45	0.001	0.01	0.012	0.12	0.030	0.30
	PGGWMA 30	2.8E-04	0.00	0.004	0.04	0.020	0.20
	PGGWMA 45	1.7E-05	0.00	4.18E-04	0.00	0.002	0.02
Fatigue Damage Surface Layer	No Overlay	0.76	100.0	0.97	100.0	1.00	100.0
	MB4 30	0.62	82.00	0.86	88.70	0.97	96.72
	MB4 45	0.54	71.85	0.81	83.11	0.92	91.67
	PGGWMA 30	0.55	72.14	0.80	82.51	0.91	91.24
	PGGWMA 45	0.43	56.55	0.72	73.97	0.84	83.90
Fatigue Damage Base Layer	No Overlay	0.95	100.0	0.95	100.0	0.95	100.0
	MB4 30	0.95	100.0	0.95	100.0	0.95	100.0
	MB4 45	0.95	100.0	0.95	100.0	0.95	100.0
	PGGWMA 30	0.95	100.0	0.95	100.0	0.95	100.0
	PGGWMA 45	0.95	100.0	0.95	100.0	0.95	100.0
Total Rut Depth	No Overlay	6.73	100.0	7.42	100.0	8.08	100.0
	MB4 30	4.30	63.93	4.87	65.65	5.51	68.17
	MB4 45	3.53	52.50	4.07	54.87	4.67	57.83
	PGGWMA 30	5.86	87.13	6.45	86.83	7.15	88.53
	PGGWMA 45	5.74	85.30	6.37	85.77	7.13	88.31
Rut Depth Surface Layer	No Overlay	5.53	100.0	5.57	100.0	5.76	100.0
	MB4 30	3.09	55.83	3.14	56.26	3.38	58.66
	MB4 45	2.17	39.24	2.21	39.62	2.43	42.24
	PGGWMA 30	3.09	55.90	3.14	56.41	3.39	58.90
	PGGWMA 45	2.19	39.64	2.23	40.08	2.46	42.72

Table 5.11. Simulation Results

5.3.2.3 Pavement Structure B and TI=11.5

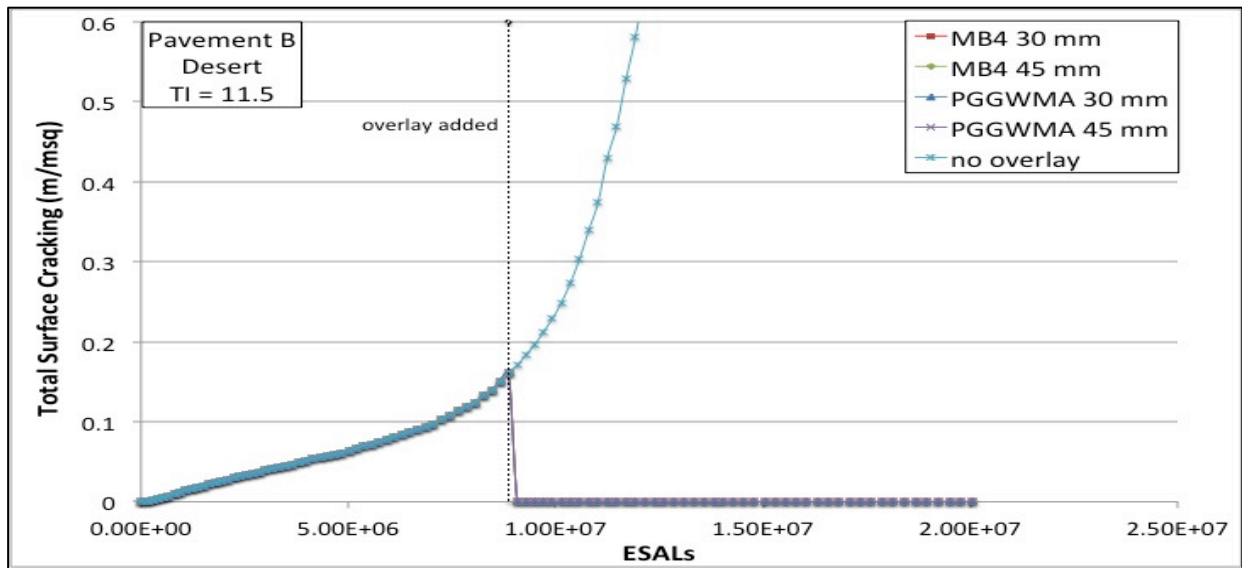


Figure 5.55. Total surface cracking in Desert

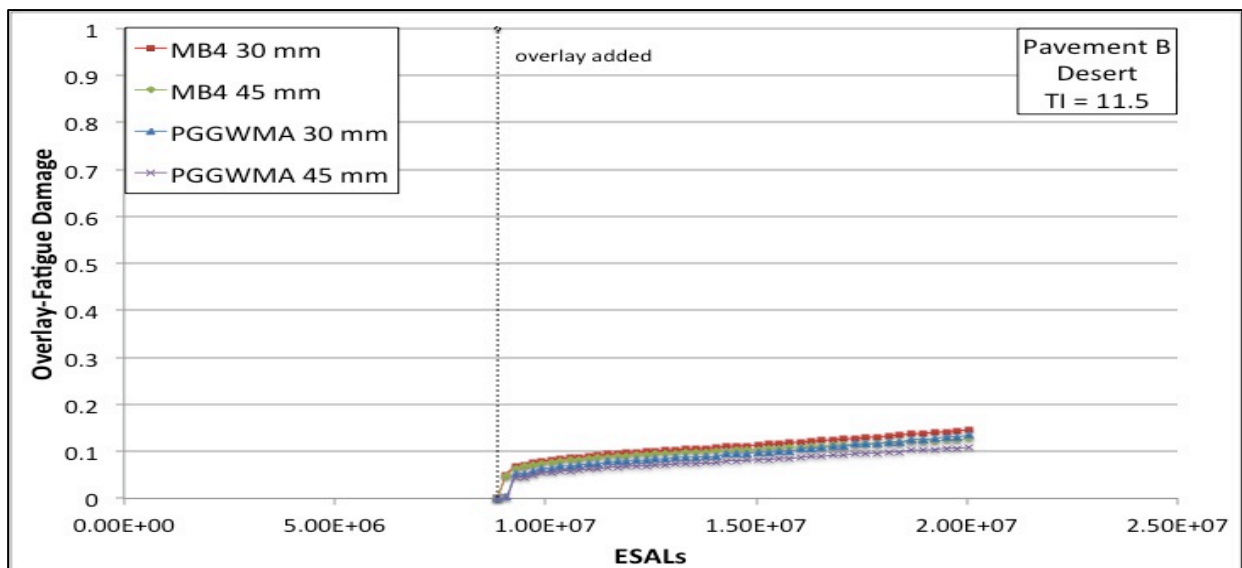


Figure 5.56. Fatigue damage in overlay in Desert.

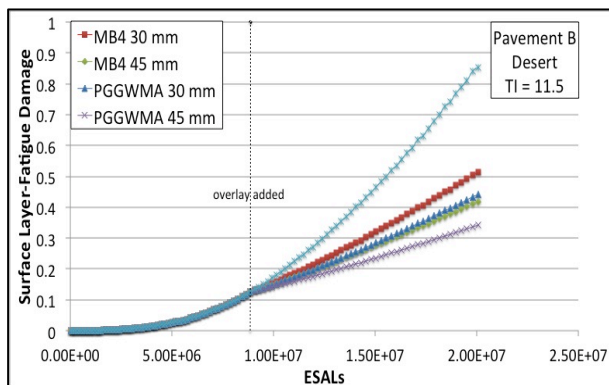


Figure 5.57. Fat. dam. surface layer in Desert

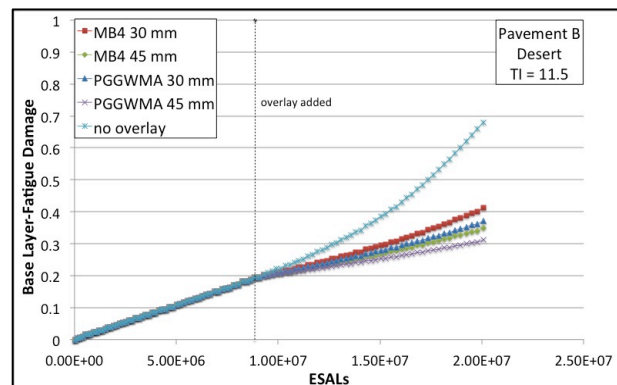


Figure 5.58. Fat. dam. base layer in Desert

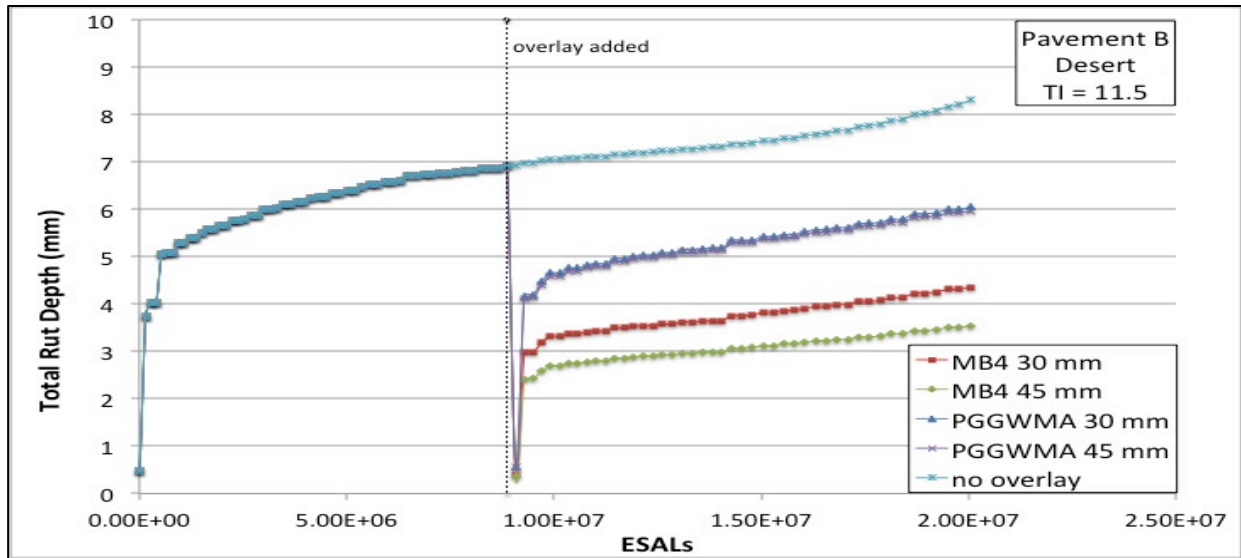


Figure 5.59. Total rut depth in Desert

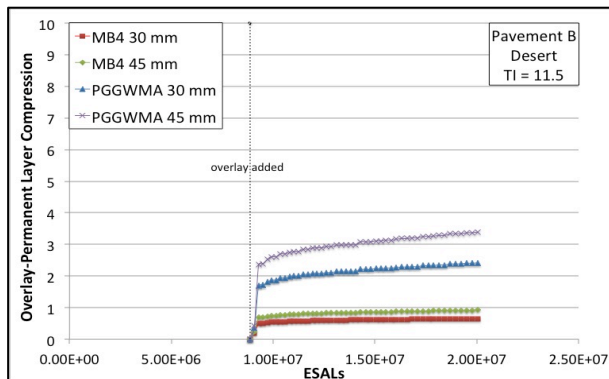


Figure 5.60. Rut depth overlay in Desert

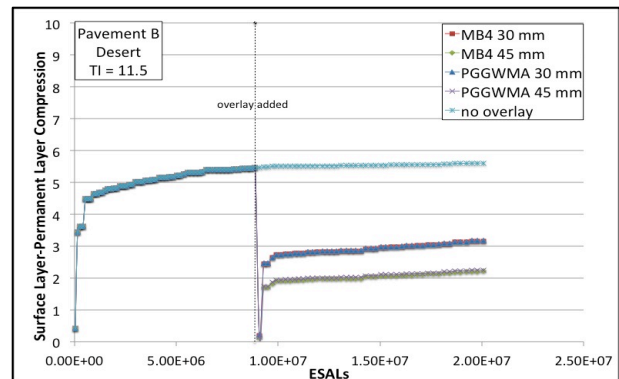


Figure 5.61. Rut depth surface layer in Desert

With none of the four overlays the pavement B is affected by surface cracking. The fatigue damage of the overlay is very similar for all overlays, with values slightly higher than 0.1. The fatigue damage for the surface layer and the base layer shows very similar outcomes with the comparable behavior of four overlays. Considering the rutting, the performance of the plots follow what was found in the Central Coast conditions. Generally speaking, the damage is higher due to the most severe climatic conditions.

Table 5.12 summarizes the results for any overlay applied, relative to 5 indicators: total surface cracking, fatigue damage surface layer, fatigue damage base layer, total rut depth and rut depth surface layer.

	Overlay	After 5*10 <sup>6</sup> ESALs	%	After 1*10 <sup>7</sup> ESALs	%
Total Surface Cracking	No Overlay	1.56	100.0	8.21	100.0
	MB4 30	9.8E-07	0.00	7.5E-06	0.00
	MB4 45	3.6E-07	0.00	1.9E-06	0.00
	PGGWMA 30	2.0E-07	0.00	3.5E-06	0.00
	PGGWMA 45	3.7E-08	0.00	4.9E-07	0.00
Fatigue Damage Surface Layer	No Overlay	0.40	100.0	0.79	100.0
	MB4 30	0.29	71.22	0.48	60.92
	MB4 45	0.25	62.03	0.39	49.90
	PGGWMA 30	0.26	63.67	0.41	52.56
	PGGWMA 45	0.22	53.80	0.32	41.07
Fatigue Damage Base Layer	No Overlay	0.34	100.0	0.62	100.0
	MB4 30	0.27	19.84	0.39	37.57
	MB4 45	0.25	25.76	0.33	46.55
	PGGWMA 30	0.26	23.35	0.35	43.30
	PGGWMA 45	0.24	29.40	0.30	51.81
Total Rut Depth	No Overlay	7.31	100.0	8.09	100.0
	MB4 30	3.65	49.92	4.25	52.61
	MB4 45	2.98	40.78	3.46	42.79
	PGGWMA 30	5.18	70.83	5.93	73.32
	PGGWMA 45	5.14	70.22	5.86	72.40
Rut Depth Surface Layer	No Overlay	5.52	100.0	5.59	100.0
	MB4 30	2.85	51.59	3.13	55.91
	MB4 45	1.98	35.92	2.19	39.13
	PGGWMA 30	2.86	51.84	3.14	56.20
	PGGWMA 45	2.02	36.57	2.23	39.82

Table 5.12. Simulation Results

5.3.2.4 Pavement Structure B and TI=13

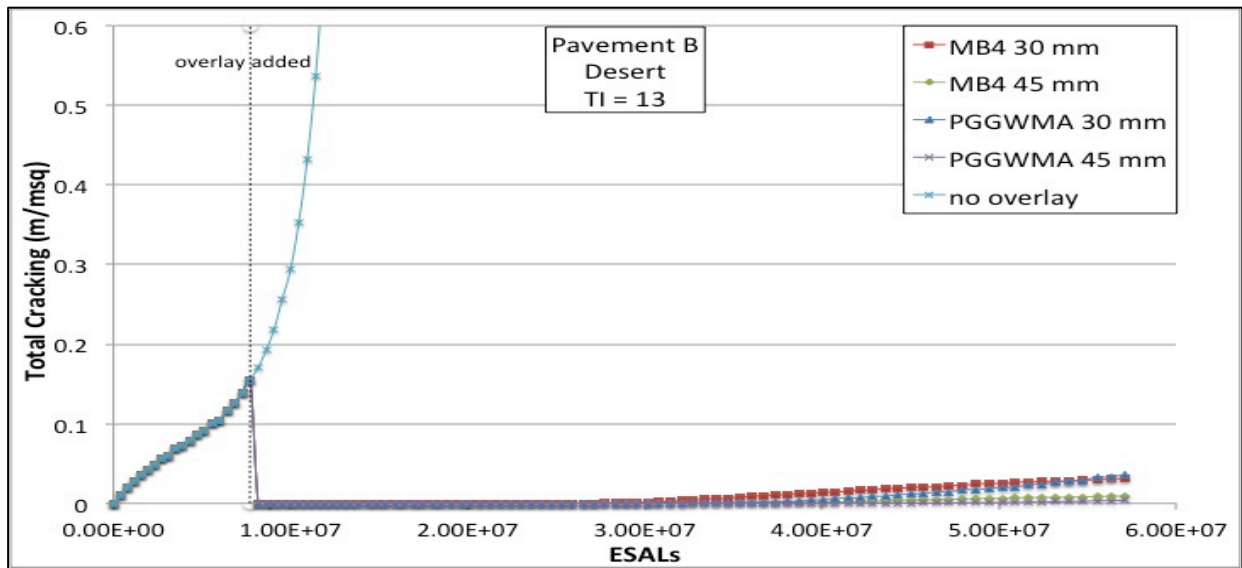


Figure 5.62. Total surface cracking in Desert

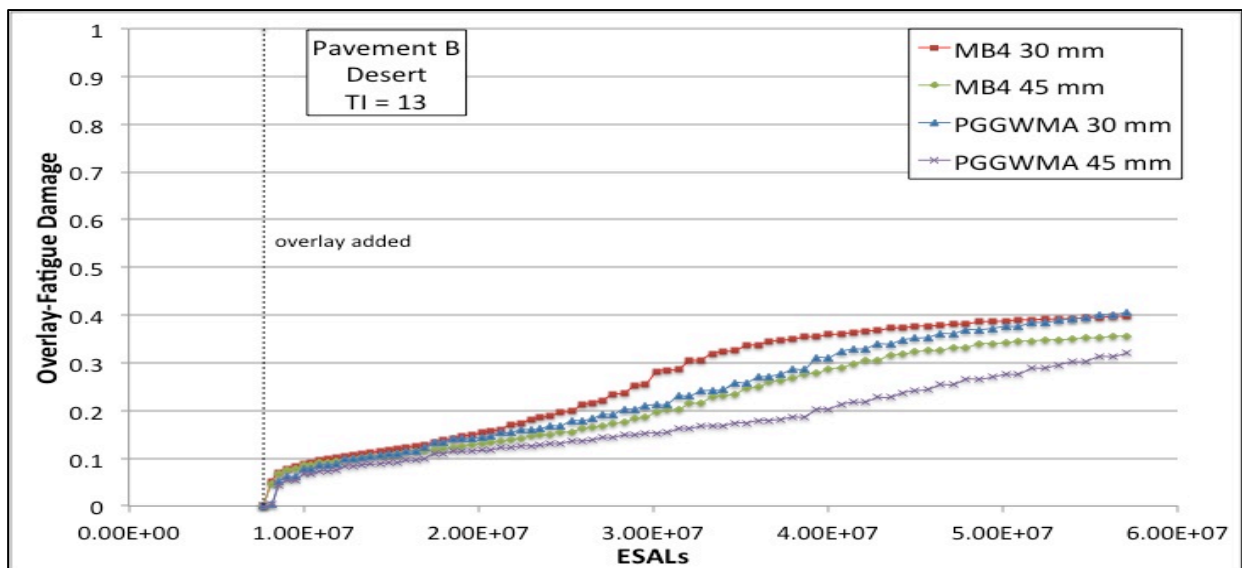


Figure 5.63. Fatigue damage in overlay in Desert

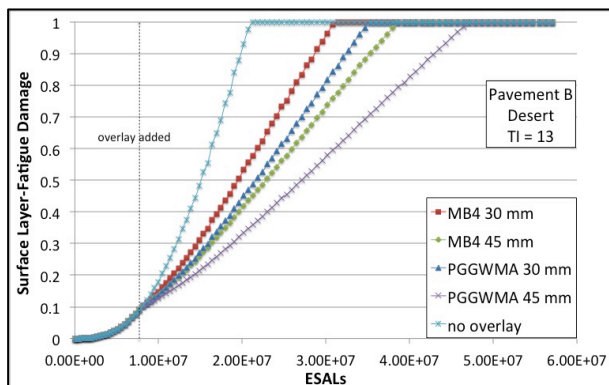


Figure 5.64. Fat. dam. surface layer in Desert

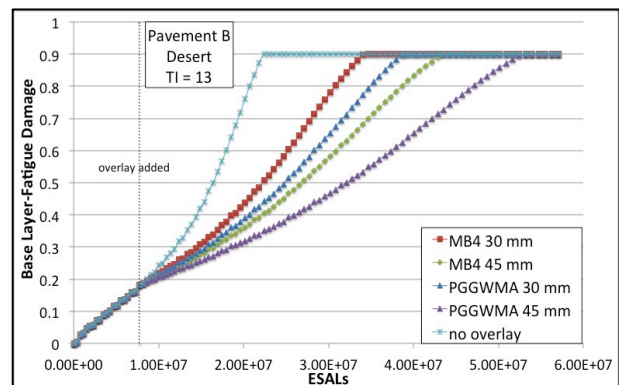


Figure 5.65. Fat. dam. base layer in Desert

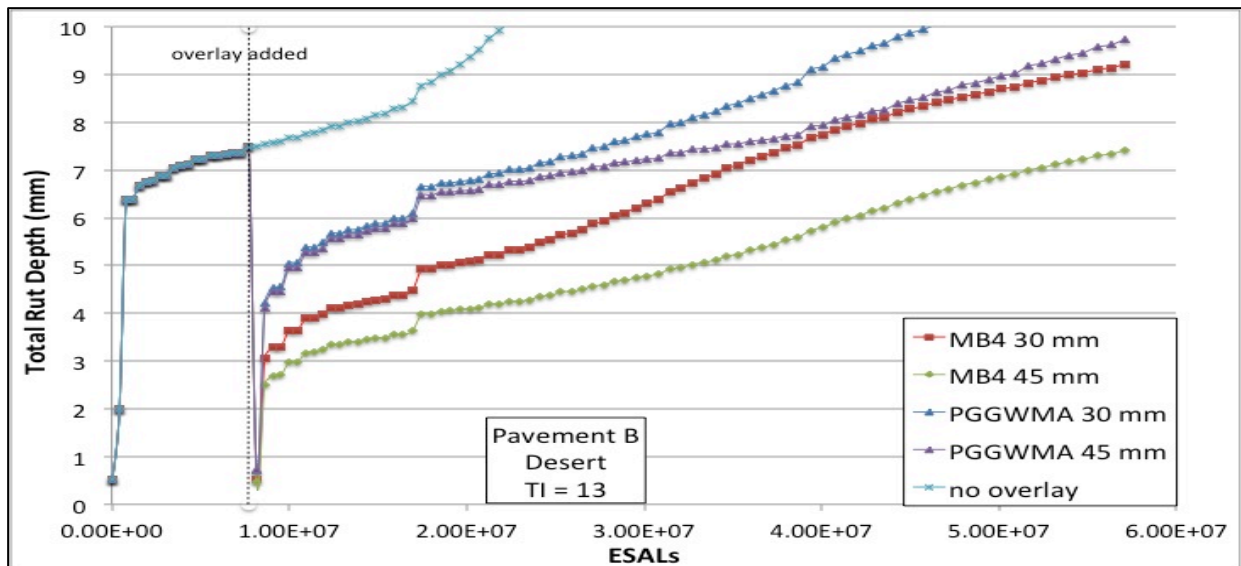


Figure 5.66. Total rut depth in Desert

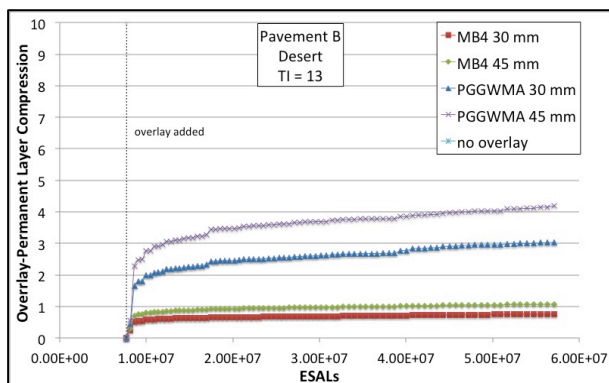


Figure 5.67. Rut depth overlay in Desert

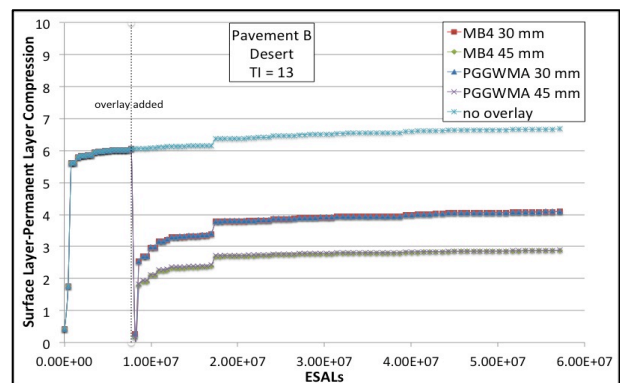


Figure 5.68. Rut depth surface layer in Desert

With a traffic index of 13 the pavement simulated shows surface cracking with MB4 30 mm and PGGWMA 30 mm overlays. In this case the thickness has more influence than the material type. In contrast with previous simulations, also with PGGWMA 45 mm, the surface layer fatigue damage reaches the limit value of 1. In the total rut depth the limit criteria is passed by the PGGWMA 30 mm overlay. With PGGWMA overlays the thickness does not affect the performance until  $1.8 \times 10^7$  ESALs. As already established, in terms of rutting, best performances are reached with MB4 45 mm. Table 5.13 summarizes the results for any overlay applied, relative to 5 indicators: total surface cracking, fatigue damage surface layer, fatigue damage base layer, total rut depth and rut depth surface layer.

	Overlay	After $5 \cdot 10^6$ ESALs	%	After $1 \cdot 10^7$ ESALs	%	After $1.5 \cdot 10^7$ ESALs	%
Total Surface Cracking	No Overlay	1.1	100.0	7.2	100.0	10.0	100.0
	MB4 30	8.2E-07	0.00	6.6E-06	0.00	5.9E-05	0.00
	MB4 45	3.2E-07	0.00	1.7E-06	0.00	7.2E-06	0.00
	PGGWMA 30	4.2E-07	0.00	5.4E-06	0.00	2.1E-05	0.00
	PGGWMA 45	8.0E-08	0.00	7.7E-07	0.00	2.2E-06	0.00
Fatigue Damage Surface Layer	No Overlay	0.35	100.0	0.74	100.0	1.00	100.0
	MB4 30	0.24	68.93	0.44	58.75	0.65	65.39
	MB4 45	0.21	59.18	0.35	47.03	0.51	50.57
	PGGWMA 30	0.21	61.03	0.37	50.09	0.55	55.05
	PGGWMA 45	0.18	50.69	0.28	37.94	0.40	40.05
Fatigue Damage Base Layer	No Overlay	0.33	100.0	0.60	100.0	0.90	100.0
	MB4 30	0.26	80.63	0.38	62.76	0.52	57.96
	MB4 45	0.24	74.63	0.32	53.68	0.41	45.93
	PGGWMA 30	0.25	77.18	0.34	57.20	0.45	50.19
	PGGWMA 45	0.23	70.99	0.29	48.50	0.35	39.41
Total Rut Depth	No Overlay	7.93	100.0	8.83	100.0	10.29	100.0
	MB4 30	4.12	51.98	4.94	55.90	5.34	51.86
	MB4 45	3.35	42.28	3.99	45.20	4.26	41.37
	PGGWMA 30	5.67	71.56	6.65	75.28	7.02	68.20
	PGGWMA 45	5.56	70.18	6.47	73.25	6.76	65.74
Rut Depth Surface Layer	No Overlay	6.14	100.0	6.36	100.0	6.41	100.0
	MB4 30	3.29	53.59	3.78	59.41	3.82	59.61
	MB4 45	2.32	37.77	2.69	42.20	2.71	42.26
	PGGWMA 30	3.30	53.82	3.79	59.58	3.83	59.77
	PGGWMA 45	2.36	38.40	2.72	42.73	2.74	42.79

Table 5.13. Simulation Results

## 5.4 Results Analysis

As far as the first simulations are concerned, Pavement A and Pavement B without overlays, the best performance in terms of cracking is in Central Coast with the base in hot mix asphalt. On the other hand, in terms of rutting, best performance is reached with the cement treated base class B. Focusing on the Desert climate, the environmental effects modified the performance, reducing both rutting and cracking resistance in each pavements. Regarding the load due to traffic, with a greater Traffic Index, the pavements considered are affected, with the same ESALs, by a slightly higher fatigue damage and rutting. This is fundamentally due to two factors:

- 1) Two aspects of loading are ESAL and temperature. Applying the same ESAL under different climate conditions (climate conditions vary during the year) will lead to different damage;
- 2) With a Traffic Index of 13 rather than 11.5, more ESALs are applied at the beginning, which is when the damage rate is faster.

Considering the other simulations, Pavements A and B with overlay, the best outcomes, with regard to cracking surface, are obtained with PGGWMA overlays. Furthermore situations in which none of the four overlays show cracking are observed. For instance with Pavement B, TI=11.5, in both climate conditions (Central Coast and Desert) and with Pavement B, TI=13, Central Coast climate (with the exception of the overlay MB4 30 mm). In addition only in two isolated cases the surface cracking criteria is exceeded: the first with Pavement A, TI=13, Central Coast climate and MB4 30 mm overlay, the second with the same overlay, the same pavement structure, the same traffic index and Desert climate.

On the other hand rubber asphalt overlays (MB4) demonstrate better performance in terms of rutting, whereas referring to PGGWMA overlays, the results show that the thickness influence is nearly irrelevant.



# *Conclusions*

Predicting asphalt fatigue cracking and rutting in a pavement structure is a difficult task, due to several aspects as the large number of variables that contribute to the deterioration process and the interaction with other distress mechanism.

Preventing pavement failure has significant economic implications at the initial construction and in addition throughout the service life. Thereupon an accurate prediction of these distresses lead to an optimization of design, maintenance and rehabilitation action to minimize the overall cost.

Until the end of 1990, the main design methods were empirical and the possibility to predict the evolution of surface cracking, rutting and other distresses was not contemplated. Thanks to several developments in the last years, advanced and efficient design methods are arisen as the Mechanistic-Empirical (ME) approaches. A ME design method consists of a structural model capable of predicting the state of stresses and strains within the pavement structure under the different traffic and environmental conditions. Effectively this study was developed by the utilization of a software based on this approach: CalME.

CalME is a software program developed by Caltrans/UCPRC using the Mechanistic-Empirical (ME) methodologies for analyzing and designing the performance of flexible pavements. CalME uses an “incremental recursive” (I-R) approach that models the entire damage process, not just the initial condition after construction and the final failure condition. Instead, CalME simulates the pavement performance starting from the initial undamaged pavement stress, strain, and deformation responses to temperature and load to the end failure state (CALTRANS).

In the first section of this research an empirical method is applied to design two different pavement structures, respectively a flexible and a semi-rigid. As the input data (traffic index and substrate resistance) are the same, the two pavements should provide the same performance. However the results derived from the simulations carried out with Calme, show that the two pavement structures have different responses during the service life. Analyzing the experimental results, the simulations exhibit that, in terms of surface cracking, a flexible pavement structure (the base layer is a hot mix asphalt) leads to better performance compared to a semi-rigid pavement structure. Moreover a comparison between two different climate situations demonstrates that severe environmental conditions affect in negative both pavements performance.

In the second section, in order to verify the properties of two different materials (a warm mix asphalt (PGGWMA) and a rubber asphalt (MB4)) and explore the Mechanistic-Empirical (I-R) approach potentiality, CalME was used to simulate the application of different typology of overlays on the above-mentioned pavement structures. The simulations demonstrate different results according to the distress analyzed. With regard to the surface cracking PGGWMA overlays reach the best performance, on the other hand concerning the rutting MB4 overlays show a better behavior. Also with the PGGWMA overlays the outcomes are under the rutting limit criteria, consequently this material type is more advisable to be adopted for a maintenance application. With respect to the thickness influence, a higher thickness leads to better performance in both rutting and cracking damage. Moreover, utilizing a thicker overlay reduce the strain level in the base layer and the correlated rate damage decreases as well, leading to a better performance in terms of fatigue damage. Nevertheless when the traffic index considered is equal to 11.5 a thickness of 30 mm produces fitting results, whereas with a traffic level of 13 a thickness of 45 mm is recommended.

To conclude, a Mechanistic-Empirical design instrument is decidedly appropriate for evaluating different design and material alternatives both in initial construction and maintenance, accounting for both laboratory performance and field conditions. The experimentation demonstrates the efficiency of the Mechanistic-Empirical (I-R) approach, whereby the empirical method limits are passed. Effectively in the ME method, the numerous variables affecting the pavement service life are considered. The procedure, utilizing models related to material properties, axle load spectra and pavement temperatures, permits a better pavement design in terms of thickness and material optimization. Based on this assumptions it would be desirable, also in Italy, the implementation of these more realistic and efficient methods, neglecting the outdated empirical design.

# *List of Reference*

- AASHTO Guide, 1972
- AASHTO Guide, 1986
- AASHTO Guide, 1993
- ACPA, 2001
- Asphalt-Institute, 1982
- Asphalt-Institute, 1991
- "Asphalt Pavement Design -The Shell Method", Claussen, A. I. M., J. M. Edwards, P. Sommer, and P. Udge., 1977
- "CalBack: Enhancing Caltrans Mechanistic-Empirical Pavement Design Process with New Back-Calculation Software", Lu Qing, James Signore, Ullidtz, 2008
- "CalME: A New Mechanistic-Empirical Design Program for Flexible Pavement Rehabilitation", P. P. Ullidtz, J. T. Harvey, I. Basheer, J. David, R. Wu, J. Lea, L. Quing, 2010
- Calme Manual, 2012
- Distress Identification Manual for The LTPP, 2003
- "Effect of Tire Parameters on Pavement Damage and Load-Equivalency Factors" Sebaaly, P. E., and N. Tabatabaee, 1992
- "Flexible Pavement Rehabilitation Manual", 2001
- "Guide to LTPP Traffic Data Collection and Processing", FHWA, 2001
- "Highway Design Manual, Chapter 600"
- "Highway Design Manual, Chapter 610"
- "Highway Design Manual, Chapter 630"
- Highway Research Board: "The AASHO Road Test. Report 61A - Pavement Research", 1961
- Highway Research Board: "The AASHO Road Test. Report 5 - Pavement Research", 1962
- "Impact of Changing Traffic Characteristics and Environmental Conditions on Flexible Pavements", Zhang, Z., J. P. Leidy, I. Kawa, and W. R. Hudson, 2000
- "Load equivalency Factors for Asphalt Pavements", Zaghoul, S., and T. White, 1994
- NCHRP 1-37A: "Mechanistic Empirical Pavement Design Guide", 2004
- Pavement International Association of Road Congress, 1994
- "Pavement Analysis and Design", Huang, Y. H., 2004

“Performance evaluation of low environmental impact asphalt concretes using the mechanistic empirical design method based on laboratory fatigue and permanent deformation models”, PhD Thesis, M. Pettinari, 2011

“Rehabilitation Strategies for Highway Pavements”, K. T. Hall, C. E. Correa, S. H. Carpenter, R. P. Elliot, 2011

"Thickness Design of Asphalt Pavements - The Asphalt Institute Method", Shook, J. F., F. N. Finn, M. W. Witzak, and C. L. Monismith, 1982

WB maintenance website

<http://training.ce.washington.edu>

<http://pavementinteractive.org>



*Con questa tesi si conclude il mio percorso universitario.*

*Ringrazio di cuore tutti coloro che mi sono stati vicini in questi anni e in questi ultimi mesi. Ognuno di loro ha contribuito a rendere questa esperienza unica.*

**GRAZIE**